THE UNIVERSITY OF CALGARY

A GEOPHYSICAL DEEP CRUSTAL STUDY OF THE FORT NORMAN AREA, NORTHWEST TERRITORIES, CANADA

by

Marlene Dredge

A THESIS

SUBMITTED TO THE FACULTY OF GRADUATE STUDIES

IN PARTIAL FULFILLMENT OF THE REQUIREMENTS FOR THE

DEGREE OF MASTER OF SCIENCE

DEPARTMENT OF GEOLOGY AND GEOPHYSICS

CALGARY, ALBERTA

SEPTEMBER, 1992

Name Marlene Dredge

Dissertation Abstracts International is arranged by broad, general subject categories. Please select the one subject which most nearly describes the content of your dissertation. Enter the corresponding four-digit code in the spaces provided.

Geophysics — SUBJECT TERM

0373 — SUBJECT CODE

U·M·I

Subject Categories

THE HUMANITIES AND SOCIAL SCIENCES

COMMUNICATIONS AND THE ARTS
Architecture 0729
Art History 0377
Cinema 0900
Dance 0378
Fine Arts 0357
Information Science 0723
Journalism 0391
Library Science 0399
Mass Communications 0708
Music 0413
Speech Communication 0459
Theater 0465

EDUCATION
General 0515
Administration 0514
Adult and Continuing 0516
Agricultural 0517
Art 0273
Bilingual and Multicultural 0282
Business 0688
Community College 0275
Curriculum and Instruction 0727
Early Childhood 0518
Elementary 0524
Finance 0277
Guidance and Counseling 0519
Health 0680
Higher 0745
History of 0520
Home Economics 0278
Industrial 0521
Language and Literature 0279
Mathematics 0280
Music 0522
Philosophy of 0998
Physical 0523
Psychology 0525
Reading 0535
Religious 0527
Sciences 0714
Secondary 0533
Social Sciences 0534
Sociology of 0340
Special 0529
Teacher Training 0530
Technology 0710
Tests and Measurements 0288
Vocational 0747

LANGUAGE, LITERATURE AND LINGUISTICS
Language
- General 0679
- Ancient 0289
- Linguistics 0290
- Modern 0291

Literature
- General 0401
- Classical 0294
- Comparative 0295
- Medieval 0297
- Modern 0298
- African 0316
- American 0591
- Asian 0305
- Canadian (English) 0352
- Canadian (French) 0355
- English 0593
- Germanic 0311
- Latin American 0312
- Middle Eastern 0315
- Romance 0313
- Slavic and East European 0314

PHILOSOPHY, RELIGION AND THEOLOGY
Philosophy 0422
Religion
- General 0318
- Biblical Studies 0321
- Clergy 0319
- History of 0320
- Philosophy of 0322

Theology 0469

SOCIAL SCIENCES
American Studies 0323
Anthropology
- Archaeology 0324
- Cultural 0326
- Physical 0327

Business Administration
- General 0310
- Accounting 0272
- Banking 0770
- Management 0454
- Marketing 0338

Canadian Studies 0385
Economics
- General 0501
- Agricultural 0503
- Commerce-Business 0505
- Finance 0508
- History 0509
- Labor 0510
- Theory 0511

Folklore 0358
Geography 0366
Gerontology 0351
History
- General 0578
- Ancient 0579
- Medieval 0581
- Modern 0582
- Black 0328
- African 0331
- Asia, Australia and Oceania 0332
- Canadian 0334
- European 0335
- Latin American 0336
- Middle Eastern 0333
- United States 0337

History of Science 0585
Law 0398
Political Science
- General 0615
- International Law and Relations 0616
- Public Administration 0617

Recreation 0814
Social Work 0452
Sociology
- General 0626
- Criminology and Penology 0627
- Demography 0938
- Ethnic and Racial Studies 0631
- Individual and Family Studies 0628
- Industrial and Labor Relations 0629
- Public and Social Welfare 0630
- Social Structure and Development 0700
- Theory and Methods 0344

Transportation 0709
Urban and Regional Planning 0999
Women's Studies 0453

THE SCIENCES AND ENGINEERING

BIOLOGICAL SCIENCES
Agriculture
- General 0473
- Agronomy 0285
- Animal Culture and Nutrition 0475
- Animal Pathology 0476
- Food Science and Technology 0359
- Forestry and Wildlife 0478
- Plant Culture 0479
- Plant Pathology 0480
- Plant Physiology 0817
- Range Management 0777
- Wood Technology 0746

Biology
- General 0306
- Anatomy 0287
- Biostatistics 0308
- Botany 0309
- Cell 0379
- Ecology 0329
- Entomology 0353
- Genetics 0369
- Limnology 0793
- Microbiology 0410
- Molecular 0307
- Neuroscience 0317
- Oceanography 0416
- Physiology 0433
- Radiation 0821
- Veterinary Science 0778
- Zoology 0472

Biophysics
- General 0786
- Medical 0760

EARTH SCIENCES
Biogeochemistry 0425
Geochemistry 0996
Geodesy 0370
Geology 0372
Geophysics 0373
Hydrology 0388
Mineralogy 0411
Paleobotany 0345
Paleoecology 0426
Paleontology 0418
Paleozoology 0985
Palynology 0427
Physical Geography 0368
Physical Oceanography 0415

HEALTH AND ENVIRONMENTAL SCIENCES
Environmental Sciences 0768
Health Sciences
- General 0566
- Audiology 0300
- Chemotherapy 0992
- Dentistry 0567
- Education 0350
- Hospital Management 0769
- Human Development 0758
- Immunology 0982
- Medicine and Surgery 0564
- Mental Health 0347
- Nursing 0569
- Nutrition 0570
- Obstetrics and Gynecology 0380
- Occupational Health and Therapy 0354
- Ophthalmology 0381
- Pathology 0571
- Pharmacology 0419
- Pharmacy 0572
- Physical Therapy 0382
- Public Health 0573
- Radiology 0574
- Recreation 0575
- Speech Pathology 0460
- Toxicology 0383

Home Economics 0386

PHYSICAL SCIENCES
Pure Sciences

Chemistry
- General 0485
- Agricultural 0749
- Analytical 0486
- Biochemistry 0487
- Inorganic 0488
- Nuclear 0738
- Organic 0490
- Pharmaceutical 0491
- Physical 0494
- Polymer 0495
- Radiation 0754

Mathematics 0405
Physics
- General 0605
- Acoustics 0986
- Astronomy and Astrophysics 0606
- Atmospheric Science 0608
- Atomic 0748
- Electronics and Electricity 0607
- Elementary Particles and High Energy 0798
- Fluid and Plasma 0759
- Molecular 0609
- Nuclear 0610
- Optics 0752
- Radiation 0756
- Solid State 0611

Statistics 0463

Applied Sciences

Applied Mechanics 0346
Computer Science 0984
Engineering
- General 0537
- Aerospace 0538
- Agricultural 0539
- Automotive 0540
- Biomedical 0541
- Chemical 0542
- Civil 0543
- Electronics and Electrical 0544
- Heat and Thermodynamics 0348
- Hydraulic 0545
- Industrial 0546
- Marine 0547
- Materials Science 0794
- Mechanical 0548
- Metallurgy 0743
- Mining 0551
- Nuclear 0552
- Packaging 0549
- Petroleum 0765
- Sanitary and Municipal 0554
- System Science 0790

Geotechnology 0428
Operations Research 0796
Plastics Technology 0795
Textile Technology 0994

PSYCHOLOGY
General 0621
Behavioral 0384
Clinical 0622
Developmental 0620
Experimental 0623
Industrial 0624
Personality 0625
Physiological 0989
Psychobiology 0349
Psychometrics 0632
Social 0451

Nom ______________________________

Dissertation Abstracts International est organisé en catégories de sujets. Veuillez s.v.p. choisir le sujet qui décrit le mieux votre thèse et inscrivez le code numérique approprié dans l'espace réservé ci-dessous.

U·M·I

______________________________ SUJET

☐☐☐☐ CODE DE SUJET

Catégories par sujets

HUMANITÉS ET SCIENCES SOCIALES

COMMUNICATIONS ET LES ARTS
- Architecture 0729
- Beaux-arts 0357
- Bibliothéconomie 0399
- Cinéma 0900
- Communication verbale 0459
- Communications 0708
- Danse 0378
- Histoire de l'art 0377
- Journalisme 0391
- Musique 0413
- Sciences de l'information 0723
- Théâtre 0465

ÉDUCATION
- Généralités 515
- Administration 0514
- Art 0273
- Collèges communautaires 0275
- Commerce 0688
- Économie domestique 0278
- Éducation permanente 0516
- Éducation préscolaire 0518
- Éducation sanitaire 0680
- Enseignement agricole 0517
- Enseignement bilingue et multiculturel 0282
- Enseignement industriel 0521
- Enseignement primaire. 0524
- Enseignement professionnel 0747
- Enseignement religieux 0527
- Enseignement secondaire 0533
- Enseignement spécial 0529
- Enseignement supérieur 0745
- Évaluation 0288
- Finances 0277
- Formation des enseignants 0530
- Histoire de l'éducation 0520
- Langues et littérature 0279
- Lecture 0535
- Mathématiques 0280
- Musique 0522
- Orientation et consultation 0519
- Philosophie de l'éducation 0998
- Physique 0523
- Programmes d'études et enseignement 0727
- Psychologie 0525
- Sciences 0714
- Sciences sociales 0534
- Sociologie de l'éducation 0340
- Technologie 0710

LANGUE, LITTÉRATURE ET LINGUISTIQUE
- Langues
  - Généralités 0679
  - Anciennes 0289
  - Linguistique 0290
  - Modernes 0291
- Littérature
  - Généralités 0401
  - Anciennes 0294
  - Comparée 0295
  - Mediévale 0297
  - Moderne 0298
  - Africaine 0316
  - Américaine 0591
  - Anglaise 0593
  - Asiatique 0305
  - Canadienne (Anglaise) 0352
  - Canadienne (Française) 0355
  - Germanique 0311
  - Latino-américaine 0312
  - Moyen-orientale 0315
  - Romane 0313
  - Slave et est-européenne 0314

PHILOSOPHIE, RELIGION ET THEOLOGIE
- Philosophie 0422
- Religion
  - Généralités 0318
  - Clergé 0319
  - Études bibliques 0321
  - Histoire des religions 0320
  - Philosophie de la religion 0322
- Théologie 0469

SCIENCES SOCIALES
- Anthropologie
  - Archéologie 0324
  - Culturelle 0326
  - Physique 0327
- Droit 0398
- Économie
  - Généralités 0501
  - Commerce-Affaires 0505
  - Économie agricole 0503
  - Économie du travail 0510
  - Finances 0508
  - Histoire 0509
  - Théorie 0511
- Études américaines 0323
- Études canadiennes 0385
- Études féministes 0453
- Folklore 0358
- Géographie 0366
- Gérontologie 0351
- Gestion des affaires
  - Généralités 0310
  - Administration 0454
  - Banques 0770
  - Comptabilité 0272
  - Marketing 0338
- Histoire
  - Histoire générale 0578
  - Ancienne 0579
  - Médiévale 0581
  - Moderne 0582
  - Histoire des noirs 0328
  - Africaine 0331
  - Canadienne 0334
  - États-Unis 0337
  - Européenne 0335
  - Moyen-orientale 0333
  - Latino-américaine 0336
  - Asie, Australie et Océanie 0332
- Histoire des sciences 0585
- Loisirs 0814
- Planification urbaine et régionale 0999
- Science politique
  - Généralités 0615
  - Administration publique 0617
  - Droit et relations internationales 0616
- Sociologie
  - Généralités 0626
  - Aide et bien-àtre social 0630
  - Criminologie et établissements pénitentiaires 0627
  - Démographie 0938
  - Études de l' individu et de la famille 0628
  - Études des relations interethniques et des relations raciales 0631
  - Structure et développement social 0700
  - Théorie et méthodes. 0344
  - Travail et relations industrielles 0629
- Transports 0709
- Travail social 0452

SCIENCES ET INGÉNIERIE

SCIENCES BIOLOGIQUES
- Agriculture
  - Généralités 0473
  - Agronomie. 0285
  - Alimentation et technologie alimentaire 0359
  - Culture 0479
  - Élevage et alimentation 0475
  - Exploitation des péturages 0777
  - Pathologie animale 0476
  - Pathologie végétale 0480
  - Physiologie végétale 0817
  - Sylviculture et faune 0478
  - Technologie du bois 0746
- Biologie
  - Généralités 0306
  - Anatomie 0287
  - Biologie (Statistiques) 0308
  - Biologie moléculaire 0307
  - Botanique 0309
  - Cellule 0379
  - Écologie 0329
  - Entomologie 0353
  - Génétique 0369
  - Limnologie 0793
  - Microbiologie 0410
  - Neurologie 0317
  - Océanographie 0416
  - Physiologie 0433
  - Radiation 0821
  - Science vétérinaire 0778
  - Zoologie 0472
- Biophysique
  - Généralités 0786
  - Medicale 0760

SCIENCES DE LA TERRE
- Biogéochimie 0425
- Géochimie 0996
- Géodésie 0370
- Géographie physique 0368
- Géologie 0372
- Géophysique 0373
- Hydrologie 0388
- Minéralogie 0411
- Océanographie physique 0415
- Paléobotanique 0345
- Paléoécologie 0426
- Paléontologie 0418
- Paléozoologie 0985
- Palynologie 0427

SCIENCES DE LA SANTÉ ET DE L'ENVIRONNEMENT
- Économie domestique 0386
- Sciences de l'environnement 0768
- Sciences de la santé
  - Généralités 0566
  - Administration des hipitaux 0769
  - Alimentation et nutrition 0570
  - Audiologie 0300
  - Chimiothérapie 0992
  - Dentisterie 0567
  - Développement humain 0758
  - Enseignement 0350
  - Immunologie 0982
  - Loisirs 0575
  - Médecine du travail et thérapie 0354
  - Médecine et chirurgie 0564
  - Obstétrique et gynécologie 0380
  - Ophtalmologie 0381
  - Orthophonie 0460
  - Pathologie 0571
  - Pharmacie 0572
  - Pharmacologie 0419
  - Physiothérapie 0382
  - Radiologie 0574
  - Santé mentale 0347
  - Santé publique 0573
  - Soins infirmiers 0569
  - Toxicologie 0383

SCIENCES PHYSIQUES

Sciences Pures
- Chimie
  - Généralités 0485
  - Biochimie 487
  - Chimie agricole 0749
  - Chimie analytique 0486
  - Chimie minérale 0488
  - Chimie nucléaire 0738
  - Chimie organique 0490
  - Chimie pharmaceutique 0491
  - Physique 0494
  - PolymÇres 0495
  - Radiation 0754
- Mathématiques 0405
- Physique
  - Généralités 0605
  - Acoustique 0986
  - Astronomie et astrophysique 0606
  - Electronique et électricité 0607
  - Fluides et plasma 0759
  - Météorologie 0608
  - Optique 0752
  - Particules (Physique nucléaire) 0798
  - Physique atomique 0748
  - Physique de l'état solide 0611
  - Physique moléculaire 0609
  - Physique nucléaire 0610
  - Radiation 0756
- Statistiques 0463

Sciences Appliqués Et Technologie
- Informatique 0984
- Ingénierie
  - Généralités 0537
  - Agricole 0539
  - Automobile 0540
  - Biomédicale 0541
  - Chaleur et ther modynamique 0348
  - Conditionnement (Emballage) 0549
  - Génie aérospatial 0538
  - Génie chimique 0542
  - Génie civil 0543
  - Génie électronique et électrique 0544
  - Génie industriel 0546
  - Génie mécanique 0548
  - Génie nucléaire 0552
  - Ingénierie des systâmes 0790
  - Mécanique navale 0547
  - Métallurgie 0743
  - Science des matériaux 0794
  - Technique du pétrole 0765
  - Technique minière 0551
  - Techniques sanitaires et municipales 0554
  - Technologie hydraulique 0545
- Mécanique appliquée 0346
- Géotechnologie 0428
- Matières plastiques (Technologie) 0795
- Recherche opérationnelle 0796
- Textiles et tissus (Technologie) 0794

PSYCHOLOGIE
- Généralités 0621
- Personnalité 0625
- Psychobiologie 0349
- Psychologie clinique 0622
- Psychologie du comportement 0384
- Psychologie du développement 0620
- Psychologie expérimentale 0623
- Psychologie industrielle 0624
- Psychologie physiologique 0989
- Psychologie sociale 0451
- Psychométrie 0632

ISBN 0-315-83139-1

THE UNIVERSITY OF CALGARY

FACULTY OF GRADUATE STUDIES

The undersigned certify that they have read, and recommend to the Faculty of Graduate Studies for acceptance, a thesis entitled "A Geophysical Deep Crustal Study of the Fort Norman Area, Northwest Territories, Canada" submitted by Marlene Dredge in partial fulfillment of the requirements for the degree of Masters of Science.

Frederick A. Cook
Supervisor
Dr. F.A. Cook
Department of Geology and Geophysics

Philip Simony
Dr. Philip Simony
Department of Geology and Geophysics

S Walker
Dr. Stuart Walker
Faculty of Environmental Design

Oct 16/92
Date

ABSTRACT

Seismic reflection data from south of Fort Norman in the Northwest Territories provide images of Proterozoic layers in the subsurface southeast of the Mackenzie Mountains. These data were obtained west of a crustal scale intra-Proterozoic ramp (homocline) as delineated on other seismic and Bouguer gravity data in the region.

Three parallel seismic reflection lines were recorded in February, 1991 by Chevron Canada to 15.0 seconds and have been provided to us for processing and interpretation of the deep structures. These data, along with four lines of industry data obtained from the National Energy Board (NEB), are being used for a regional study of the Proterozoic structure and stratigraphy within the Fort Norman area.

The processed sections display a thick (more than 5.0 seconds or 15.0 km) sequence of strongly layered Proterozoic reflectors to approximately 8.0 seconds (about 24.0 km depth) that are uplifted on the west side of the profiles. These reflectors may be strata of a westward thickening miogeocline that existed in the area between about 1.8 and 1.3 Ga. Steeply west-dipping reflections at about 5.0 to 8.0 seconds on the east side of the unmigrated data flatten beneath the uplifted layered sequence at about 10.0 to 11.0 seconds (about 30-33 km) and appear to be related to a deep basal detachment.

Potential field data assist in outlining the structure of the Hudsonian basement beneath the Proterozoic strata because the basement appears to have a much higher density and magnetic susceptibility than overlying sedimentary strata. These results are combined with the seismic reflection data to provide a three dimensional view of the Proterozoic homocline and its associated overlying structures.

ACKNOWLEDGEMENTS

I would like to sincerely thank my supervisor, Dr. Frederick Cook, for his scientific guidance throughout my masters program.

I would like to thank Chevron Canada for the donation of seismic data, Mobil Canada for the use of their mapping package, and the Geological Survey of Canada (G.S.C.) for access to the potential field database.

I am also indebted to the staff at the LSPF managed by Kris Vasudevan, especially, Rolf Maier, Arie Vander Velden, and Mark Lane who helped immensely in processing part of my thesis, Jeff Thurston for his help with the potential field data, Betty Clark and John Varsek for their discussions.

Special thanks to my husband, Boris Mitchelmore, and to my parents, Curtis and Mary Dredge. These are the people who gave me the encouragement and support to further my education, thank you.

TABLE OF CONTENTS

LIST OF TABLES

LIST OF FIGURES

CHAPTER 1 : INTRODUCTION

Introduction

The Fort Norman study area (Figure 1.1) is located within the Interior Platform of northwestern Canada west of Great Bear Lake between latitudes 64° to 65° north and longitudes 124° to 126° west. The Interior Platform of Northwestern Canada is bounded on the east by the Proterozoic rocks of the Canadian Shield and on the west by rocks of the Cordillera. It is characterized by thin Paleozoic and Mesozoic cover rocks that are relatively undeformed (Cook, 1988).

Two Proterozoic orogenic episodes, the Racklan orogeny and the Hayhook orogeny have been identified in the Mackenzie Mountains area. The Racklan orogeny occurred prior to deposition of the Mackenzie Mountains Supergroup and is not well understood. It is defined essentially on the basis of folded and cleaved Wernecke Supergroup strata that are unconformably overlain by the Mackenzie Mountains Supergroup (Young et al., 1979). The Hayhook orogeny occurred after deposition of the Mackenzie Mountains Supergroup and is characterized by block faulting and the development of extensional basins within the upper Mackenzie Mountains Supergroup and lower Ekwi Supergroup (or equivalent Windermere Supergroup; Young et al., 1979).

Figure 1.1

Regional geological map of northwestern Canada illustrating the locations of exposed Proterozoic rocks. The study area is outlined by a box located immediately west of Great Bear Lake (modified from Cook and Taylor, 1991).

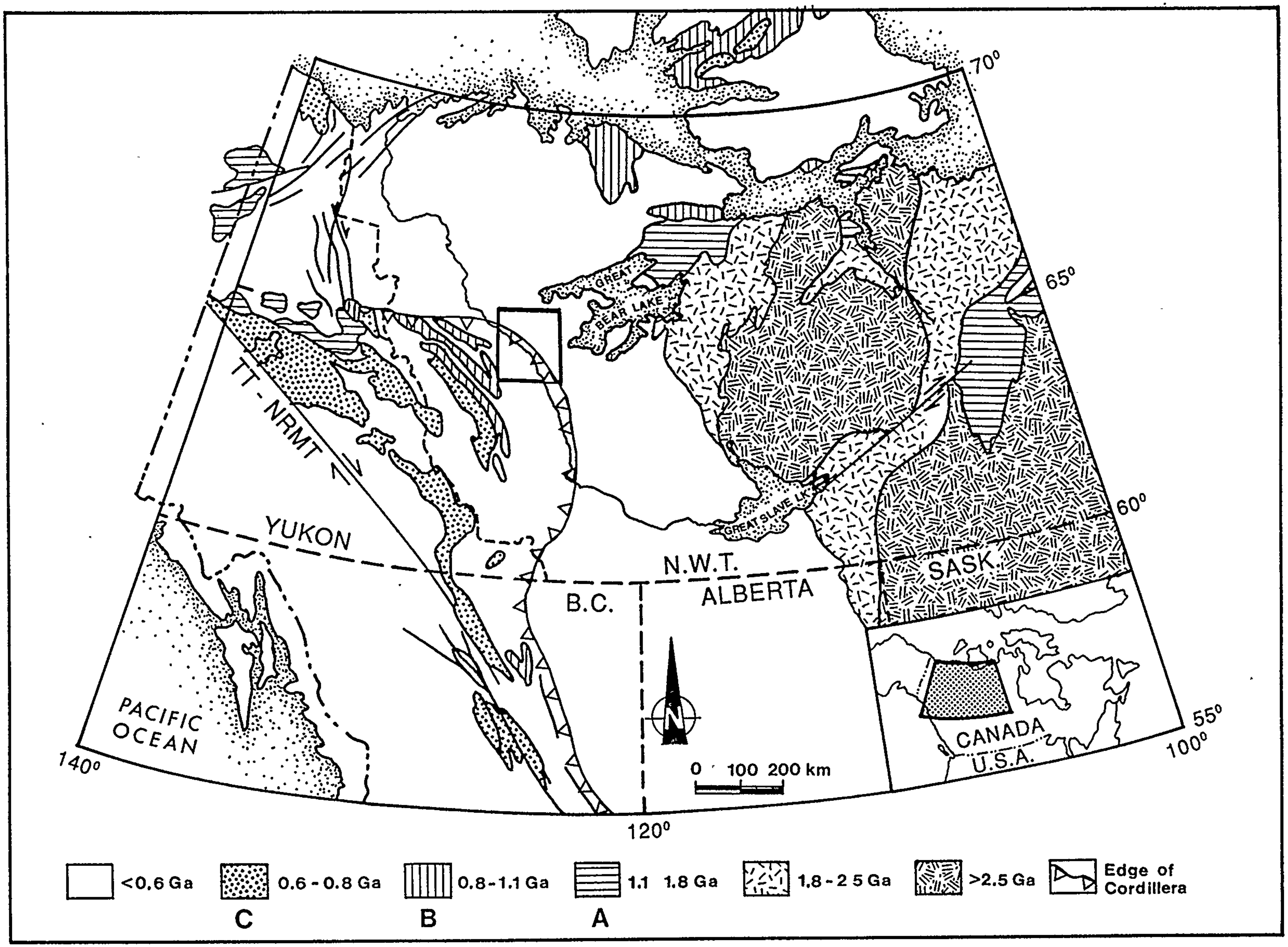
70°
65°
60°
55°
100°
140°
120°
GREAT BEAR LAKE
GREAT SLAVE L.
TT - NRMT
YUKON
N.W.T.
B.C.
ALBERTA
SASK.
PACIFIC OCEAN
N
0 100 200 km
CANADA
U.S.A.
<0.6 Ga
0.6 - 0.8 Ga
C
0.8 - 1.1 Ga
B
1.1 1.8 Ga
A
1.8 - 2 5 Ga
>2.5 Ga
Edge of Cordillera

The major structures known in northwestern Canada include a crustal-scale basement ramp and some uplifts that are cored by Proterozoic strata: the Fort Simpson structural highs (magnetic anomalies) in the east. The 'ramp' has been interpreted by Cook et al. (1991) to represent a regionally extensive west-facing transition from thick craton on the east to thin crust on the west which likely formed during passive margin development following the Hudsonian Orogeny (ca. 1.8 Ga). It has been observed in four other areas within the Cordillera: the Fort Good Hope area (Profile A), an area ca. 200 km south of profile A (Profile B), the Monashee Complex in southern British Columbia (Profile C), and in northern United States (Profile D; Figure 1.2).

The Fort Simpson anomaly is caused by variations in the magnetic properties of Proterozoic rocks at depth (Cook et al., 1992). The structural high is caused by west-east contraction resulting in the uplifting of Hudsonian basement rocks. There are no direct ties to Proterozoic outcrops available and well control is limited, both in areal extent and in penetration. Nevertheless, stratigraphic correlations for the Interior Platform of the Northwest Territories by Young et al. (1979), Kerans et al. (1981), Delaney (1981), Aitken and Pugh (1984), and Young (1984) allow rock units in one area to be generally related to those in another. For example, Young (1984), suggests a correlation of the Proterozoic rocks from the Wernecke Mountains, N.W.T. to the Churchill Province of Quebec (Figure 1.3). In western Canada, this correlation suggests Dismal Lakes and Hornby Bay Groups, comprising two clastic-carbonate shoaling upwards sequences of the Coppermine Homocline, correlate to the Fairchild Lake Group and Quartet and Gillespie Lake Groups of the Wernecke Supergroup in the Cordillera, respectively (Figure 1.3).

Similarly, the volcanic rocks of the Coppermine River Group and the probably coeval Muskox intrusion intrude and overlie these clastic-carbonate megacycles and are a locally developed remnent of the widespread Mackenzie igneous episode (Young, 1984; LeCheminart and Hearn, 1989). The lower formations of the Mackenzie Mountains Supergroup in the Cordillera, consisting of the H1 carbonate unit, the Tsezotene Formation, and the Katherine Group have been correlated with the Rae and Shaler Groups in the Coppermine area and unconformably overlie strata of the Wernecke Supergroup (or correlative strata).

These general relationships, while allowing regional stratigraphic characteristics to be established, offer little information on the structural and stratigraphic variations in the subsurface between the Cordillera and the Shield. Geophysical data, including seismic, gravity and magnetics, coupled with some information from drill holes provide this link.

Objectives of this Research

The objectives of this research are: 1) to process deep seismic reflection data provided by Chevron Canada, 2) to relate the observations made from the Chevron data to the surrounding seismic data and to stratigraphic data available to the east (Coppermine Area) and to the west (Cordillera), and 3) to incorporate these data along with the potential field data available from the Geological Survey of Canada (G.S.C.) into an

Figure 1.2

Map of western Canada showing the location of the Cordillera (shaded) and the location of the crustal scale ramp as defined by seismic and gravity north of 56 degrees, and seismic south of 56 degrees (hachured line). The study area is boxed in immediately west of Great Bear Lake (modified from Cook et al., 1991).

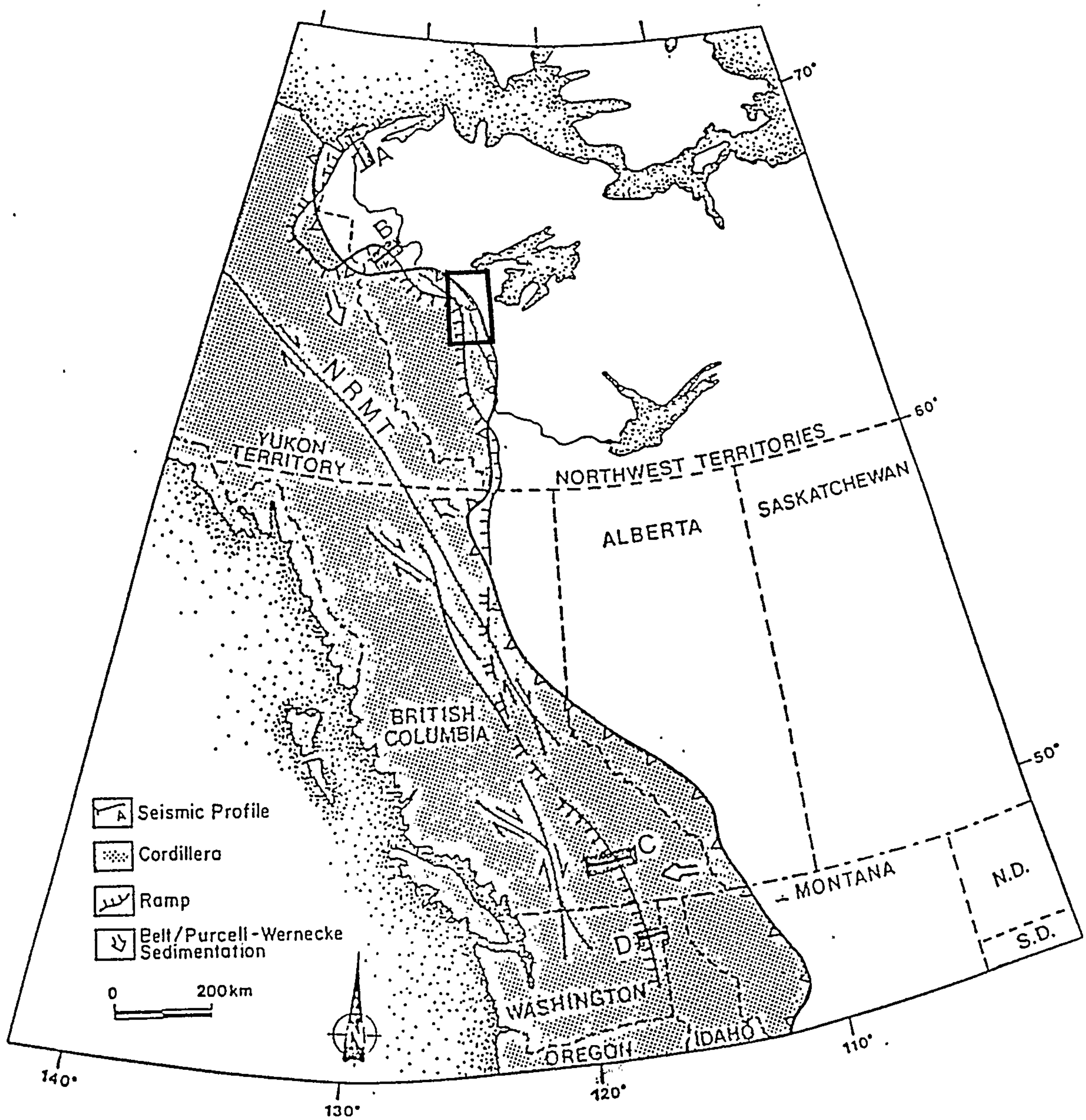
70°
60°
50°
110°
120°
130°
140°
A
B
C
D
NRMT
YUKON TERRITORY
NORTHWEST TERRITORIES
ALBERTA
SASKATCHEWAN
BRITISH COLUMBIA
MONTANA
N.D.
S.D.
WASHINGTON
OREGON
IDAHO
Seismic Profile
Cordillera
Ramp
Belt/Purcell-Wernecke Sedimentation
0 200km
N

integrated interpretation of the structure and stratigraphy of the Proterozoic rocks in the Fort Norman area.

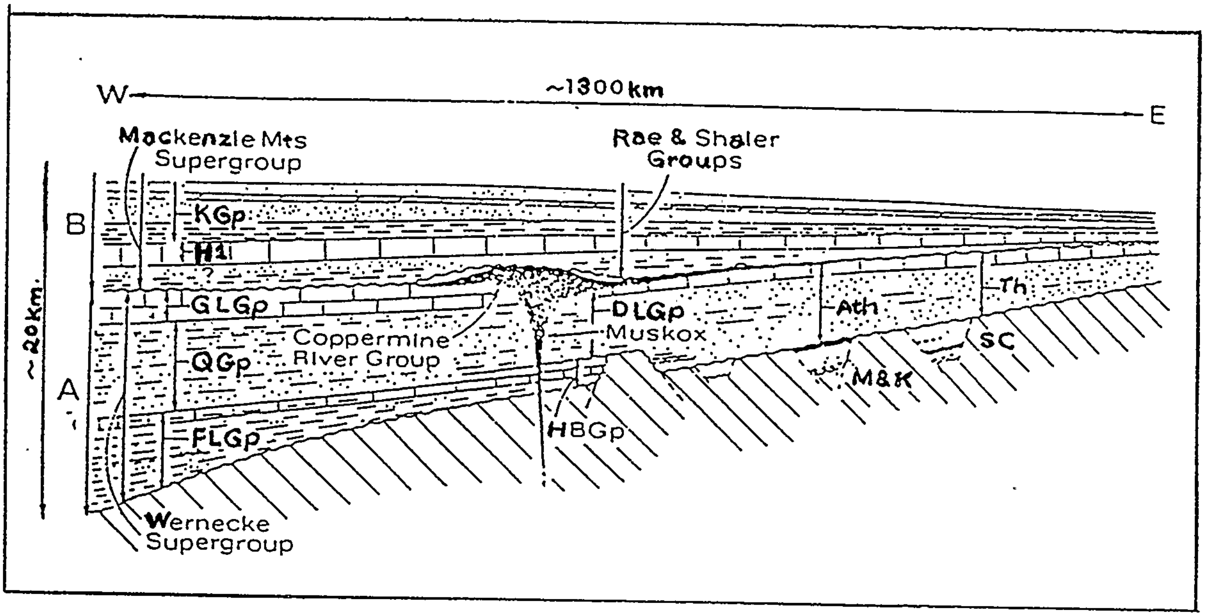

Figure 1.3

Stratigraphic correlation of the Proterozoic strata from the Wernecke Mountains to the Churchill Province (Young, 1984). Abbreviations used are: KGp - Katherine Group, H1 - H1 carbonate map unit, GLGp - Gillespie Lakes Group, QGp - Quartet Group, FLGp - Fairchild Lake Group, DLGp - Dismal Lakes Group, HBGp - Hornby Bay Group, Ath - Athabasca Basin, Th - Thelon Basin, M & K - Martin and Kazan Formations, and SC - South Channel Formation.

CHAPTER 2 : BACKGROUND AND PREVIOUS WORK

Regional Setting

This study builds upon and extends previous work in the area that includes regional studies of the Proterozoic stratigraphy (Young et al., 1979, Aitken and Pugh, 1984), and structures based upon seismic and potential field data (Cook, 1988, Cook et al., 1992). Large exposures of Proterozoic rocks are known only from the Cordillera some 200 km to the west and from the Coppermine Homocline some 100 km to the east. Nevertheless, evidence from drill holes and a few isolated outcrops east of the Cordillera indicates that strata that can be correlated to Coppermine Homocline rocks are present beneath this region (Aitken and Pugh, 1984). In addition, Proterozoic rocks exposed within the Cordillera can be stratigraphically correlated to rocks of the Coppermine Homocline (Young et al., 1979, Aitken and Pugh, 1984). Taken together, these results suggest that Proterozoic strata are present beneath the Phanerozoic in the study area. Following is an account of the regional stratigraphic characteristics of these rocks.

Regional Proterozoic Stratigraphy

The study area lies in the Interior Platform of the Northwest Territories west of the crustal-scale intra-Proterozoic ramp (homocline) as delineated on other seismic reflection data and Bouguer gravity data in the region. In general, Proterozoic rocks of the Interior platform unconformably overlie the metamorphic and plutonic rocks of the Hudsonian basement (Kerans et al., 1981) and are in turn overlain by more or less horizontal Paleozoic sediments.

Young et al. (1979) subdivided the Proterozoic successions of Northwestern Canada into three sequences on the basis of lithostratigraphic correlations (Figure 2.1). They named these sequences A, B, and C and suggested they were deposited from about 1.7-1.2 Ga, 1.2-0.8 Ga, and 0.8-0.57 Ga respectively (Delaney, 1981). Each stratigraphic sequence is separated by regionally extensive unconformities.

The oldest sequence, sequence A, was deposited on metamorphic and igneous rocks of the Hudsonian Orogen and includes up to 5.0-5.5 km of clastic and carbonate rocks of the Hornby Bay and Dismal Lakes Groups in the Coppermine Homocline in the east. These sediments are overlain by 2.5-3.0 km of continental tholeiitic basalt of the Coppermine River Group. The rocks of the Dismal Lakes and Hornby Bay Groups are correlated with a much thicker (up to 15 km; Delaney, 1981) Wernecke Supergroup in the Cordillera which consists of shoaling upward basinal to miogeoclinal strata. Surface exposures and well penetrations of rocks of sequence A are extremely limited in the area between the Coppermine Homocline and the Cordillera. The deposition of sequence A was followed by a major period of orogenic activity causing erosion and uplift.

According to Sevigny et al. (1991), there are at least three periods of deformation that affected sequence A strata prior to deposition of sequence B which had been previously considered as forming one event; the Racklan Orogeny (Young et al., 1979). Sequences B and C were separated by a tensional orogenic event named the Hayhook

Figure 2.1

Schematic cross-section of Proterozoic stratigraphy for three areas of northwestern Canada. Major subdivisions into three sequences is shown by letters A, B, and C at left. Proposed correlations of sequences by Young et al. (1979) are illustrated by dashed lines. Abbreviations used are: GL - Greenhorn Lake Formation, FC - Fort Confidence Formation, ER - East River Formation, G - Group, and SG - Supergroup (modified from Young et al., 1979).

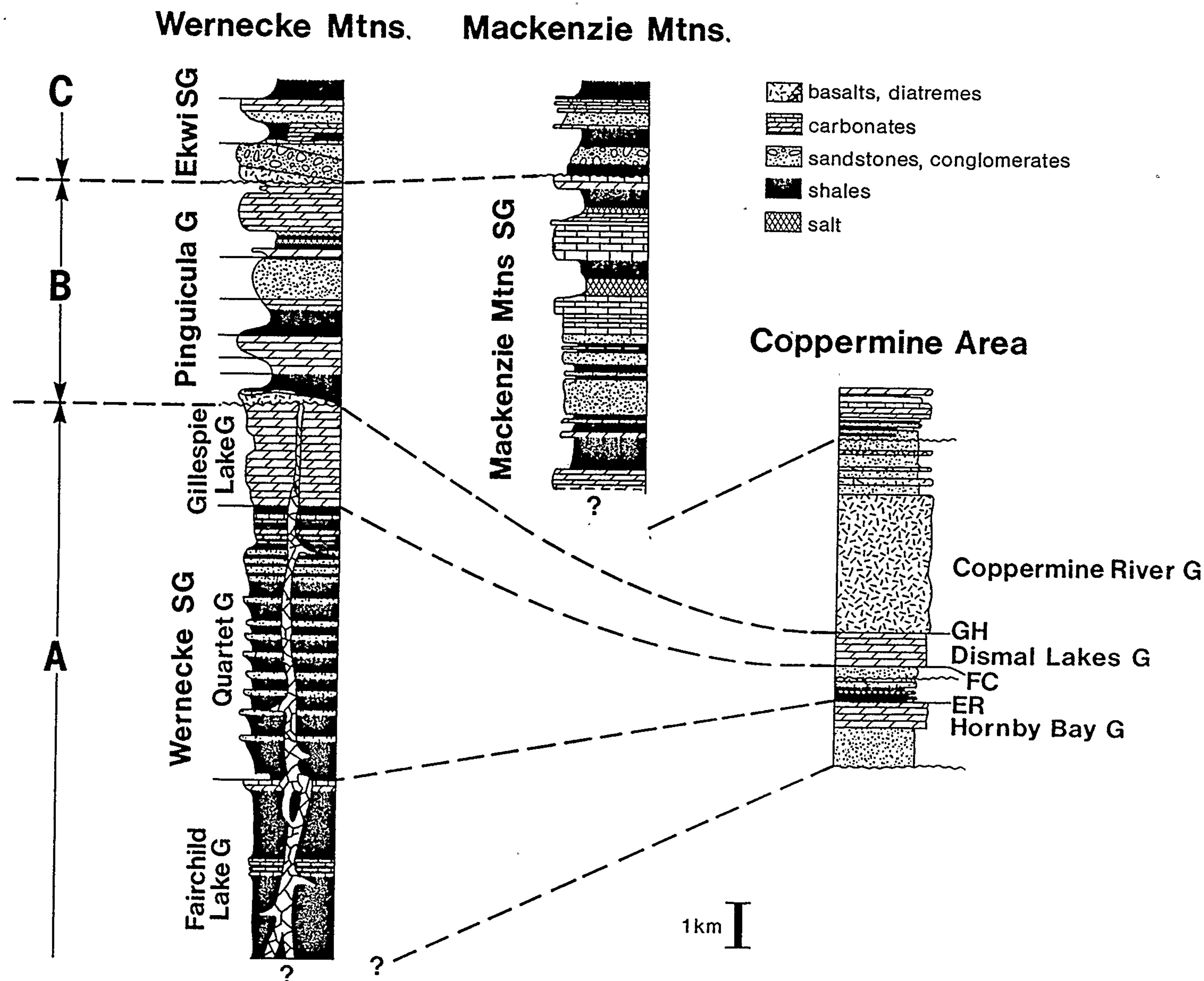

Wernecke Mtns.
Mackenzie Mtns.
C
B
A
Ekwi SG
Pinguicula G
Gillespie Lake G
Wernecke SG
Quartet G
Fairchild Lake G
Mackenzie Mtns SG
basalts, diatremes
carbonates
sandstones, conglomerates
shales
salt
Coppermine Area
Coppermine River G
GH
Dismal Lakes G
FC
ER
Hornby Bay G
1km
?
?
?

orogeny at about 0.8 Ga (Young et al., 1979).

Sequence B is represented by a relatively thin (1.0-1.5 km) Rae Group in the Coppermine Homocline which consists of carbonates and clastics. In the Cordillera, sequence B is represented by about 5 km of sedimentary strata of the Pinguicula Group (or the equivalent Mackenzie Mountains Supergroup; Young et al., 1979). The I-74 well, located in the northeastern part of the study area, penetrated Mackenzie Mountains Supergroup rocks beneath the Paleozoic (Aitken and Pugh, 1984). Available radiometric age determinations and stratigraphic relationships suggest that sequences A and B correspond to the Belt-Purcell Supergroup of the Southern Cordillera (Young et al., 1979). Sequences A and B are separated by a tensional orogenic event, the Hayhook orogeny.

Sequence C strata are found only in the Cordillera of northwestern Canada and thus are not likely present in the study area. These rocks are considered to be correlative with the ca. 600-700 Ma Windermere strata of the southern Canadian Cordillera (Young et al., 1979).

Wernecke Supergroup - Hornby Bay/Dismal Lakes Groups

In the west, the Wernecke Supergroup is a 15 km thick sequence of fine grained terrigenous and carbonate sediments which records a shoaling-upward miogeoclinal depositional regime. These rocks have been subdivided into three groups, from youngest to oldest, the Gillespie Lake Group, the Quartet Group, and the Fairchild Lake Group. The Gillespie Lake Group consists of more than 4 km of carbonate strata. The Quartet

Group consists mostly of layered clastics and is at least 5 km thick. Nowhere has the base of the Fairchild Lake Group been observed, but it is generally conformably overlain by the Quartet Group. It is at least 4 km of carbonates and clastics (Delaney, 1981).

The Hornby Bay and Dismal Lakes Groups in the east comprise two clastic-carbonate cycles which Young et al. (1979) have correlated with the Fairchild Lake Group and the Quartet and Gillespie Lake Groups, respectively. The correlations are shown on Figure 2.1.

Drill Hole Data and Outcrop Information

There are few wells that penetrate Proterozoic strata in and around the Fort Norman study area, but some valuable information is available from the limited data available (Figure 2.2). The northern I-74 well was interpreted to penetrate Mackenzie Mountains Supergroup strata (unit H1) beneath the Paleozoic (Aitken and Pugh, 1984). About 50-60 kilometres to the southwest (Figure 2.1), the B-62 well penetrated a white to light grey quartzite below the Paleozoic. This quartzite was compared to the lithology of the Katherine Formation (part of the Mackenzie Mountains Supergroup) encountered in the the P.C.I. Sammons well drilled in 1984. The two are quite similar and had similar drilling properties (National Energy Board, 1986). Thus it is very possible that the B-62 well penetrates the Upper Proterozoic Katherine Formation. Approximately 60-70 km west of B-62, the D-61 well encountered the East River Formation of the Hornby Bay Group (Aitken and Pugh, 1984). About 80-100 km south of the B-62 well, the L-04 well

Figure 2.2

Surface geology map of northwestern Canada illustrating well locations and ages of rocks in surface exposures (modified from Cook and Yorath, 1981).

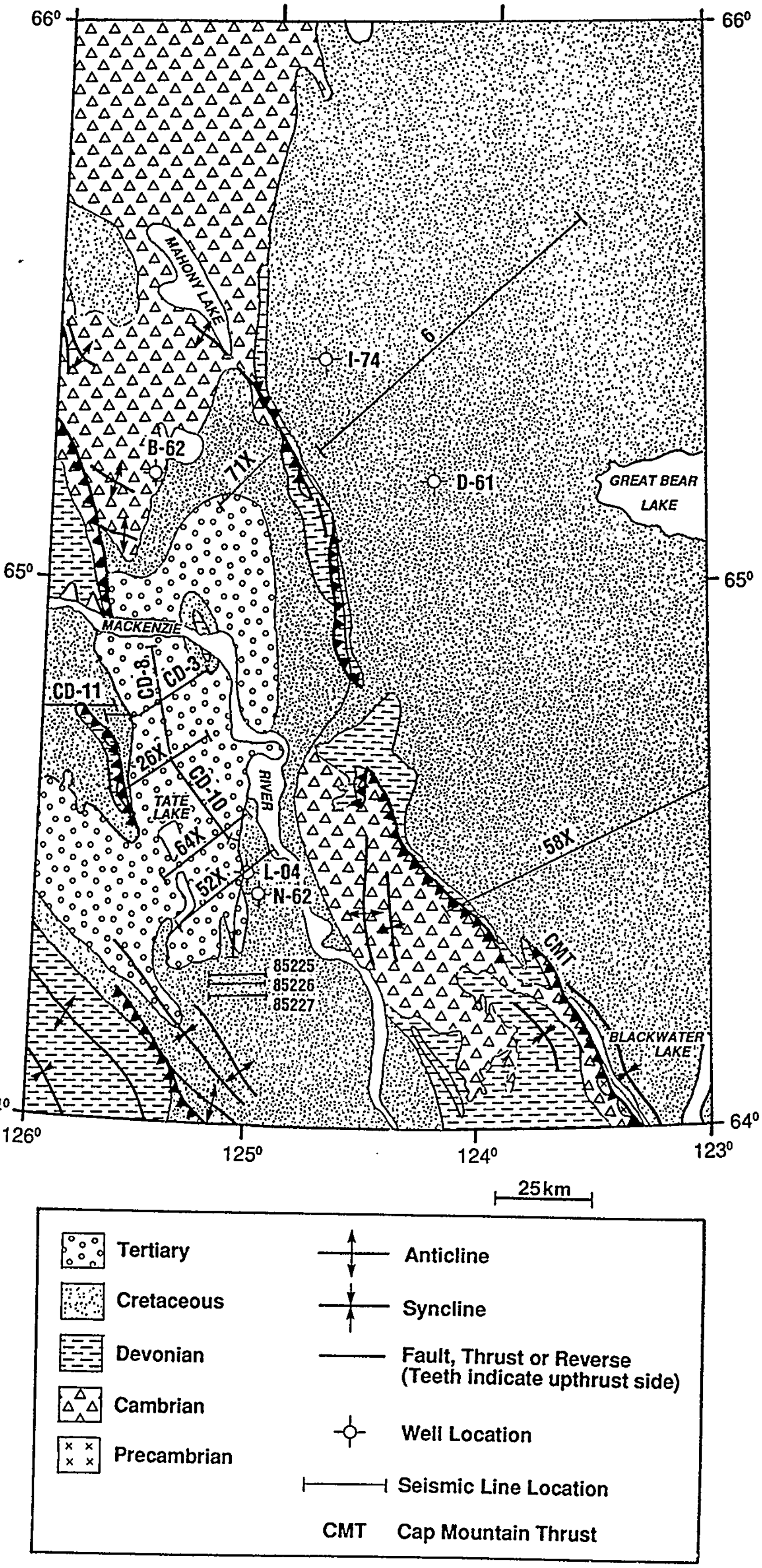
66°
65°
64°
126°
125°
124°
123°
MAHONY LAKE
I-74
6
B-62
71X
D-61
GREAT BEAR LAKE
MACKENZIE
RIVER
CD-8
CD-3
CD-11
26X
CD-10
TATE LAKE
64X
52X
L-04
N-62
58X
CMT
85225
85226
85227
BLACKWATER LAKE
25km
Tertiary
Cretaceous
Devonian
Cambrian
Precambrian
Anticline
Syncline
Fault, Thrust or Reverse
(Teeth indicate upthrust side)
Well Location
Seismic Line Location
CMT Cap Mountain Thrust

penetrates into the Cambrian and is situated adjacent to one of the Chevron reflection seismic lines described here. The well control thus enables us to identify the top of the Proterozoic on seismic data, and to some extent the stratigraphy at the top of the Proterozoic in the area.

In addition to the drill hole data, Proterozoic strata exposed at Cap Mountain, a Cordilleran structure located some 100 km southeast of the study area and uplifted along the Cap Mountain Thrust (CMT) which crosses the study area (Figure 2.2), are likely correlative with sedimentary rocks of the lowermost Dismal Lakes and the uppermost Hornby Bay Groups (Aitken and Pugh, 1984). Accordingly, these strata are present in the subsurface of this region and can be correlated to the seismic data.

CHAPTER 3 : SEISMIC DATA BASE

Seismic Data Acquisition

Chevron Canada acquired approximately 90 km of seismic data about 25 to 30 km south of the townsite of Fort Norman (Figure 3.1). These data were recorded to 15.0 seconds during February 1991 and were donated to the Lithoprobe Seismic Processing Facility (LSPF) for analysis of deep structure. Line 40X was a short (7.47 km) line which extended west of line 52X. The data quality of 40X is very poor, therefore the line was not used for this study. The other three lines; 52X, 64X, and 26X, were 30.06 km, 26.37 km, and 26.06 km long respectively (Figure 3.1). These three lines are parallel to one another and are positioned more or less perpendicular to the magnetic and gravity trend which is likely a good approximation of the regional strike of deep structure in the area. Table 3.1 outlines the parameters used in acquiring the data.

Other seismic reflection lines (Table 3.2) used in the study were obtained from the National Energy Board (NEB) and were typically recorded to 4.0 seconds. There are many more seismic lines (Figure 3.1) within the study area but they were either of poor data quality or were insignificant for the purpose of this study.

Seismic Data Processing

The seismic data processing was done on the SUN ITA workstation at the LSPF. The data were processed through a standard common mid-point (CMP) processing

Figure 3.1

Map of the study area illustrating the available seismic database. Dashed lines are the three Chevron seismic lines, all other solid lines represent seismic lines available from the NEB database.

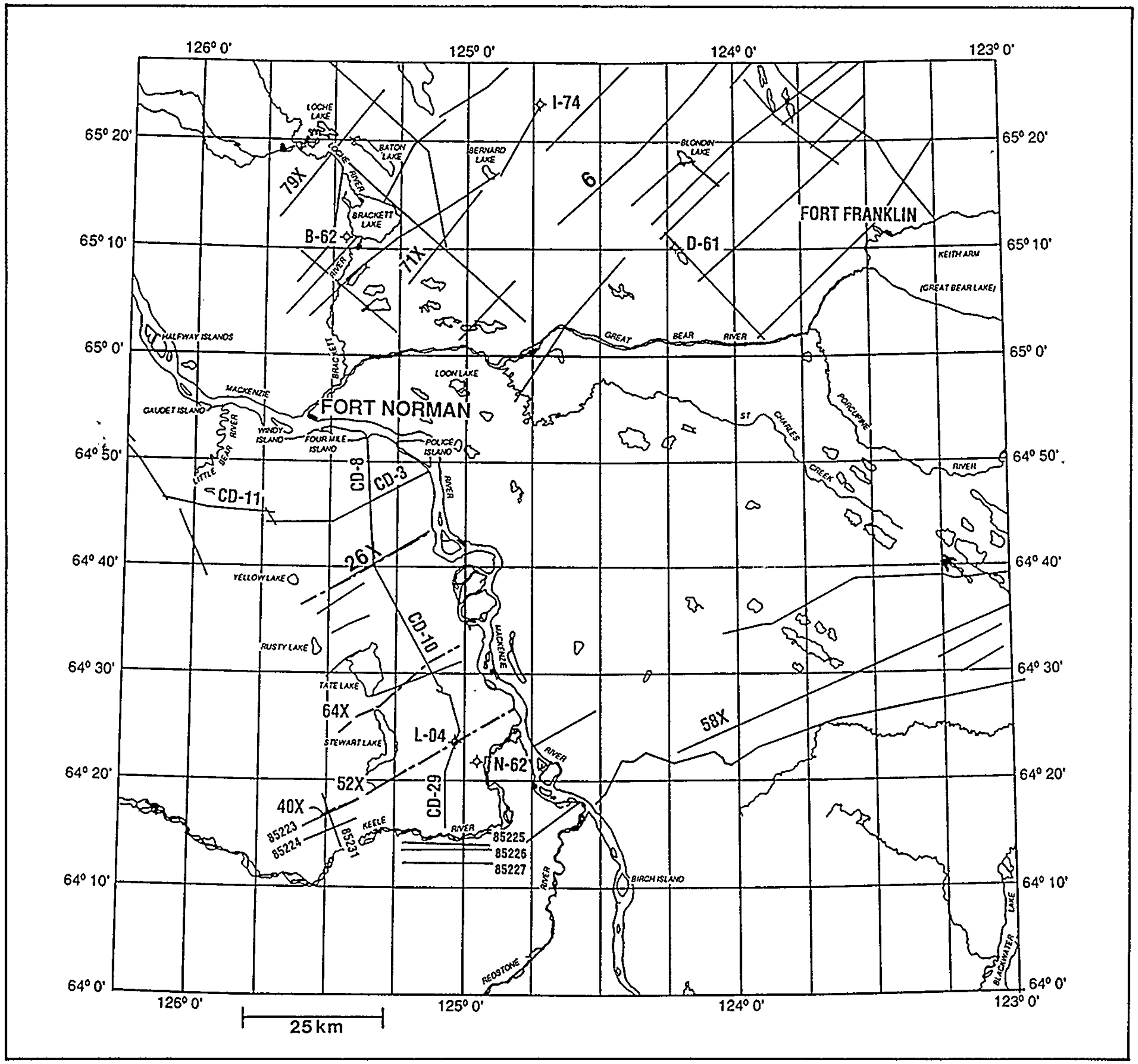
126° 0'
125° 0'
124° 0'
123° 0'
65° 20'
65° 10'
65° 0'
64° 50'
64° 40'
64° 30'
64° 20'
64° 10'
64° 0'
LOCHE LAKE
BATON LAKE
BERNARD LAKE
BLONDIN LAKE
BRACKETT LAKE
I-74
79X
6
B-62
71X
D-61
FORT FRANKLIN
KEITH ARM
(GREAT BEAR LAKE)
HALFWAY ISLANDS
GREAT BEAR RIVER
LOON LAKE
FORT NORMAN
MACKENZIE RIVER
GAUDET ISLAND
WINDY ISLAND
FOUR MILE ISLAND
POLICE ISLAND
ST CHARLES CREEK
PORCUPINE RIVER
LITTLE BEAR RIVER
CD-11
CD-8
CD-3
26X
YELLOW LAKE
RUSTY LAKE
CD-10
TATE LAKE
64X
STEWART LAKE
L-04
N-62
58X
52X
40X
CD-29
85223
85224
85231
KEELE RIVER
85225
85226
85227
BIRCH ISLAND
REDSTONE RIVER
BLACKWATER LAKE
25 km

sequence. The parameters used in the processing are summarized in Table 3.3.

The first line processed was line 52X and will be used to illustrate some of the processing steps listed in Table 3.3. The shot records, with a 500 ms AGC applied, indicate noise problems (Figures 3.2a and b). For example, artifacts labelled A on Figure 3.2a look like surface waves and are caused by activity at the shot location. Another noise problem is that of atmospheric electrical discharge observed on Figure 3.2a (B) where high amplitude, horizontal lines (infinite velocity) cross the shot record.

On the left side of Figures 3.2a and b there is a small zone of constant frequency traces becoming wider deeper in the section with the frequencies varying from trace to trace. In other words, there are 60 Hz, 30 Hz and 16 Hz frequencies in this group of traces. Therefore, applying notch filters would not remove the problem without seriously affecting the data. The constant frequency bands may have been caused by machinery vibrating close to the receivers or overhead noise. These traces, along with bad traces labelled D, were removed during the edit stage.

Since the seismic lines were nearly straight, straight line geometries were used such that a shot was placed at every third receiver location. Figure 3.3 is a screen image from an ITA workstation illustrating the symmetrical split spread design. An enlargement of the end of the line (Figure 3.4) demonstrates the rolling in of the data. The fold coverage is roughly 22 throughout the line. The survey notes indicate a fairly rugged topograpy (Figure 3.5).

Table 3.1 : Acquisition parameters of the Chevron seismic reflection lines.

Data Acquisition Parameters	
Source Information	
Energy source	DFS-V : Dynamite
charge size	2 kg
Shot interval	90 m
Receiver Information	
Geophone	
type	SM-4
frequency	14 Hz
Field filters	anti-alais
Sample rate	2 ms (resampled to 4 ms)
Group interval	30 m
Channels	120
Coverage	2000%
Spread design	Symmetric split
	60 station west
	30 station gap
	61 station east

Table 3.2 : List of the NEB seismic reflection lines used in the study.

Line	Operator	Year	Source
CD-29	Sigma Explorations Ltd.	1971	dynamite
CD-10	Sigma Explorations Ltd.	1971	dynamite
71X	Petro-Canada	1982	dynamite
6	B.P.O.G.	1974	dynamite

Table 3.3 : Processing parameters for the Chevron seismic reflection lines.

Demultiplex	(completed in field)
Gain Recovery	
Geometry	Straight Line
levation Statics	Datum : 500 m
	Replacement Velocity : 3500 m/s
First Break Mutes	
CMP Gather	
Velocity Analysis	
Normal Moveout Corrections	
Residual Static Corrections	
Bandpass Filtering	12/15 - 65/75 Hz
Gain	500 ms AGC
Stack	Nominally 20 Fold
Coherency/Semblance Filtering	
Migration	

Figures 3.2a and b

Examples of shot records from seismic line 52X illustrating noise problems. Artifacts labelled A-D are discussed in text.

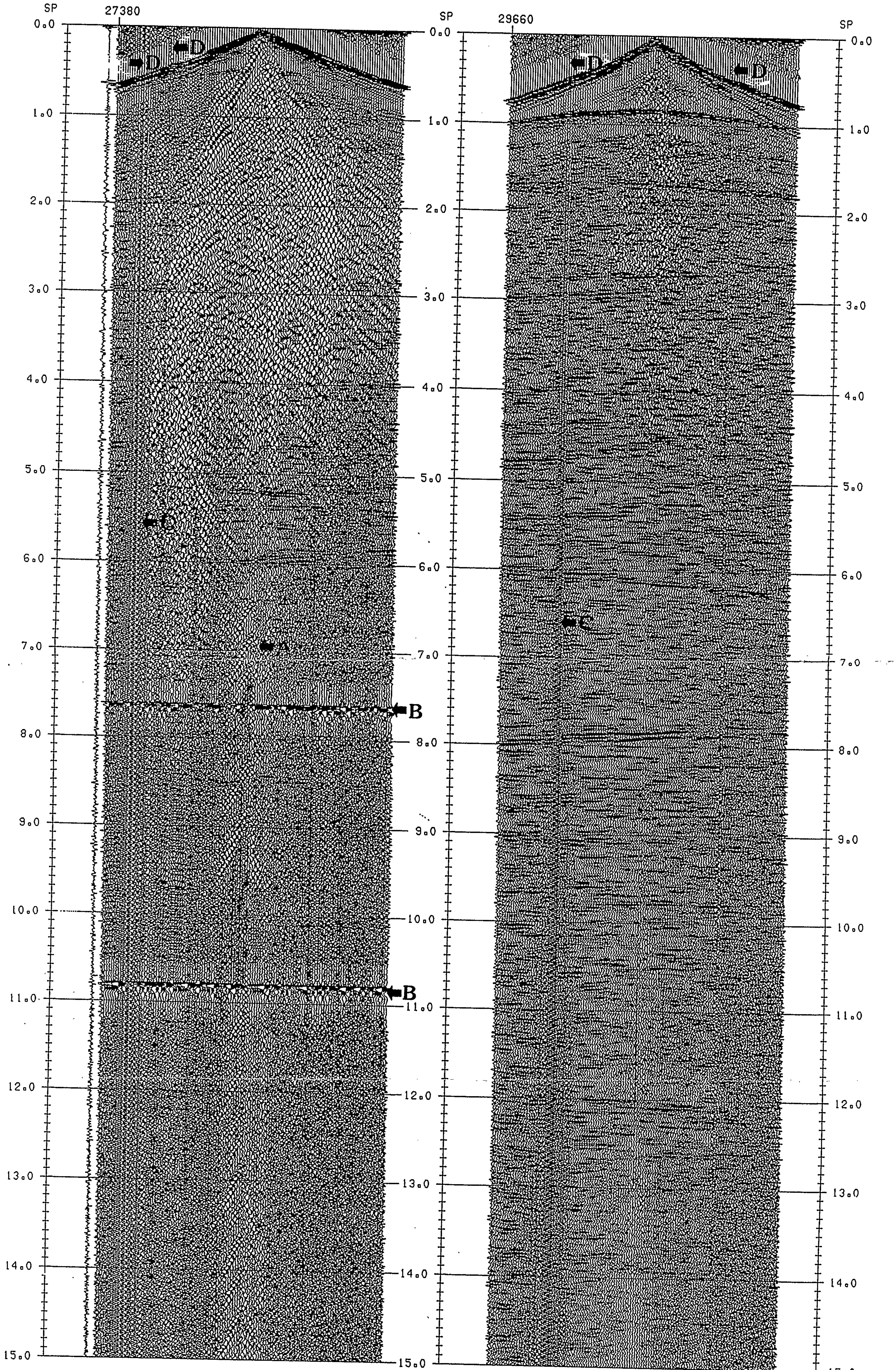

SP
27380
SP
29660
SP
D
D
D
D
C
C
A
B
B
0.0
1.0
2.0
3.0
4.0
5.0
6.0
7.0
8.0
9.0
10.0
11.0
12.0
13.0
14.0
15.0

First break picks for refraction statics were made and statics were then applied to the data but the result was not satisfactory. The shallow events were more continuous prior to the application of the refraction statics solution. The reason for this deterioration may have been the fact that the first breaks were not always well defined. Figure 3.6a illustrates a shot record with a well defined first break whereas Figure 3.6b illustrates a very poor, difficult to pick, first break. This may be due to ice cracking at the surface.

For velocity analyses "super common depth points" (CDPs) were created. Super CDPs are CDPs that consist of more than one CDP merged together. The reason for this was that limited disc space was available and the combining of CDPs to create one super CDP should generate better semblances than possible with only one. In this case, five CDPs were summed together every 100 CDPs and semblance plots were generated (Figures 3.7a and 3.7b). Figure 3.7a illustrates a plot of good semblances and Figure 3.7b shows a poor semblance plot (much smearing). Velocities were picked as shown in Figure 3.7c and the result of applying this velocity function is illustrated in Figure 3.7d, in which both the uncorrected and NMO corrected CDP gather is shown. As observed from the flattened events, the velocity function chosen was appropriate.

Figure 3.3

A screen image of the spread design of seismic line 52X from the ITA workstation. The numbers across the top represent shot locations. The middle dots represent receiver locations and outsidedots represent shot locations. The solid lines going through the shot illustrate the number of CDPs at that shot. At the bottom of the figure a graph is shown indicating the fold coverage of the data. On the right, shot depths and uphole times are given. Here the shot depth was always 20 m and the uphole times were always 10 ms.

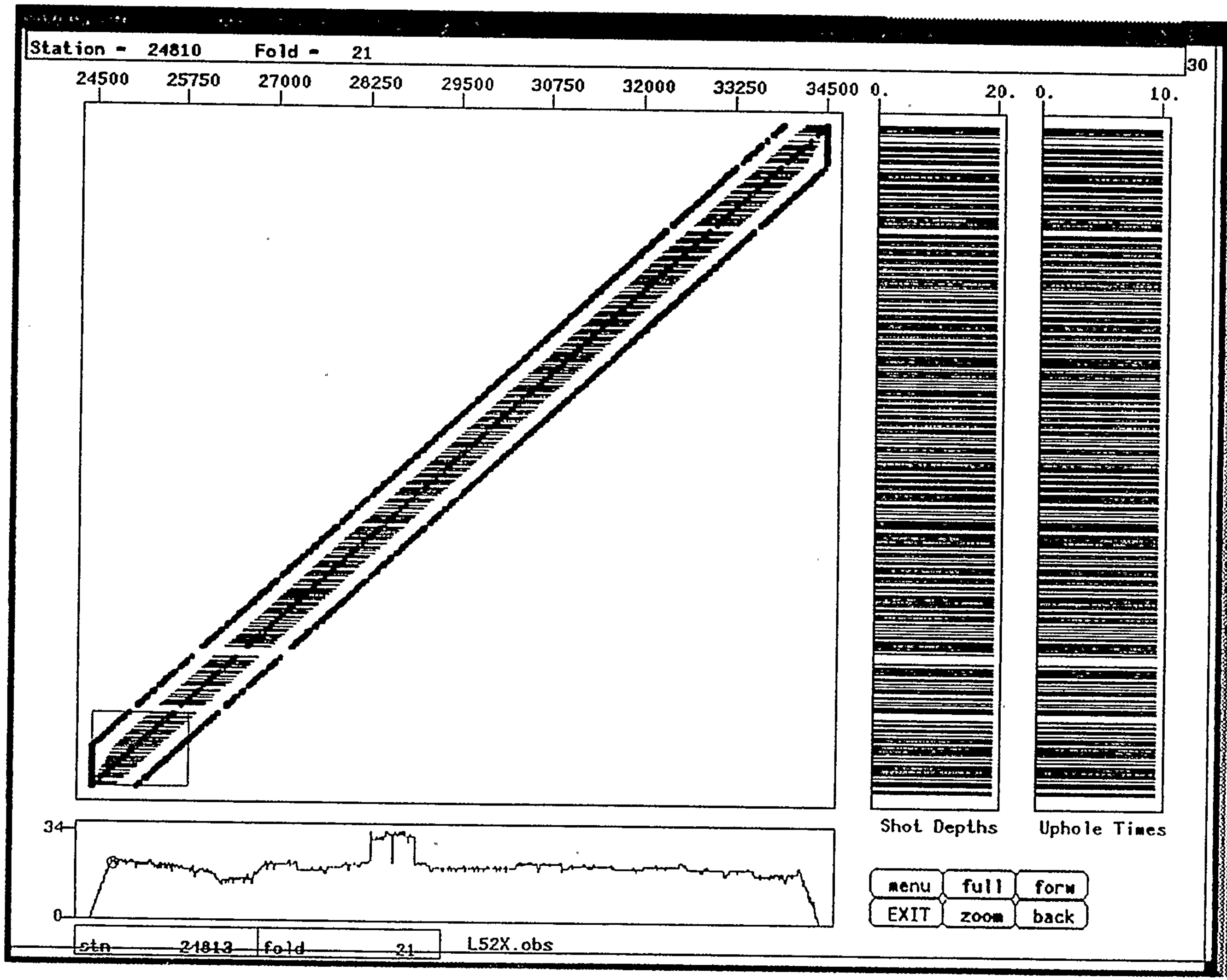
Station = 24810 Fold = 21
30
24500
25750
27000
28250
29500
30750
32000
33250
34500
0.
20.
0.
10.
34
0
Shot Depths
Uphole Times
menu
full
forw
EXIT
zoom
back
stn 24813
fold 21
L52X.obs

Figure 3.4

An enlargement of the area outlined by a box in the lower left hand corner of Figure 3.3 demonstrating the data during the rolling in stage of acquisition. Note the low fold coverage at the start of the line. Other features in this diagram are discribed in the figure caption for Figure 3.3.

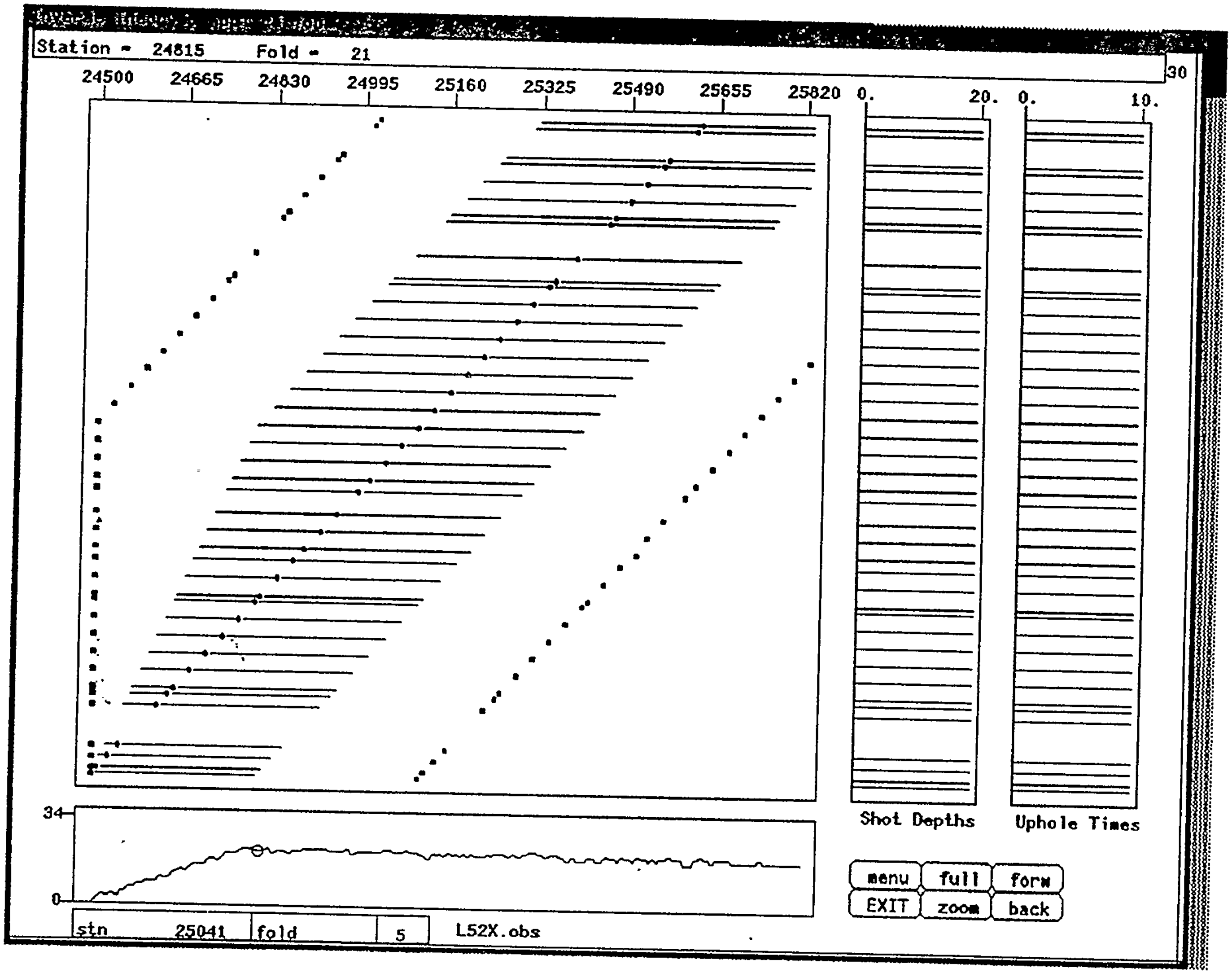
Station = 24815
Fold = 21
24500
24665
24830
24995
25160
25325
25490
25655
25820
0.
20.
0.
10.
30
34
0
Shot Depths
Uphole Times
menu
full
forw
EXIT
zoom
back
stn
25041
fold
5
L52X.obs

Figure 3.5

A screen image of a survey file showing the elevation along seismic line 52X from east to west. The top diagram is a cross-sectional view of the elevation, the bottom diagram is a plan view of line 52X. The numbers at the base are the easting coordinates for the seismic line.

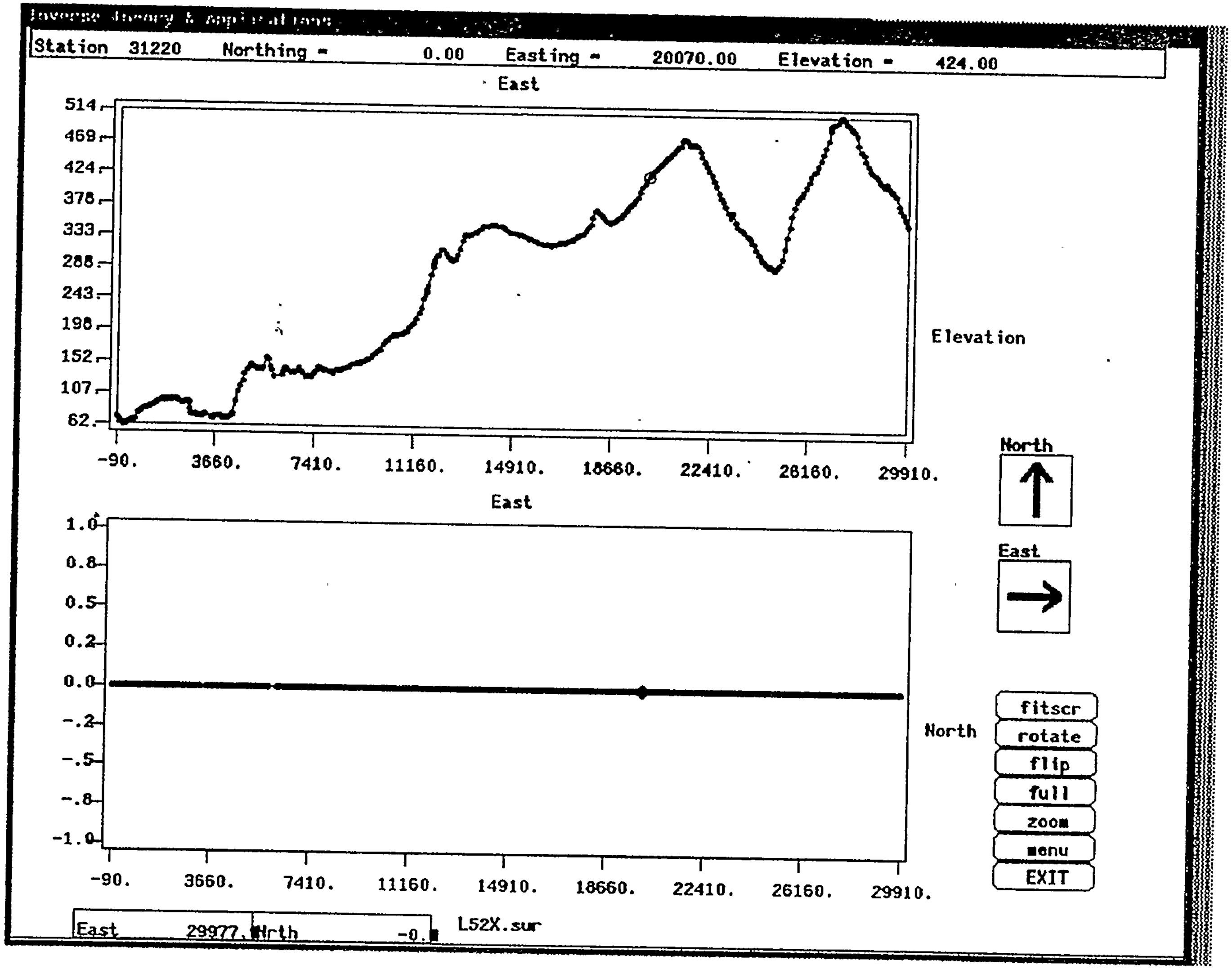
Station 31220 Northing = 0.00 Easting = 20070.00 Elevation = 424.00
East
514.
469.
424.
378.
333.
288.
243.
198.
152.
107.
62.
-90.
3660.
7410.
11160.
14910.
18660.
22410.
26160.
29910.
Elevation
East
1.0
0.8
0.5
0.2
0.0
-.2
-.5
-.8
-1.0
-90.
3660.
7410.
11160.
14910.
18660.
22410.
26160.
29910.
North
North
East
fitscr
rotate
flip
full
zoom
menu
EXIT
East 29977.
-0.
L52X.sur

Figure 3.6a and b

Plots of shot records from seismic line 52X to 2.0 seconds.

a) This shot record illustrates a well defined first break.

b) This shot record illustrates a poorly defined first break.

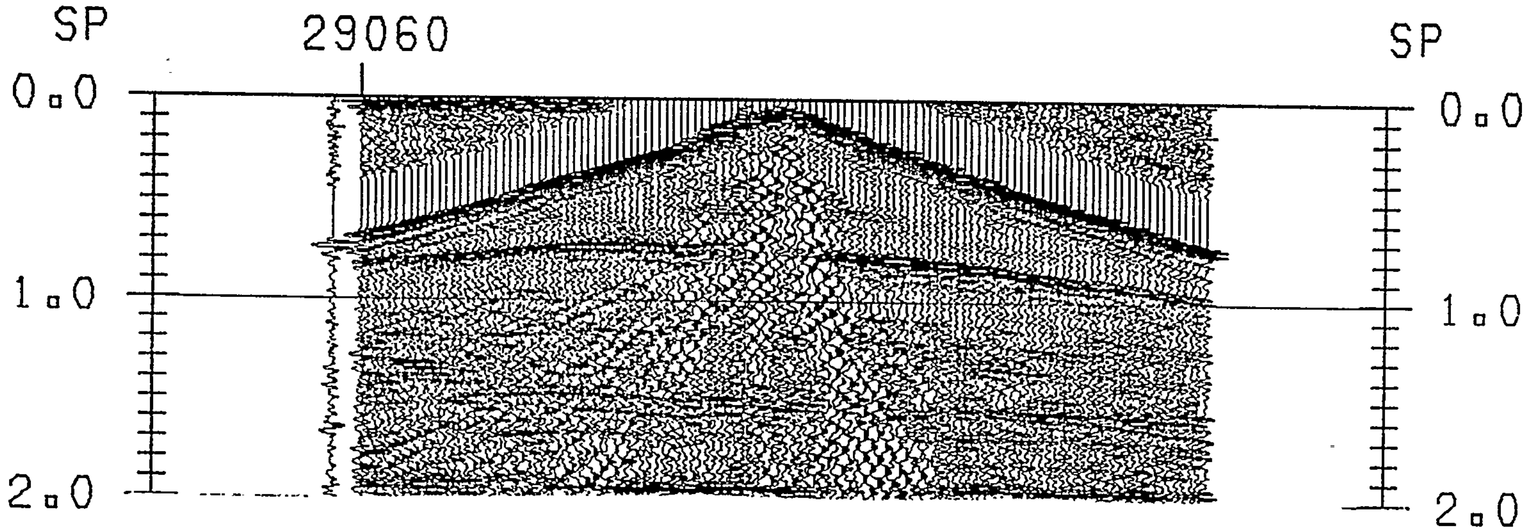
SP
29060
SP
0.0
1.0
2.0
0.0
1.0
2.0

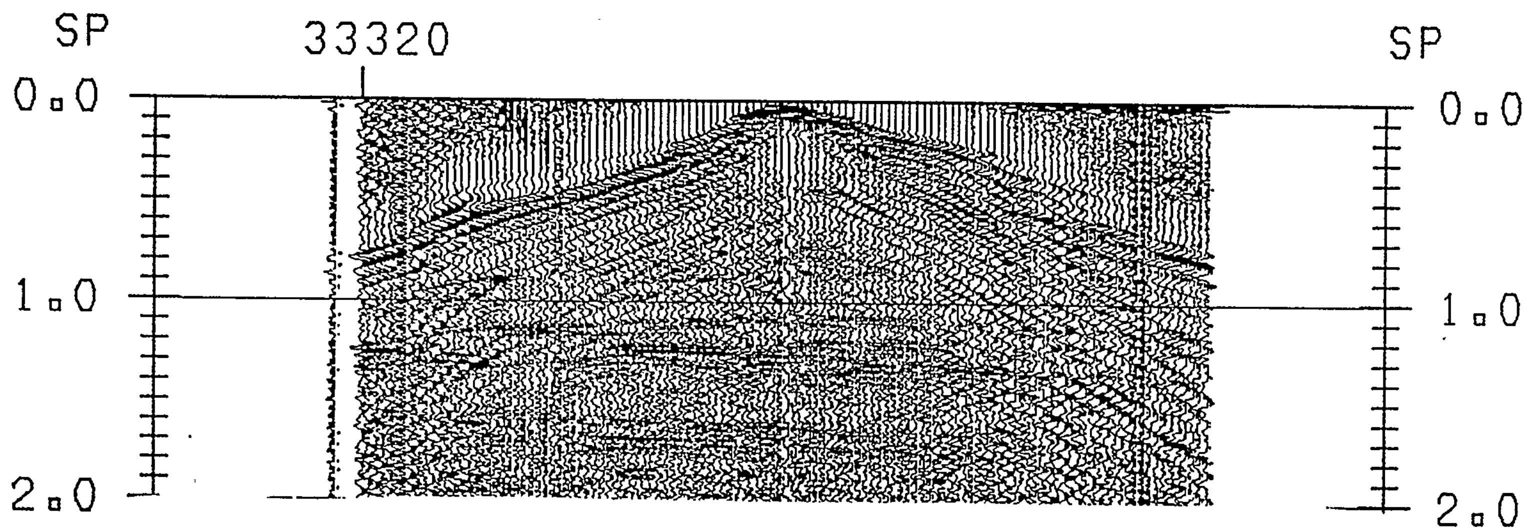
SP
33320
SP
0.0
1.0
2.0
0.0
1.0
2.0

Figure 3.7

Semblance Plots

a) Screen image of an example of a good semblance. On the left is the super CDP gather, next is the semblance plot. The lighter the shade encased by black observed on the semblance plot, the stronger the coherent event. Numbers across the top of the semblance are velocity numbers. At the far right, peaks on the graph represent locations in the data with the strongest coherent energy.

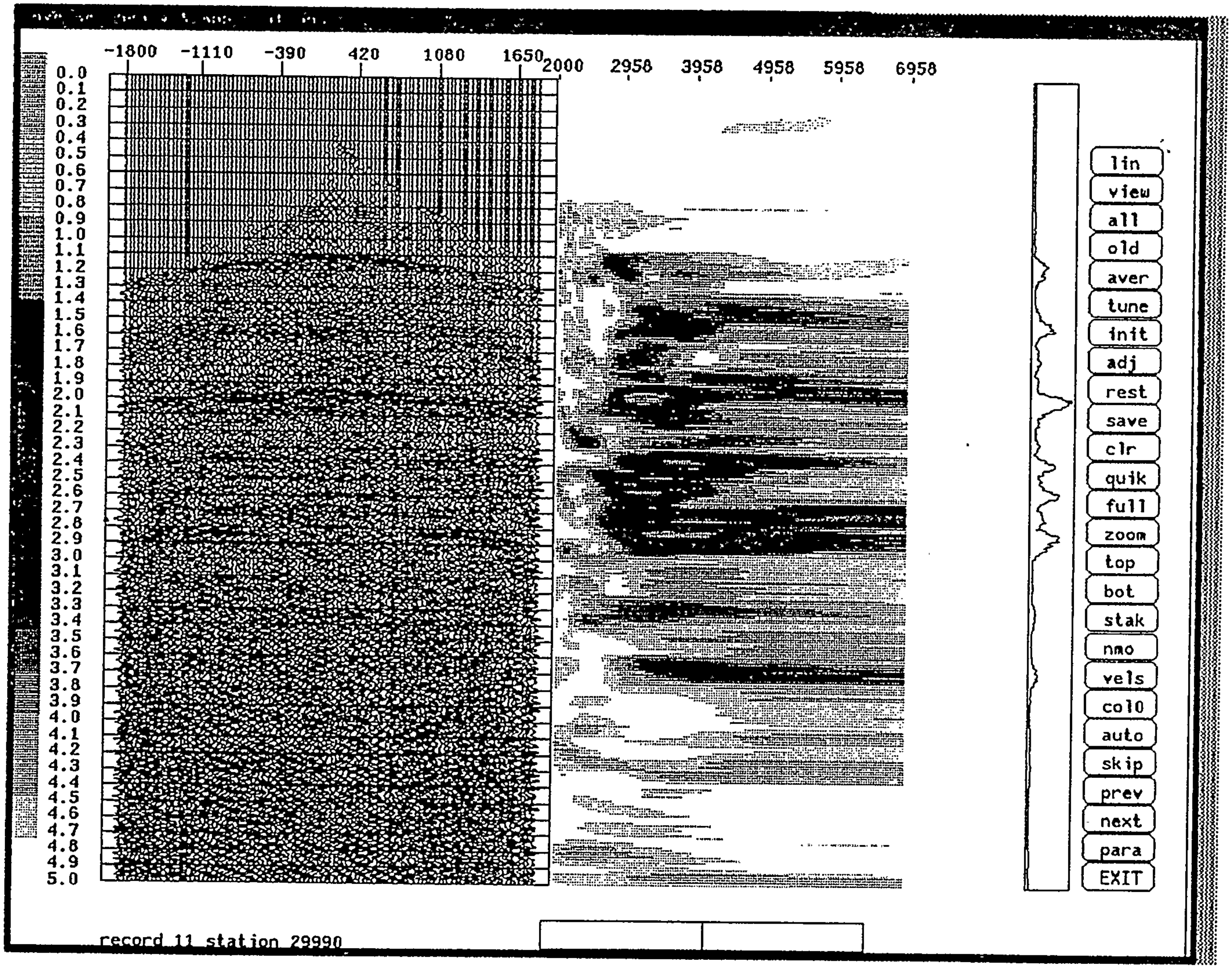
-1800 -1110 -390 420 1080 1650
2000 2958 3958 4958 5958 6958
0.0 0.1 0.2 0.3 0.4 0.5 0.6 0.7 0.8 0.9 1.0 1.1 1.2 1.3 1.4 1.5 1.6 1.7 1.8 1.9 2.0 2.1 2.2 2.3 2.4 2.5 2.6 2.7 2.8 2.9 3.0 3.1 3.2 3.3 3.4 3.5 3.6 3.7 3.8 3.9 4.0 4.1 4.2 4.3 4.4 4.5 4.6 4.7 4.8 4.9 5.0
lin
view
all
old
aver
tune
init
adj
rest
save
clr
quik
full
zoom
top
bot
stak
nmo
vels
col0
auto
skip
prev
next
para
EXIT
record 11 station 29990

Figure 3.7b

Screen image of an example of a poor semblance.

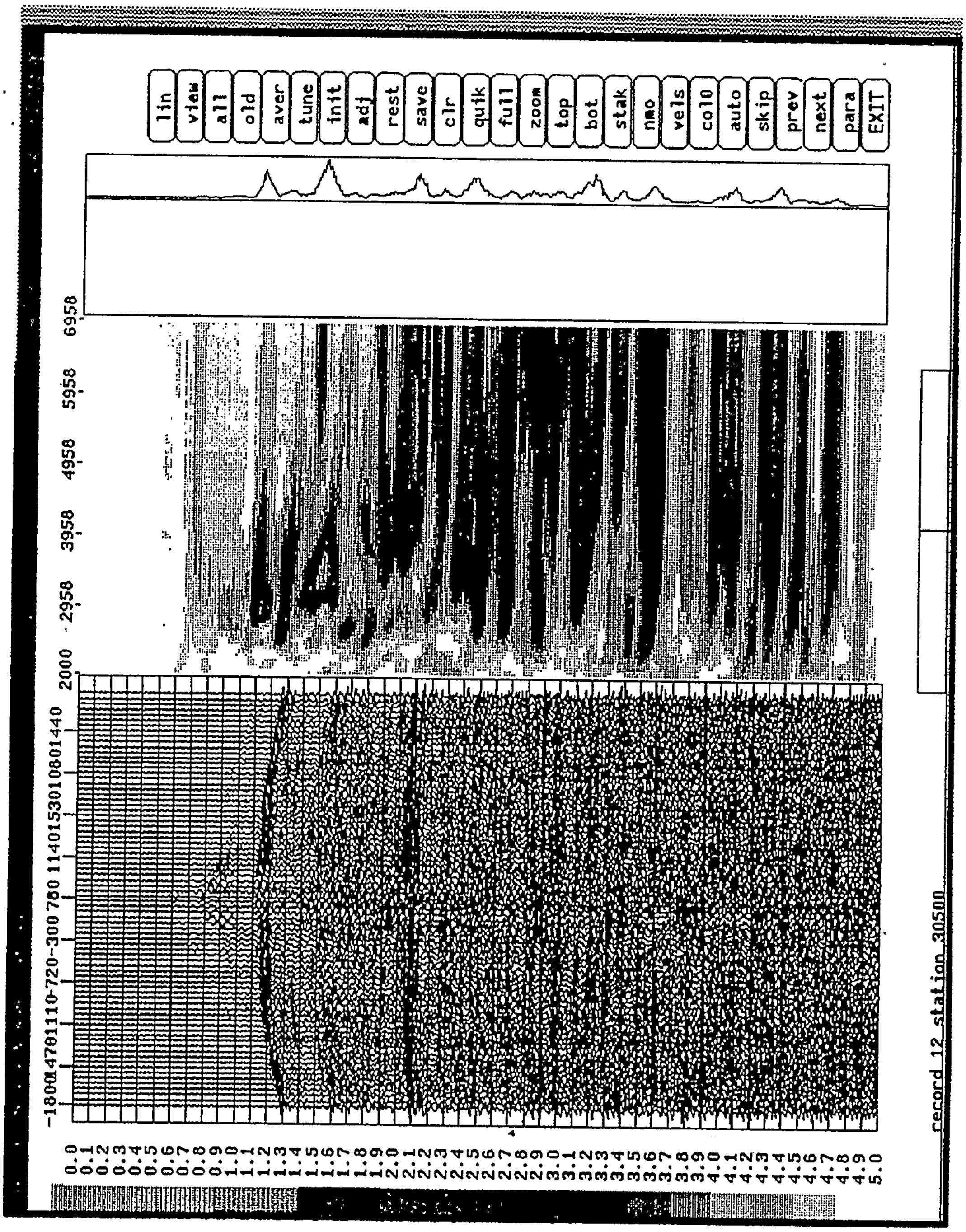
lin
view
all
old
aver
tune
init
adj
rest
save
clr
quik
full
zoom
top
bot
stak
nmo
vels
colo
auto
skip
prev
next
para
EXIT
2000
2958
3958
4958
5958
6958
record 12 station 30500

Figure 3.7c

Semblance plot illustrating how velocities are picked. The hyperbolic lines on the CDP gather indicates the event for which the velocity was picked. The line in the center of the semblance indicates the velocity function chosen increases in velocity with depth. Velocities range between 2000 m/s-5000 m/s and are noted at the top of the semblance plot. The blocky graph to the right illustrates interval velocities calculated for each interval picked on the semblance.

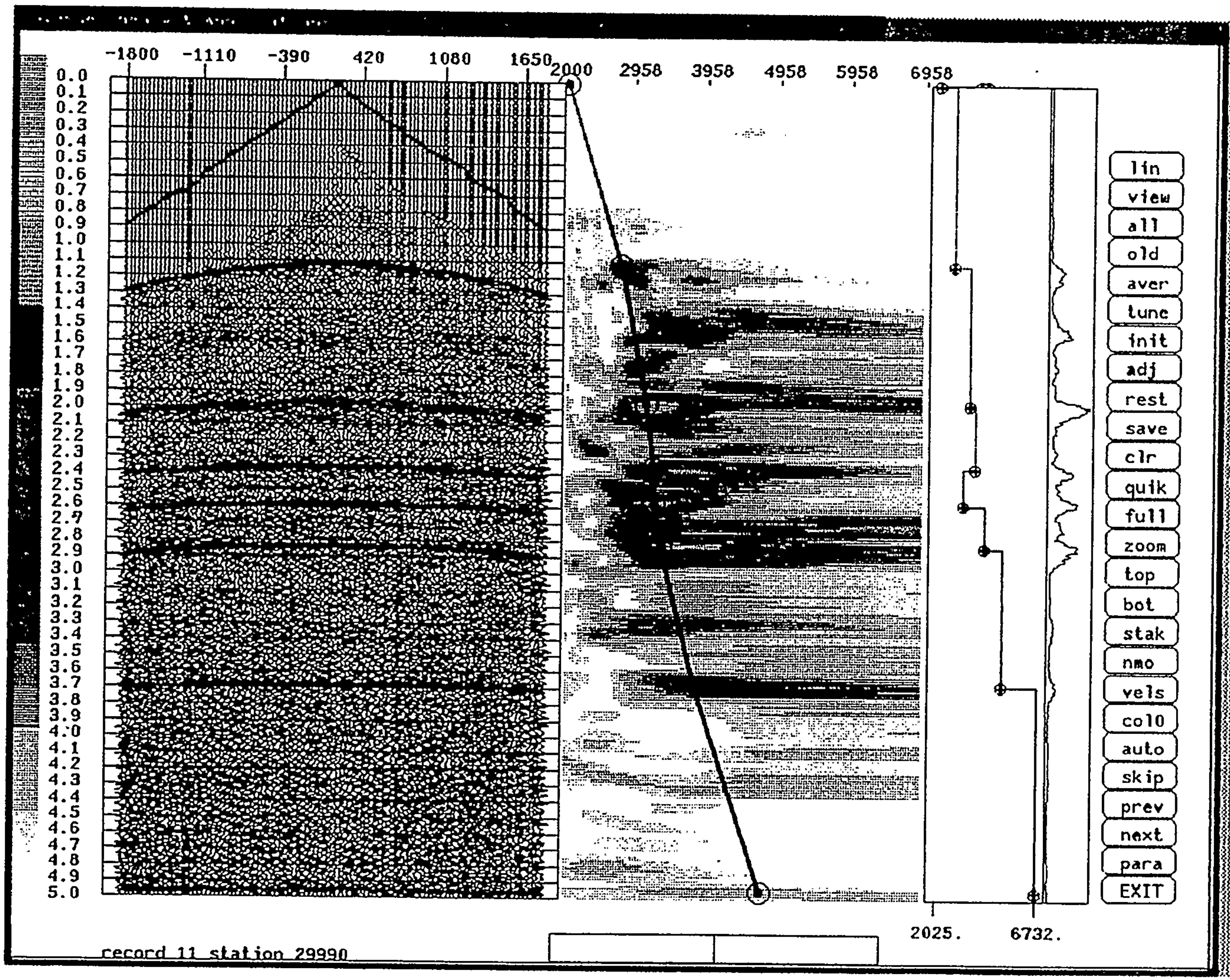
-1800 -1110 -390 420 1080 1650
2000 2958 3958 4958 5958 6958
0.0 0.1 0.2 0.3 0.4 0.5 0.6 0.7 0.8 0.9 1.0 1.1 1.2 1.3 1.4 1.5 1.6 1.7 1.8 1.9 2.0 2.1 2.2 2.3 2.4 2.5 2.6 2.7 2.8 2.9 3.0 3.1 3.2 3.3 3.4 3.5 3.6 3.7 3.8 3.9 4.0 4.1 4.2 4.3 4.4 4.5 4.6 4.7 4.8 4.9 5.0
2025.
6732.
lin
view
all
old
aver
tune
init
adj
rest
save
clr
quik
full
zoom
top
bot
stak
nmo
vels
col0
auto
skip
prev
next
para
EXIT
record 11 station 29990

Figure 3.7d

The resulting NMO corrected gather (on the right) from the velocities picked in Figure 3.7c plus the uncorrected gather (on the left) for comparison. Notice on the NMO corrected gather reflectors are flattened thus the velocity function chosen was appropriate.

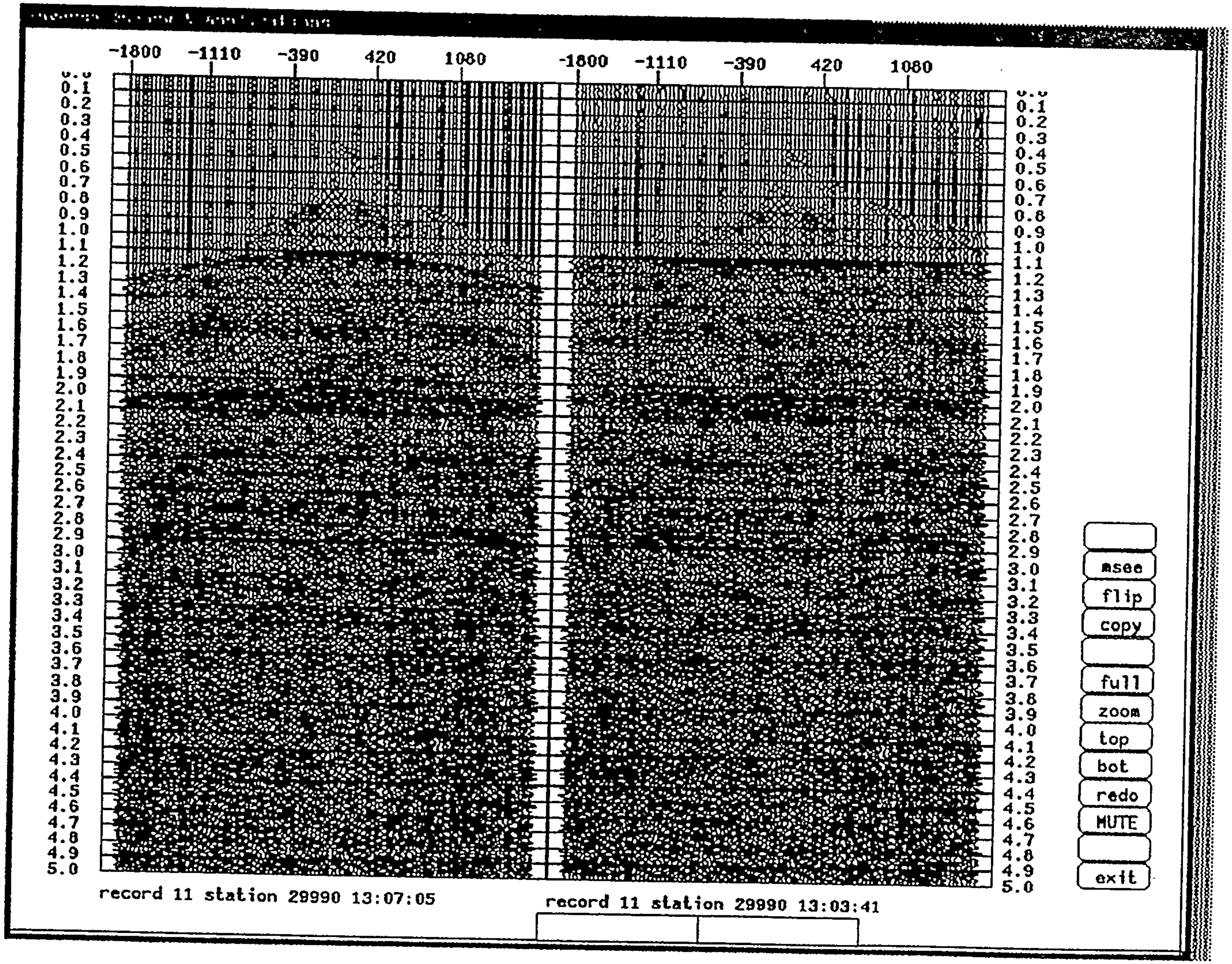
-1800 -1110 -390 420 1080
-1800 -1110 -390 420 1080
0.1 0.2 0.3 0.4 0.5 0.6 0.7 0.8 0.9 1.0 1.1 1.2 1.3 1.4 1.5 1.6 1.7 1.8 1.9 2.0 2.1 2.2 2.3 2.4 2.5 2.6 2.7 2.8 2.9 3.0 3.1 3.2 3.3 3.4 3.5 3.6 3.7 3.8 3.9 4.0 4.1 4.2 4.3 4.4 4.5 4.6 4.7 4.8 4.9 5.0
msee
flip
copy
full
zoom
top
bot
redo
MUTE
exit
record 11 station 29990 13:07:05
record 11 station 29990 13:03:41

The frequency content of the data was analysed for application of a good filter. This was done by plotting frequency panels and by plotting the Fourier spectra. Figure 3.8 is a plot of the spectra for traces 21 and 61 of a record taken from seismic line 52X after automatic gain control (AGC) has been applied. The frequency filter selected for the data was a bandpass filter having a low cutoff at 12/15 and a high cutoff at 65/75.

There appears to be a problem with multiples with the 52X seismic line in the lower portion of the data (8.0 to 15.0 sec), therefore, predictive deconvolution was applied to try and remove the multiples. This was attempted by applying a deconvolution with a small operator length so that the result would tend to suppress short period multiples. This worked (Figure 3.9 a-d) but the difference before and after the application of the deconvolution was so little it was not used. Figure 3.10a and b are the final stack and the coherency filter of line 52X, respectively.

Coherency/Semblance Filtering

One of the main objectives of processing deep crustal seismic data is the identification and correlation of coherent events. As these events are often coherent only over short distances, local coherency is more relevant than global continuity. A relatively new technique for event detection has been proposed by Kong et al. (1985). This uses local semblances, derived from a slant-stack approach, which are used to calculate coherency. When applied to the stack data, this technique enhances local coherent events and suppresses incoherent random noise. The degree of noise suppression can be

Figure 3.8

Fourier spectra for a shot record from seismic line 52X. This diagram indicates the frequency content of the data. This is determined by picking out the frequency span with highest amplitude (above that of the background noise. In this case the frequency span encompasses the area where the amplitude is between 0 and -40 DB.

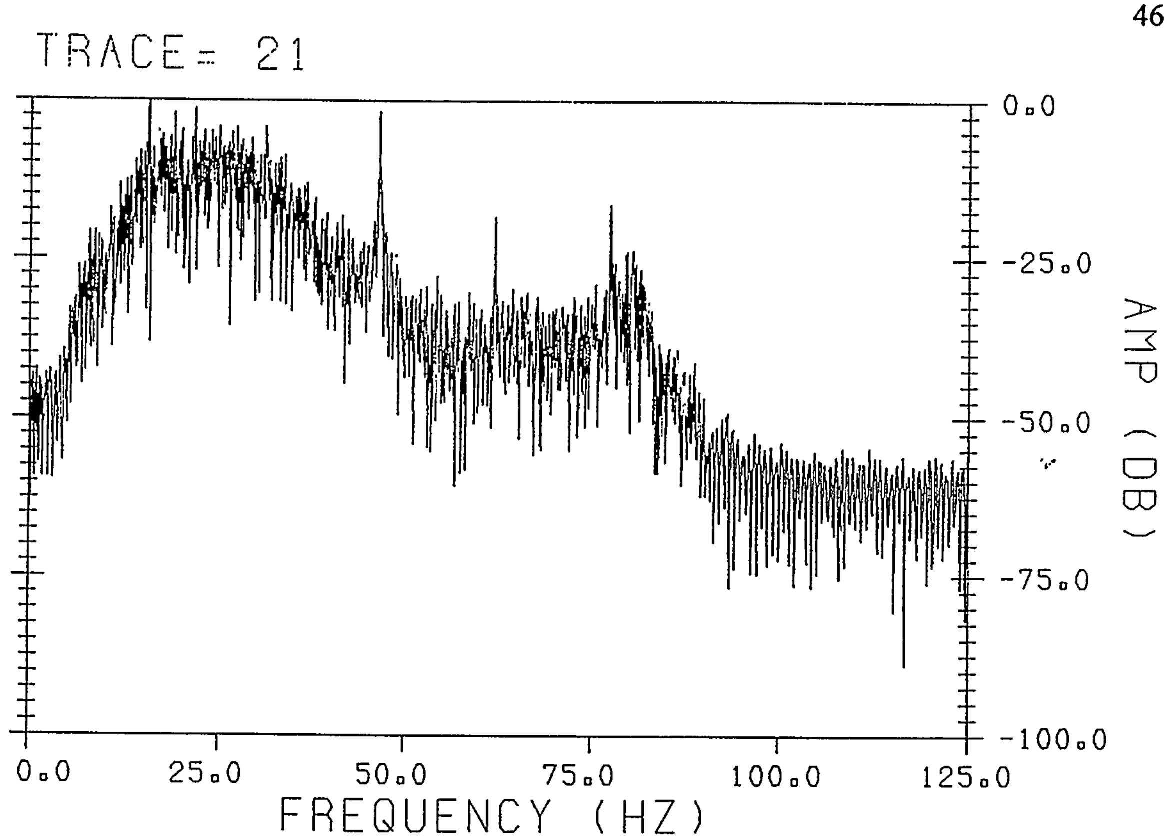
TRACE= 21
0.0
-25.0
-50.0
-75.0
-100.0
AMP (DB)
0.0
25.0
50.0
75.0
100.0
125.0
FREQUENCY (HZ)

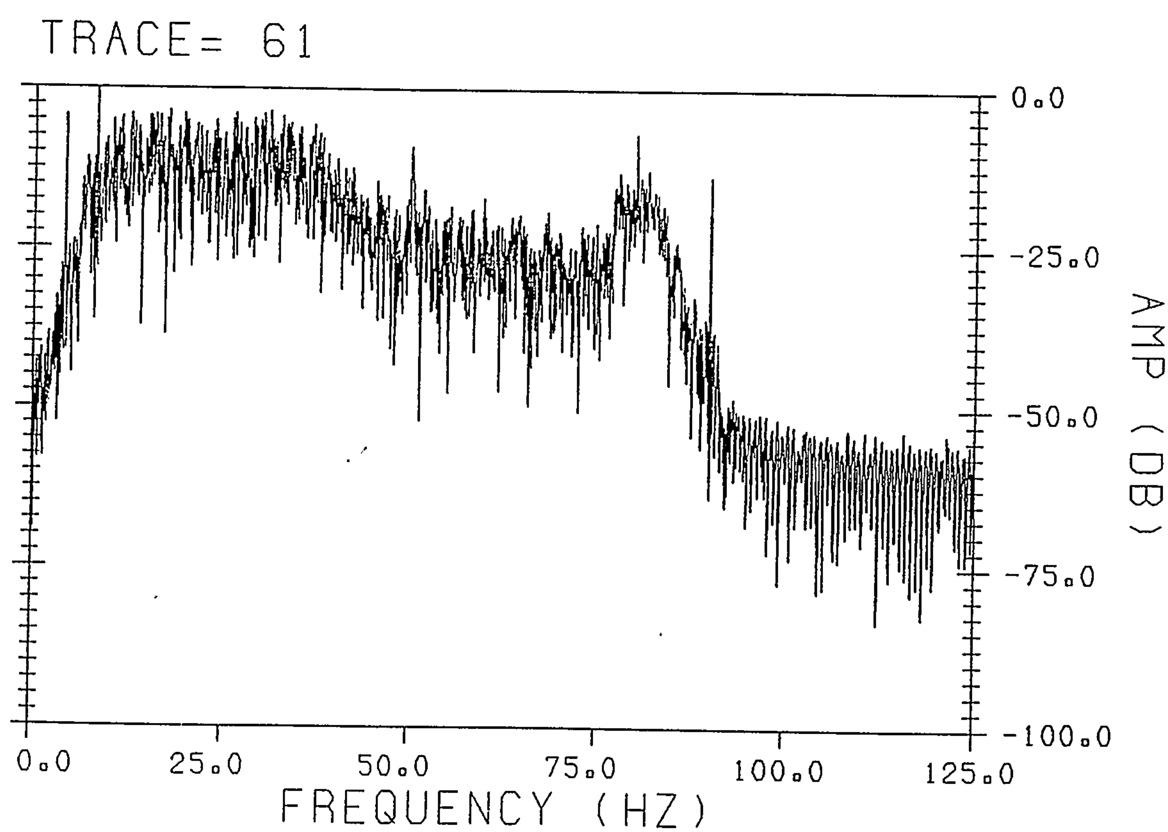
TRACE= 61
0.0
-25.0
-50.0
-75.0
-100.0
AMP (DB)
0.0
25.0
50.0
75.0
100.0
125.0
FREQUENCY (HZ)

Figure 3.9

Deconvolution example

a) Plot of the stack for line 52X prior to the application of deconvolution.

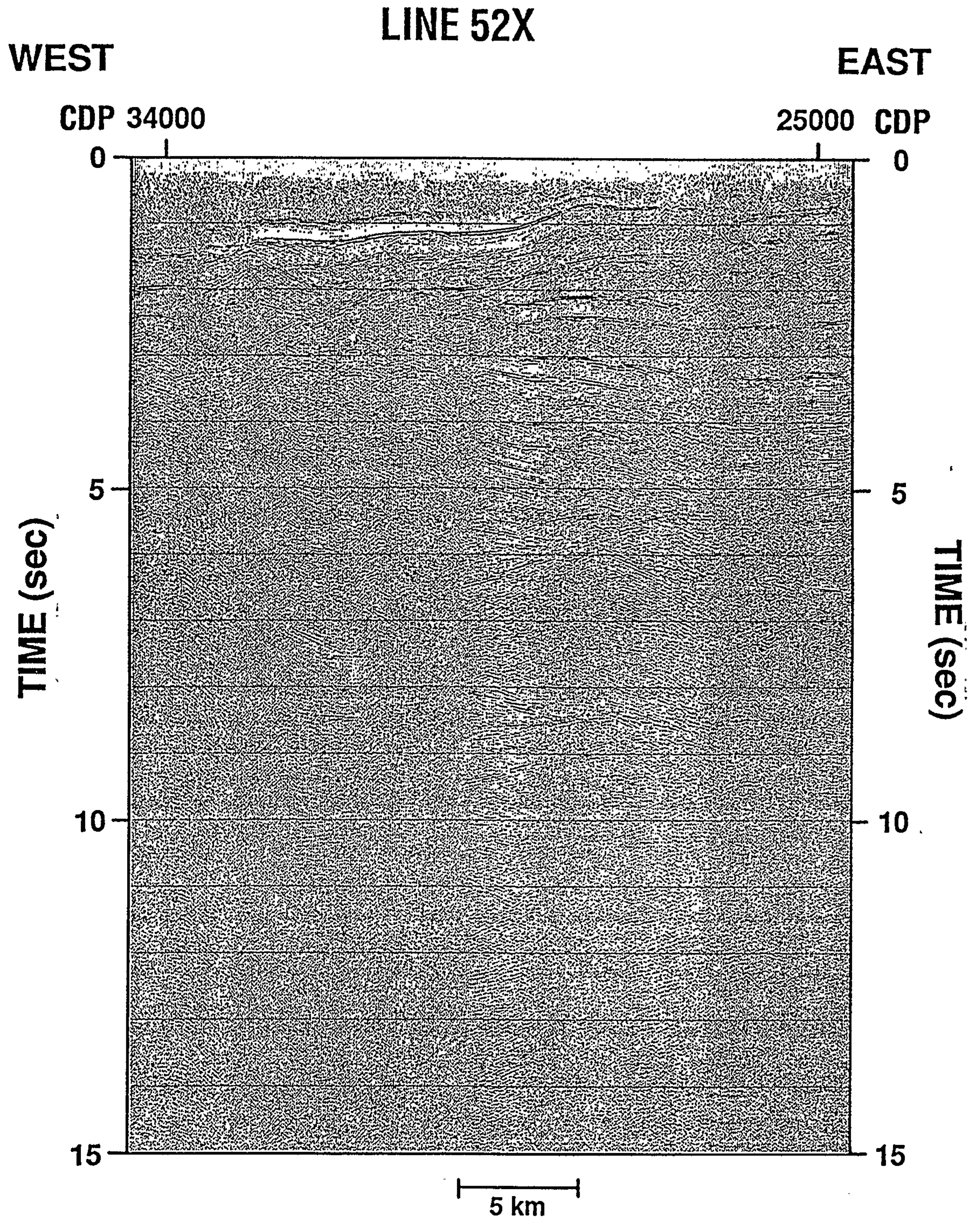

LINE 52X
WEST
EAST
CDP 34000
25000 CDP
0
5
10
15
TIME (sec)
5 km

Figure 3.9b

Plot of the autocorrelation of the original stack for line 52X.

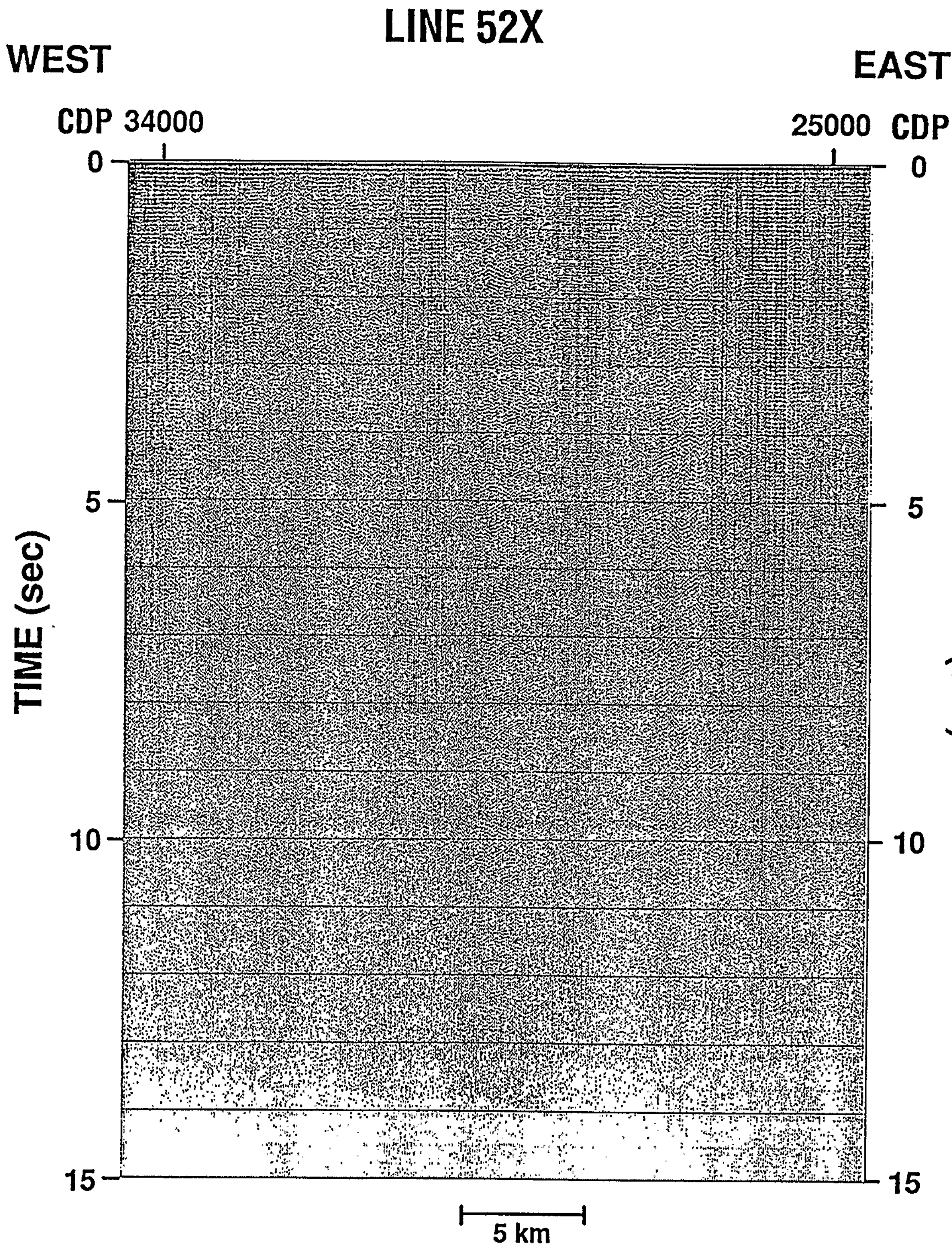
LINE 52X
WEST
EAST
CDP 34000
25000 CDP
0
5
10
15
TIME (sec)
5 km

Figure 3.9c

Plot of the autocorrelation of the 52X stack after deconvolution was applied.

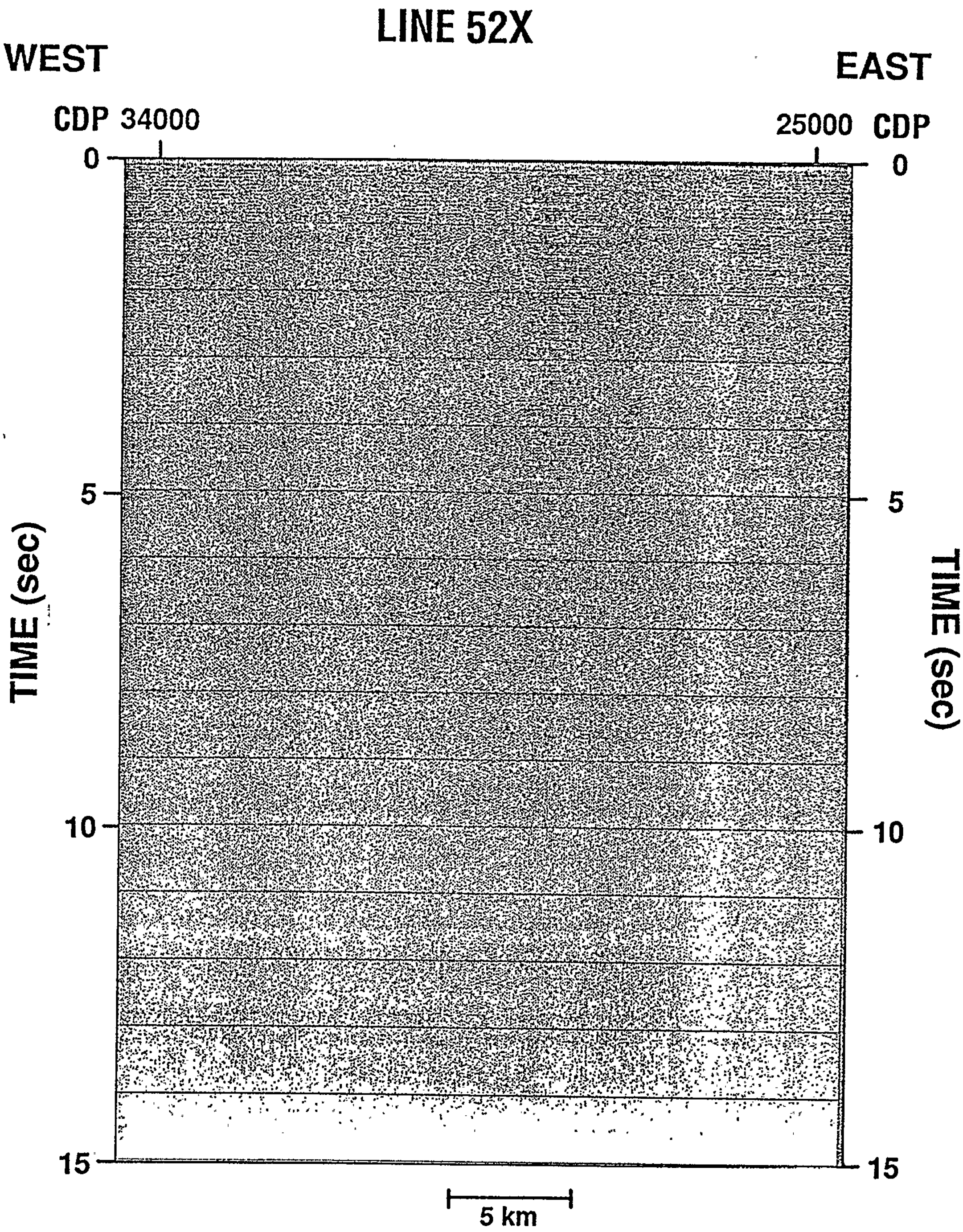
LINE 52X
WEST
EAST
CDP 34000
25000 CDP
0
5
10
15
TIME (sec)
0
5
10
15
TIME (sec)
5 km

Figure 3.9d

Resulting stack after predictive deconvolution was applied.

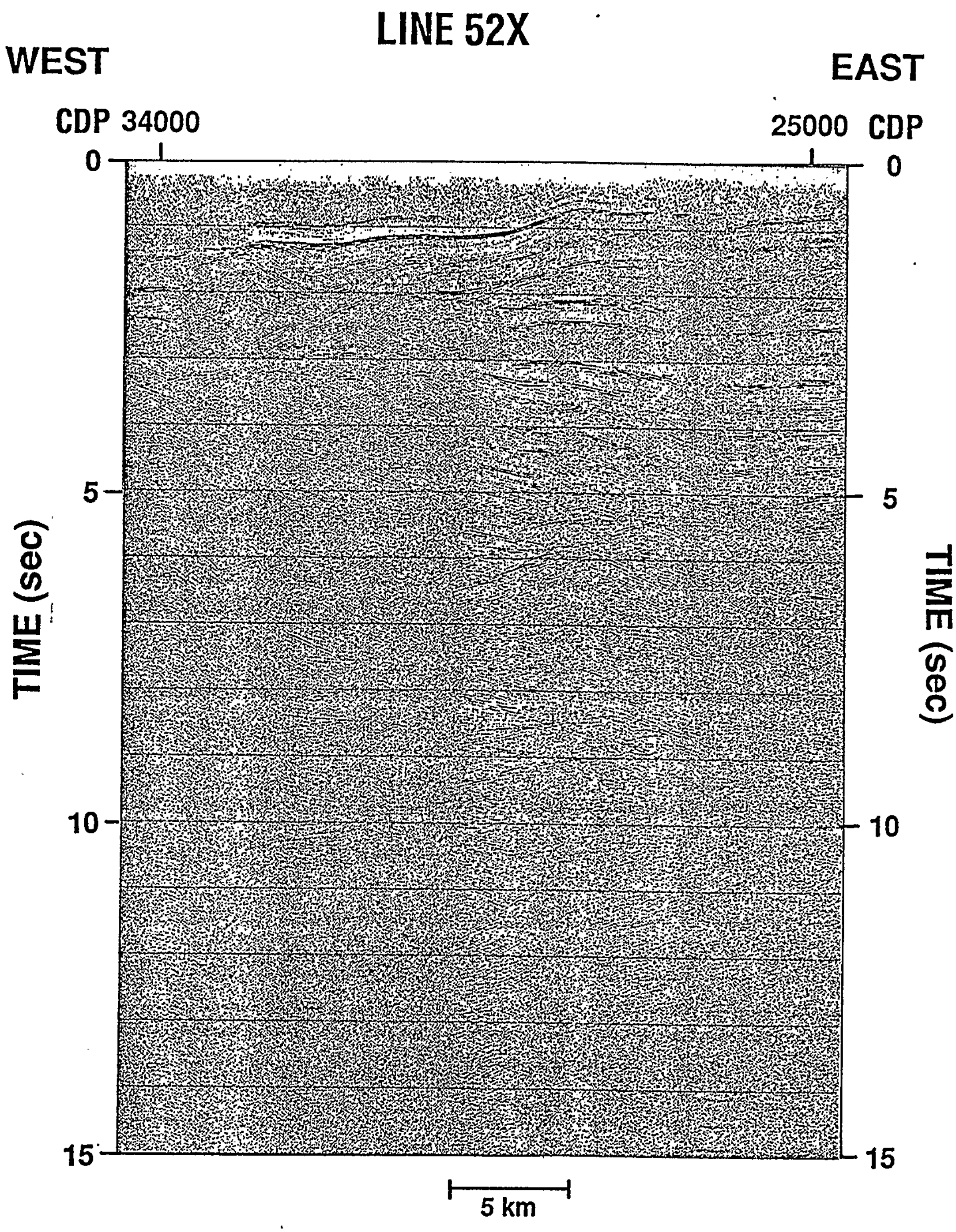
LINE 52X
WEST
EAST
CDP 34000
25000 CDP
0
5
10
15
0
5
10
15
TIME (sec)
TIME (sec)
5 km

Figure 3.10

An example of :

a) the stack for line 52X and

b) coherency filter of the stack.

Above each is a plot of the total residual receiver and shot statics, the CDP elevation and the fold.

Line 52X

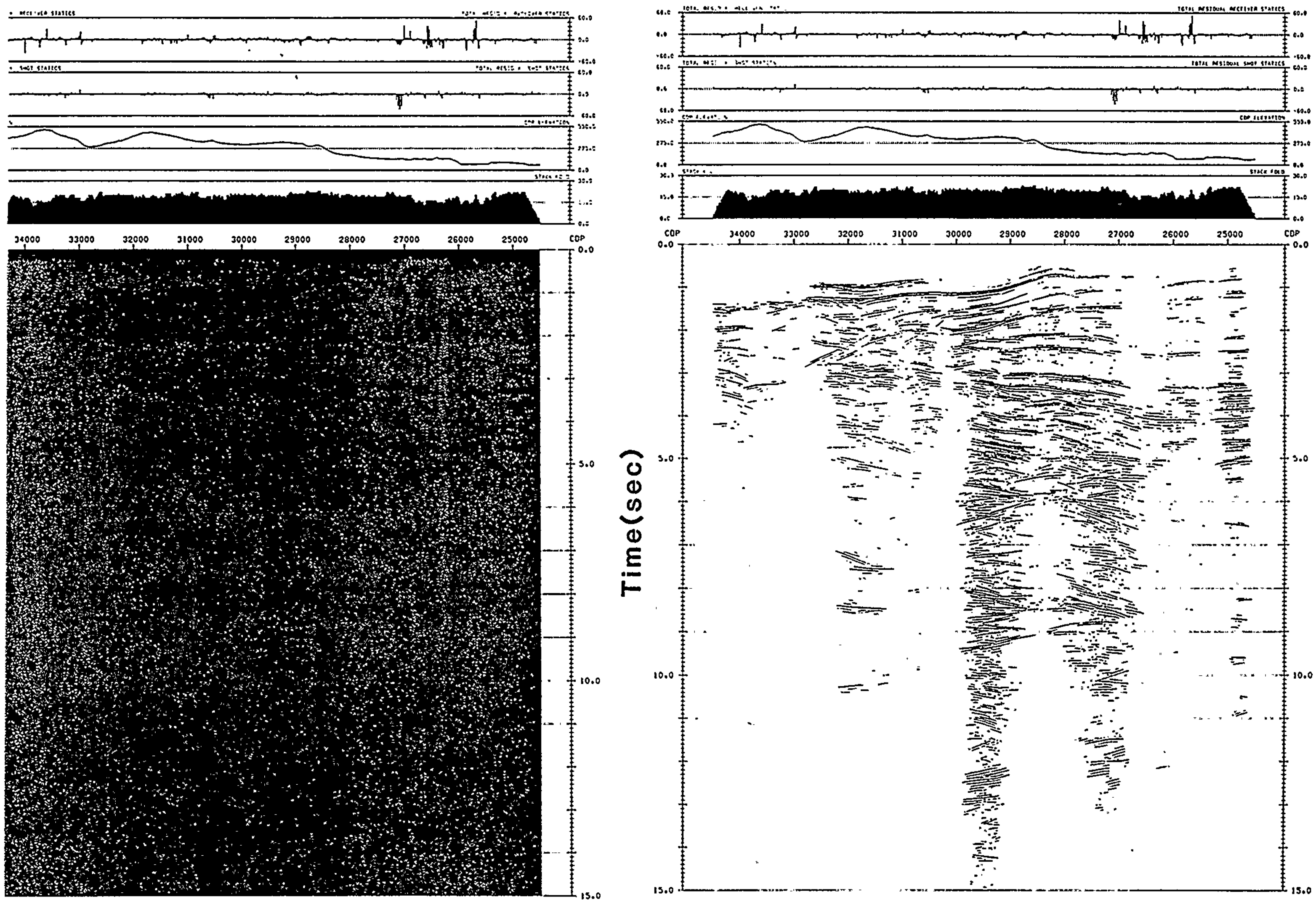
Time(sec)
CDP
34000
33000
32000
31000
30000
29000
28000
27000
26000
25000
0.0
5.0
10.0
15.0

controlled by the user, through a series of parameters, including semblance exponent, bias, slope and window length.

The essential steps of the algorithm are : 1) compute local semblances using a stant-stack method, 2) compute a coherency using the semblances and multiply the input data by the coherency. The result of this process is a semblance value for each dip at each input data point. These coherency filtered results are used in chapter 5 in the data description and interpretation sections as lines 52X, 64X and 26X (Figures 5.1-5.3).

Migration

Time migrations were completed on seismic reflection lines 52X, 64X, and 26X (Figures 3.11-3.13). The migration used was a phase shift migration which took into account vertical change in velocity and frequency. This served to migrate the steep, west-dipping reflector deep within the seismic sections but did little to otherwise flat to gently dipping data. The steep event in question migrated to the east approximately 6 km, 8 km, and 12 km for lines 52X, 64X, and 26X, respectively. On line 26X, the east-dipping thick package of reflections which appears to merge with the west-dipping event on the unmigrated data, now appears to flatten and then follow the trend of the west-dipping event (Figure 3.13).

Figure 3.11

Time migration for seismic line 52X.

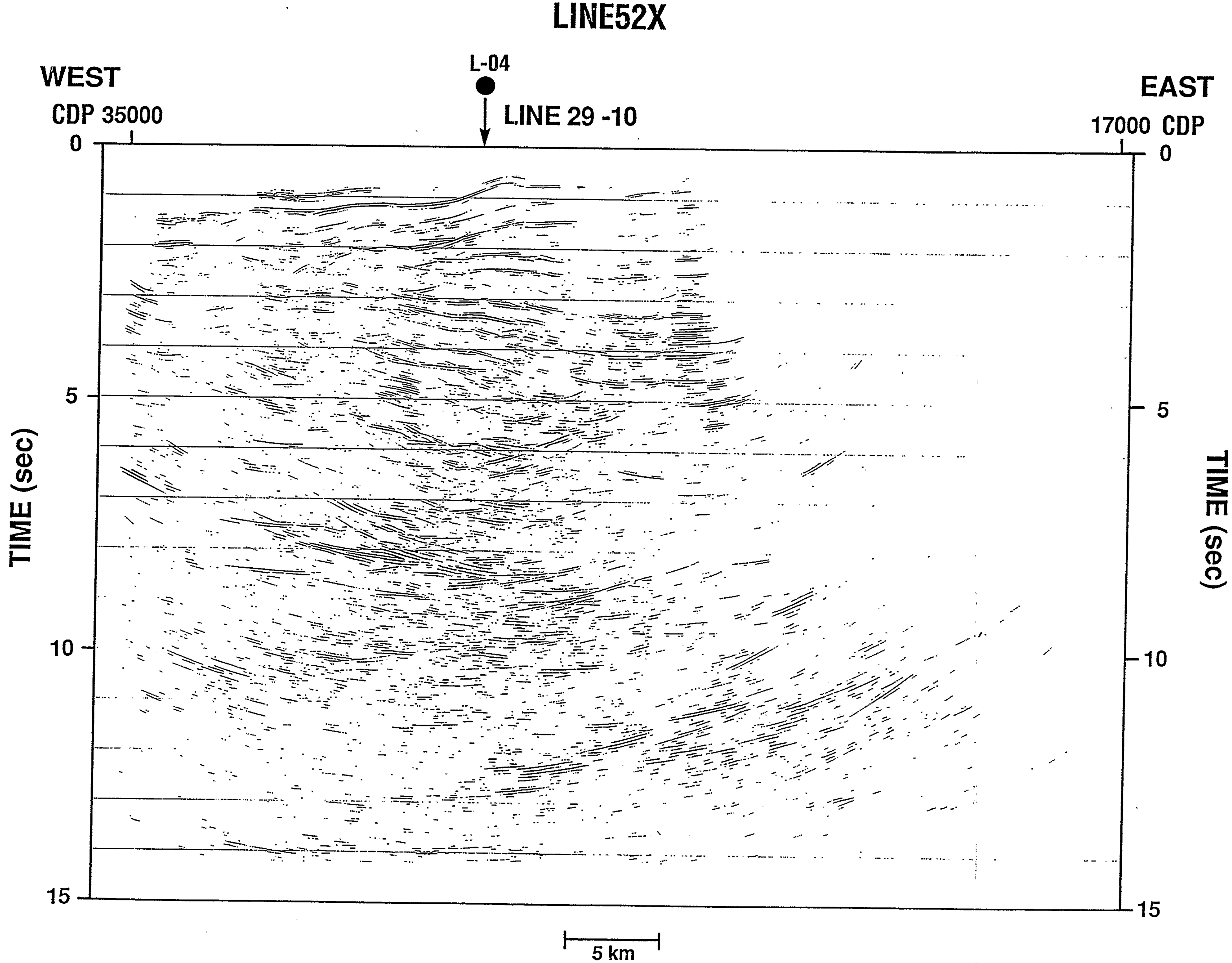
LINE52X
WEST
L-04
LINE 29 -10
EAST
CDP 35000
17000 CDP
0
5
10
15
TIME (sec)
TIME (sec)
5 km

Figure 3.12

Time migration for seismic line 64X.

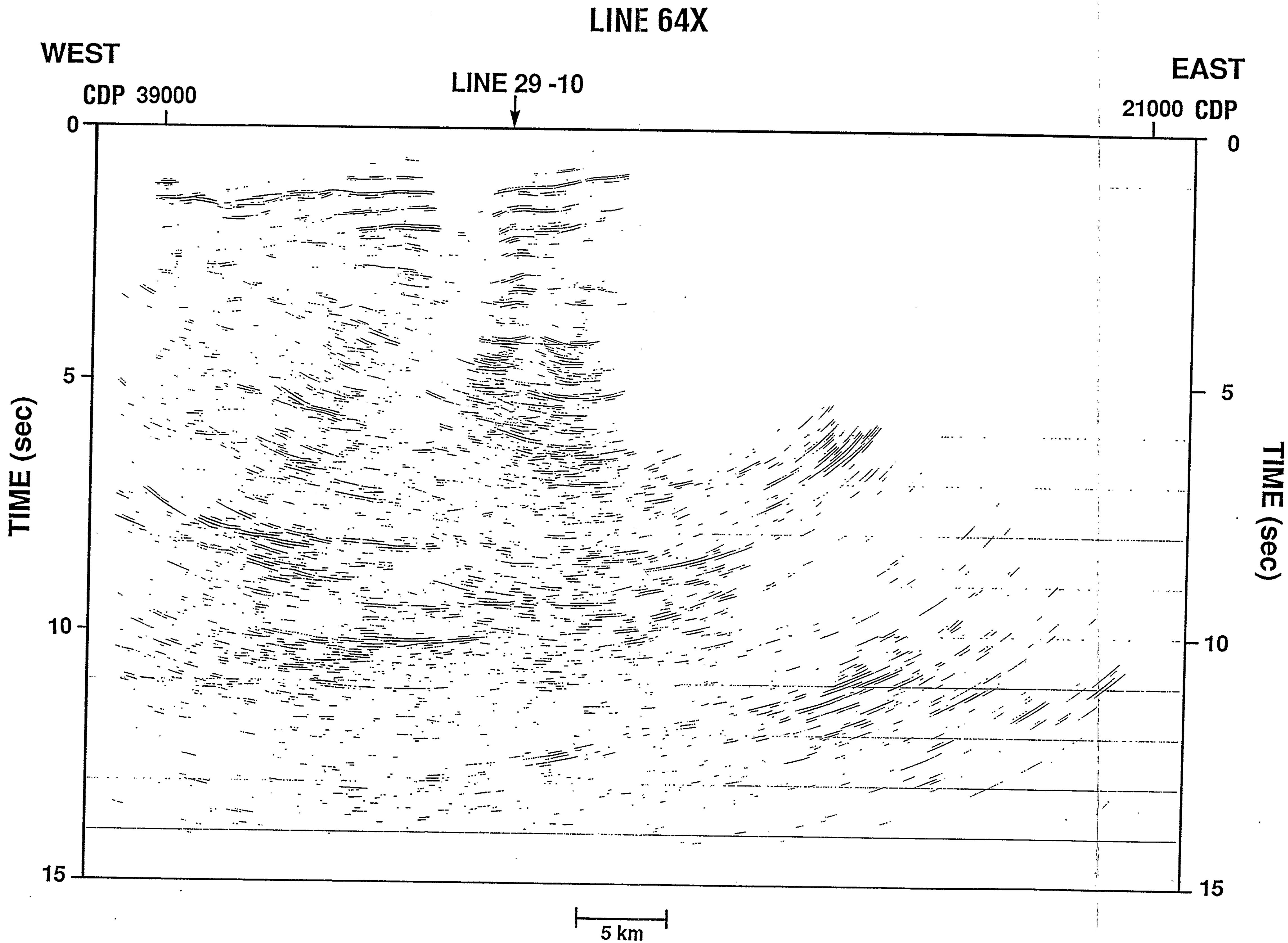

LINE 64X
WEST
EAST
LINE 29 -10
CDP 39000
21000 CDP
0
5
10
15
TIME (sec)
0
5
10
15
TIME (sec)
5 km

Figure 3.13

Time migration for seismic line 26X.

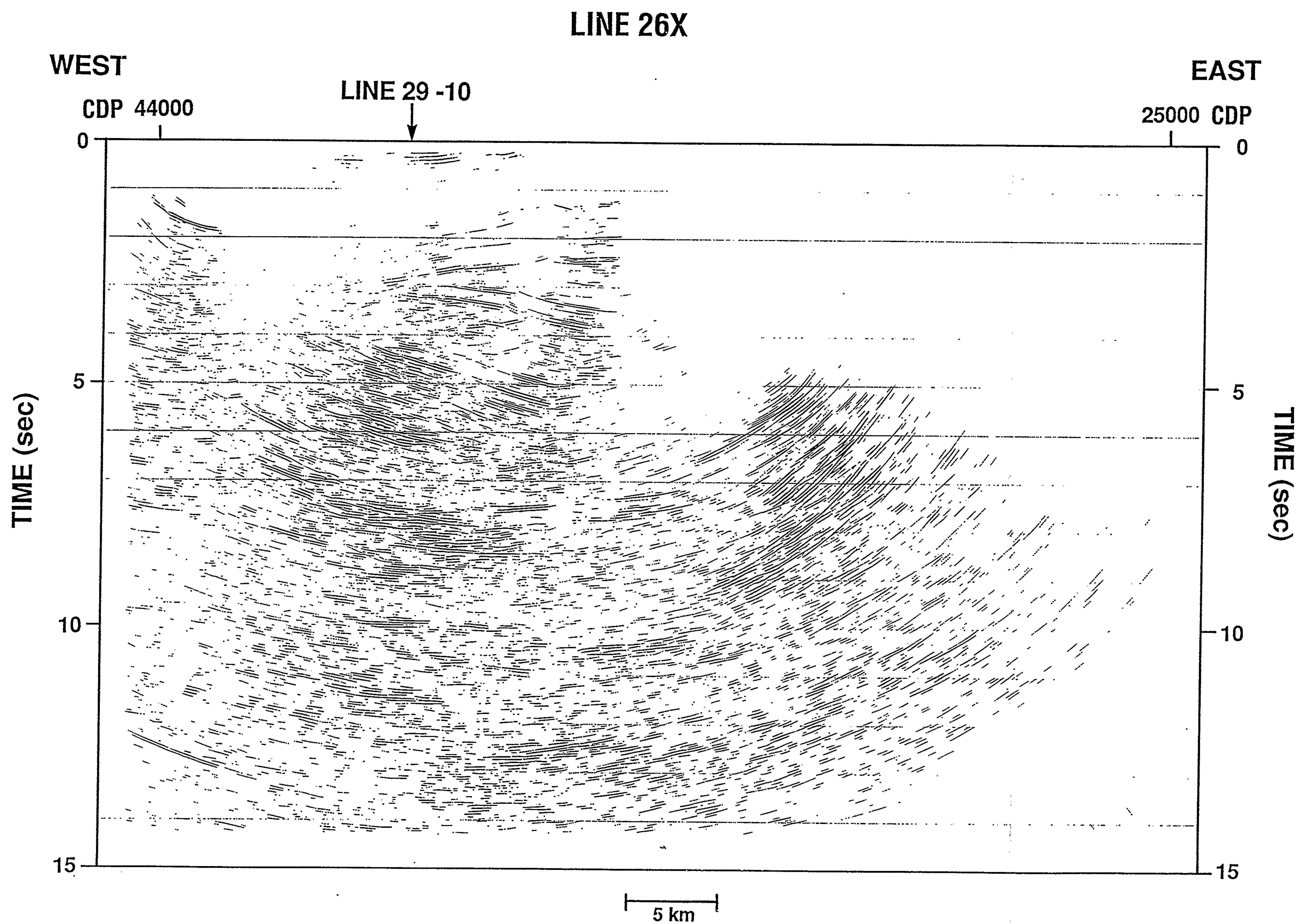
LINE 26X
WEST
EAST
LINE 29 -10
CDP 44000
25000 CDP
0
5
10
15
TIME (sec)
5 km

CHAPTER 4 : POTENTIAL FIELD DATA

Introduction

Potential field anomalies reveal patterns that can be correlated to some subsurface structures. Regional Bouguer gravity and residual aeromagnetic maps (Figures 4.1 and 4.2) illustrate the different anomalies characteristic of the Canadian Shield and the Cordillera. On the east, a series of northeast - southwest trending gravity and magnetic anomalies between Great Slave Lake shear zone and the U.S. border are related to the rocks of the Canadian Shield. On the west, a series of northwest-southeast trending anomalies characterize Cordilleran structures. Two major gravity and magnetic anomalies north of the Great Slave Lake shear zone (GSLsz), the Great Bear Batholith (GBB) and the Fort Simpson anomalies (FSa), exhibit north-south trends. These anomalies, as well as the northeast - southwest ones characterizing the shield rocks, are overprinted by the later anomalies related to the Cordillera at the position marked X on the gravity map (Figure 4.1).

Rocks that may be responsible for the high magnetic response of the Fort Simpson anomaly have been drilled near 60° north. Crystalline rocks that have dates of approximately 1.85 Ga (Villeneuve et al., 1991) were encountered below flat lying Paleozoic rocks and have since been interpreted to be the cause of the Fort Simpson magnetic anomalies (Cook et al., 1992).

A major north-south trending gravity gradient (GG, Figure 4.1), is parallel but somewhat west of the Fort Simpson magnetic anomaly. This feature marks the transition

Figure 4.1

Regional bouguer map of western Canada and the Northwestern U.S. (Geological Society of America, 1987a; Map modified from Cook et al., 1991). The dark shades represent low gravity values and the light shades represent high gravity values; contour interval is 5 mGals. The front of the Cordillera is shown as the line with the teeth on the west.

BOUGUER GRAVITY

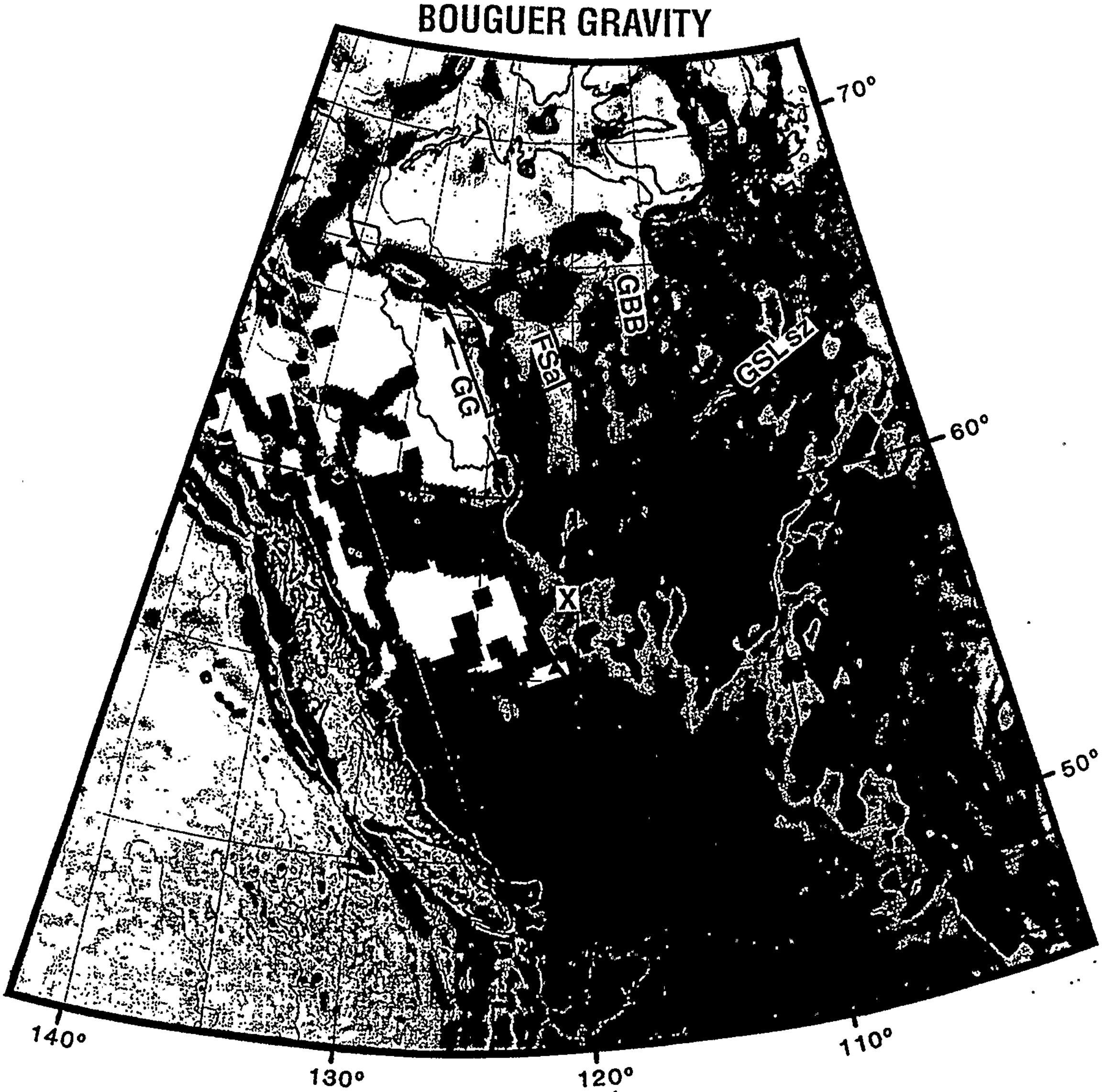

Figure 4.2

Regional aeromagnetic anomaly map of western Canada and northwestern U.S. (Geological Society of America, 1987b; Map modified from Cook et al., 1991.

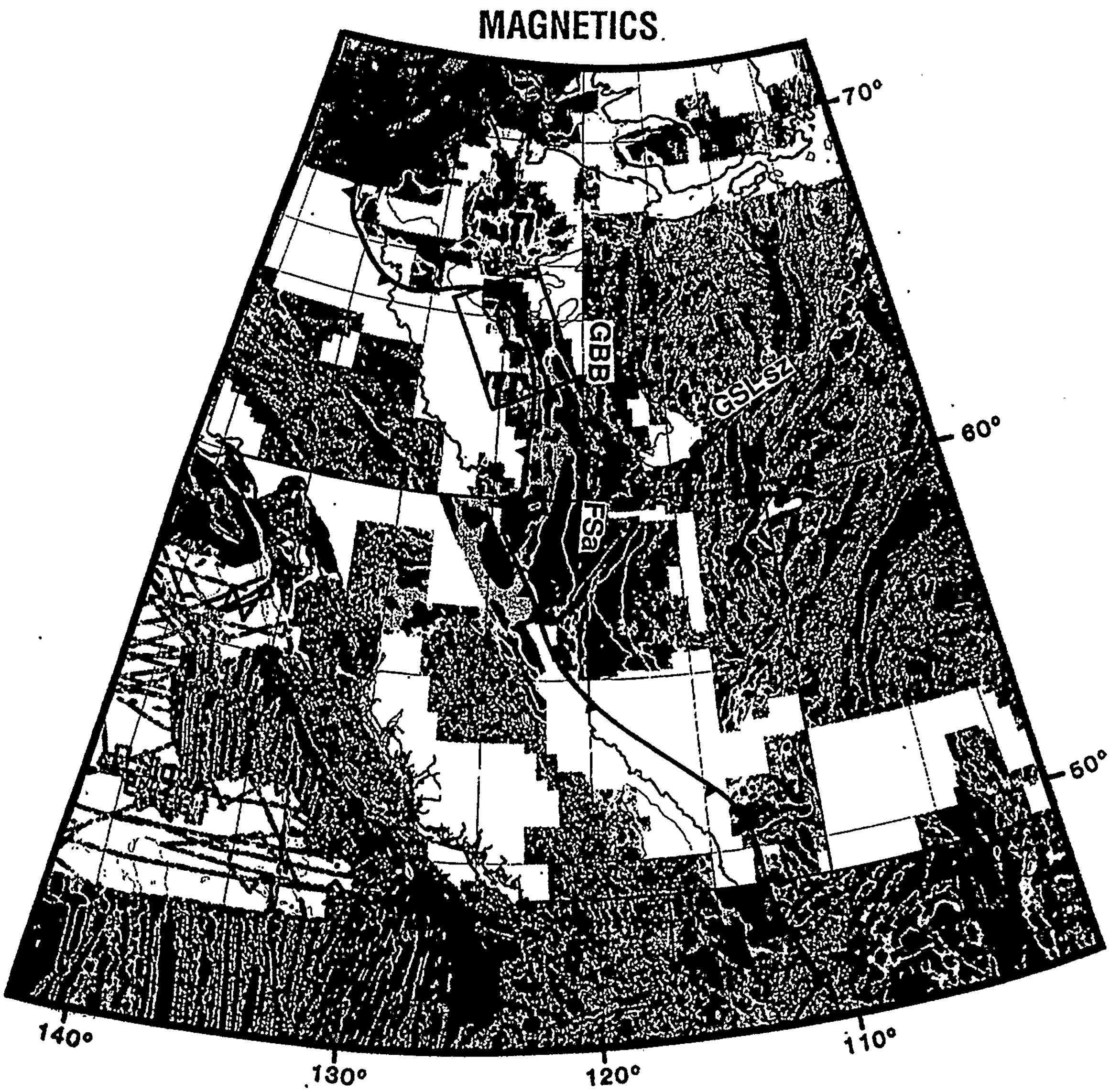
MAGNETICS
70°
60°
50°
GBB
GSLsz
FSa
140°
130°
120°
110°

from regionally high gravity values on the east to low values on the west (from greater than 0 mGals to less than -80 mGals; Clark and Cook, 1989). The ramp structure observed on the crustal seismic profiles within northern British Columbia and the Northwest Territories appears to follow this gravity gradient.

In the Fort Norman study area, the gravity map shows a gradual decrease in gravity values from east to west with two large north-south trending anomalies east of the study area. The magnetics show a similar picture, but the two eastern anomalies are smaller and slightly shifted in location as compared to the gravity anomalies (Figures 4.3 and 4.4).

Gravity Modelling

A gravity profile (Figure 4.5) was extracted from the G.S.C. database along line 64X. The profile was extended to both the northeast and the southwest of the seismic line. The area northeast of line 64X was constrained by seismic lines 71X and 6 (Figure 4.6). The area southwest had no seismic constraints. The observed gravity anomaly for the profile reached a high of -22 mGals and a low of -88 mGals. Only one gravity profile was extracted because the features observed were large in areal extent, covering a major portion of the study area, and because the gravity stations were widely spaced, about 5 km, therefore any small changes would not be recorded.

The gravity data were modelled using G.S.C. modelling software. Although no density information was available the area occupied by profile 1 was constrained by the structure imaged on the seismic reflection data. Where no seismic data were available, the model body could be changed to best fit the observed gravity values. For simplicity, two 2-dimensional model bodies, body 1 and body 2 were used having a density contrast of -0.061 and 0.000 g/cc respectively. Body 1 represented the Hudsonian basement; body 2 represented the sediments of the Wernecke Supergroup.

The large gravity high located on the west side of the profile is probably due to an anomalous mass that is off the profile to the southwest.

The results of the modelling indicate the rocks of body 1 are higher density than those that overlie them and are therefore consistent with the interpretation of these rocks as Hudsonian crystalline basement rock. The model also indicates that while uplift in the basement contributes to the gravity high on the east, the regional gravity anomaly is due to a larger feature such as the westward thickening of low density Proterozoic and Phanerozoic rocks, above the Hudsonian crystalline basement.

Magnetic Modelling

Magnetic and gravity methods have much in common, but magnetics are generally more complex and variations in the magnetic field are more erratic and localized. A residual magnetic profile (Figure 4.7) was extracted along the same line as the gravity profile. The observed magnetic values reach a maximum of 564 nT and a minimum of -76 nT in the region. Although the magnetic profile is not exactly perpendicular to the magnetic contours, comparison of the chosen profile to a profile drawn perpendicular to

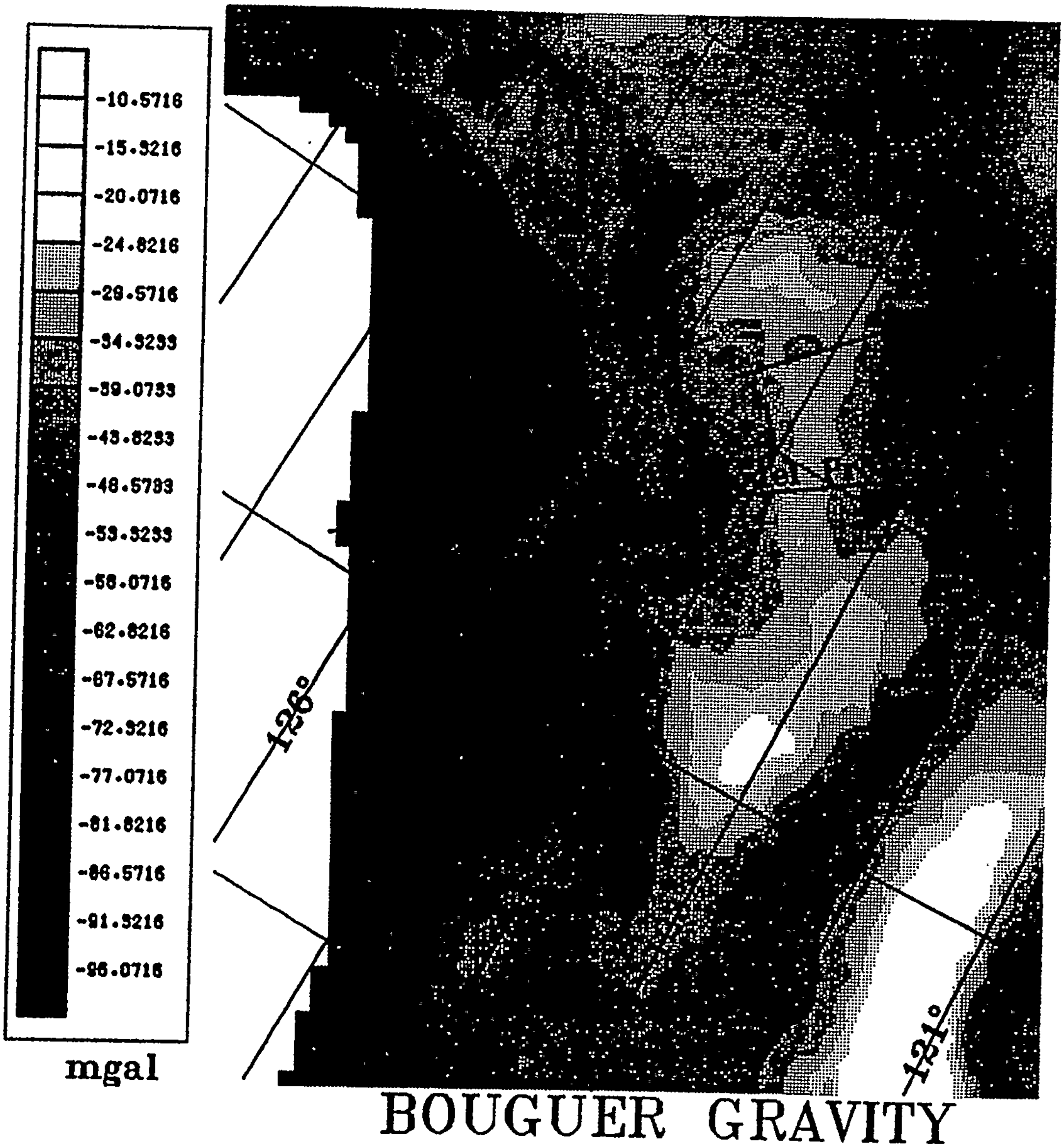

Figure 4.3

An enlargement of the Bouguer gravity map for the Fort Norman study area which is surrounded by a black box in Figure 4.1. The colors are the same as in Figure 4.1. The solid black line extending across the study area represents the location of the profile that is used in the gravity modelling. Other solid black lines represent the location of the seismic lines used in the study.

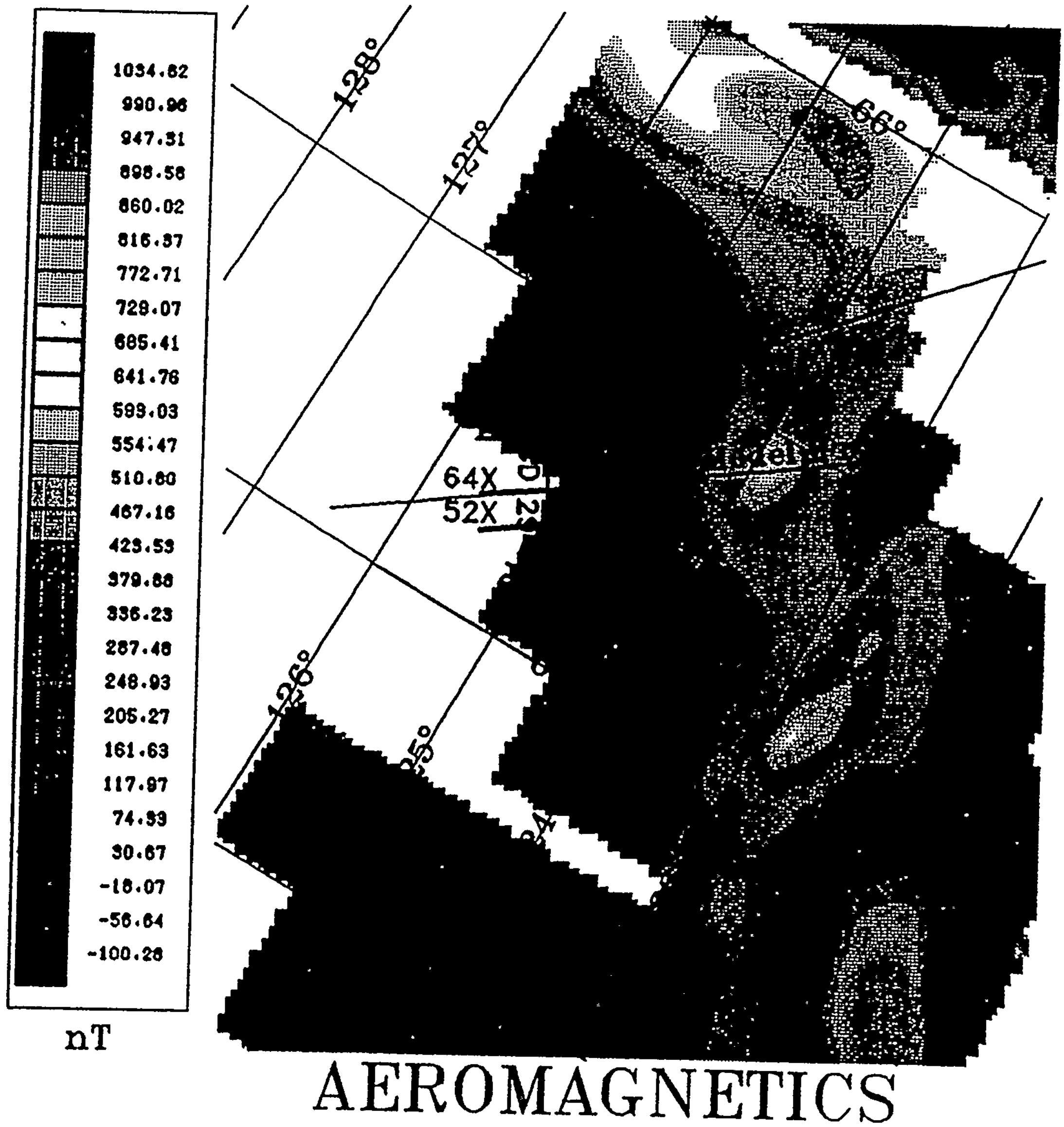

Figure 4.4

An enlargement of the aeromagnetic map for the Fort Norman study area which is surrounded by a black box in Figure 4.2. The colors differ from those used in Figure 4.2, the lighter shades reds represent high values and the darker shades represent low values. The solid black line extending across the study area represents the location of the profile that is used in the gravity modelling. Other solid black lines represent the location of the seismic lines used in the study.

Figure 4.5

Gravity profile extracted along seismic line 64X and extended to both the northeast and southwest.

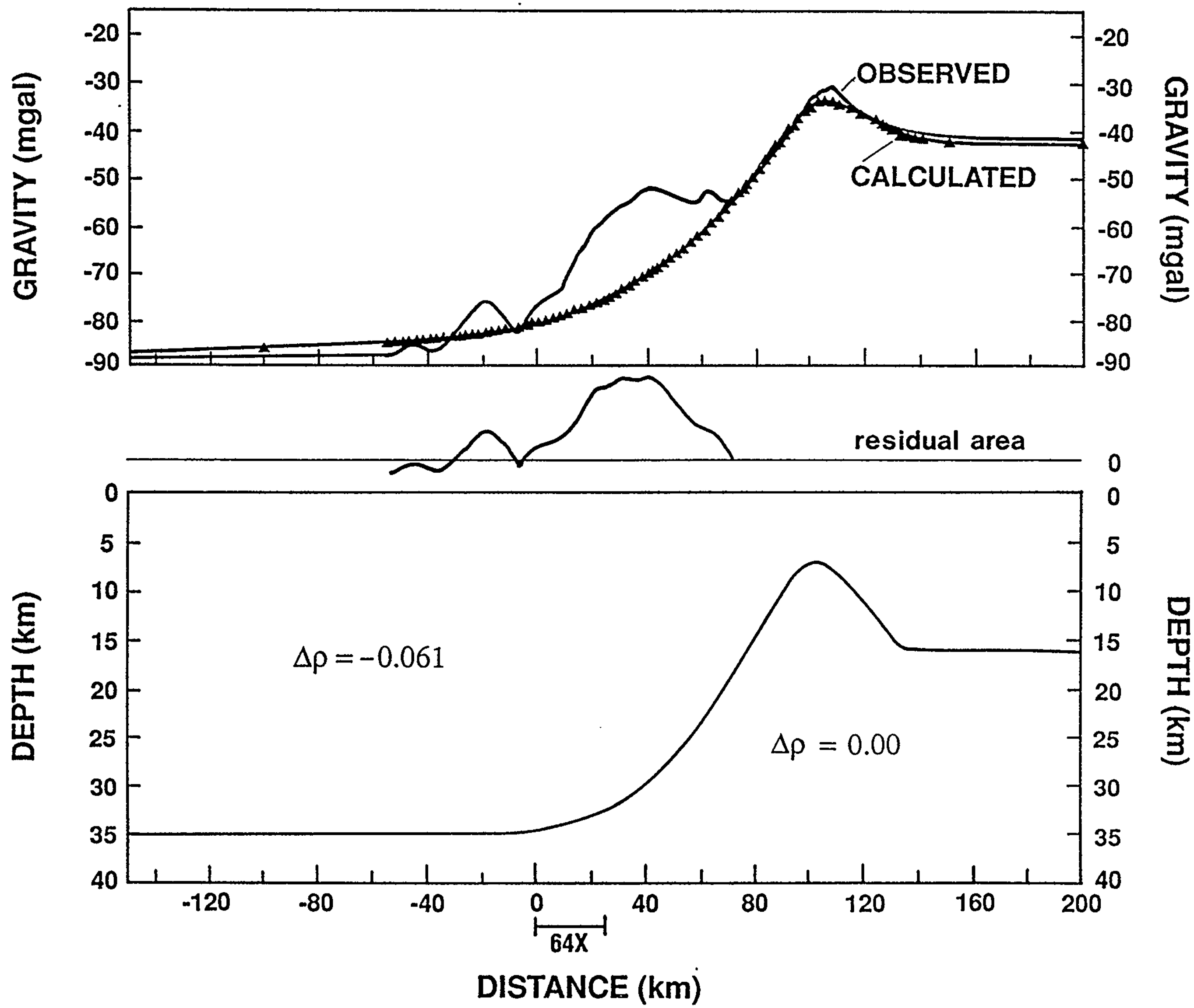

GRAVITY (mgal)
-20
-30
-40
-50
-60
-70
-80
-90
OBSERVED
CALCULATED
residual area
0
DEPTH (km)
0
5
10
15
20
25
30
35
40
Δρ = −0.061
Δρ = 0.00
-120
-80
-40
0
40
80
120
160
200
64X
DISTANCE (km)

Figure 4.6

Gravity profile plotted to the same scale as the seismic constraint used for the modelling along with an interpretation of seismic and gravity. The observed gravity high on the west side of the profile is probably due to an anomalous mass that is off the profile to the southeast (see text). The different zones I-IV are based on seismic character and correlatability as described in Chapter 5. The different patterns are used to delineate these zones.

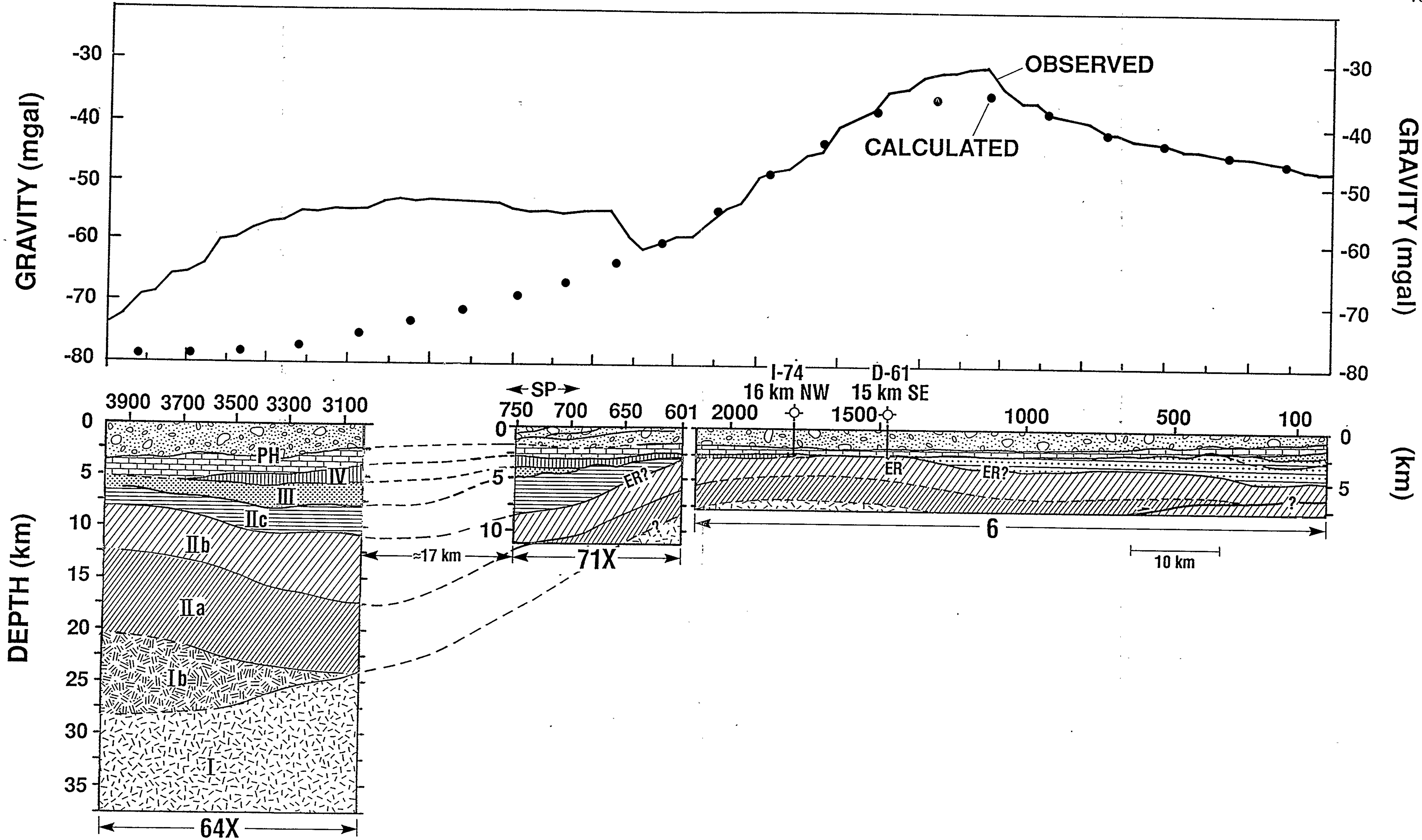
GRAVITY (mgal)
OBSERVED
CALCULATED
I-74
16 km NW
D-61
15 km SE
SP
PH
IV
III
IIc
IIb
IIa
Ib
I
ER?
ER
≈17 km
64X
71X
6
10 km
DEPTH (km)
(km)

strike reveals the anomaly is very similar on both (Figure 4.7). For comparison purposes, therefore, the perpendicular profile was not used in the modelling of the magnetic anomaly.

The modelling technique used for the magnetics was the same as that discussed above for the gravity modelling. The magnetic inclination and declination for the Fort Norman area are about 32.23° N and 80° E, respectively. No magnetic susceptibilities were known, but again structural information from the seismic data was used as a constraint (Figure 4.8). The contrast in magnetization between body 1 and the overlying strata is modelled at 225 emu/cc. In this case, the 10-15 km ramp (homocline) was not needed to model the regional magnetic anomaly, perhaps because it is at a significant depth. The magnetic anomaly appears to be caused by a more local feature; the uplift of the Hudsonian crystalline basement in the area east of line 64X.

Relationship of Potential Field Data to Seismic Data

The potential field and seismic data both indicate an uplift in the east referred to as the Fort Simpson magnetic anomaly by Cook et al. (1992). From drill hole and outcrop data the Fort Simpson anomaly is known to be cored by rocks of the Hudsonian basement (greater than 1.8 Ga) and flanked by sedimentary rocks of the Dismal Lakes and Hornby Bay groups (Cook et al.,1992). The high density and magnetic susceptibility of the uplifted basement rocks correlate well with the anomalies observed on the potential field data.

The deepening of the Wernecke basin west of the intra-Proterozoic ramp allowed much low density rocks to accumulate. A regional gravity gradient occurring west of the ramp (homocline) is a direct result of the thickening of these low density sedimentary or metasedimenary rocks overlying the Hudsonian basement.

Figure 4.7

Magnetic profile extracted along the same line as the gravity profile. Note that no large high is present to the southwest as in the case with the gravity. This is likely because the gravity response tends to be longer wavelength.

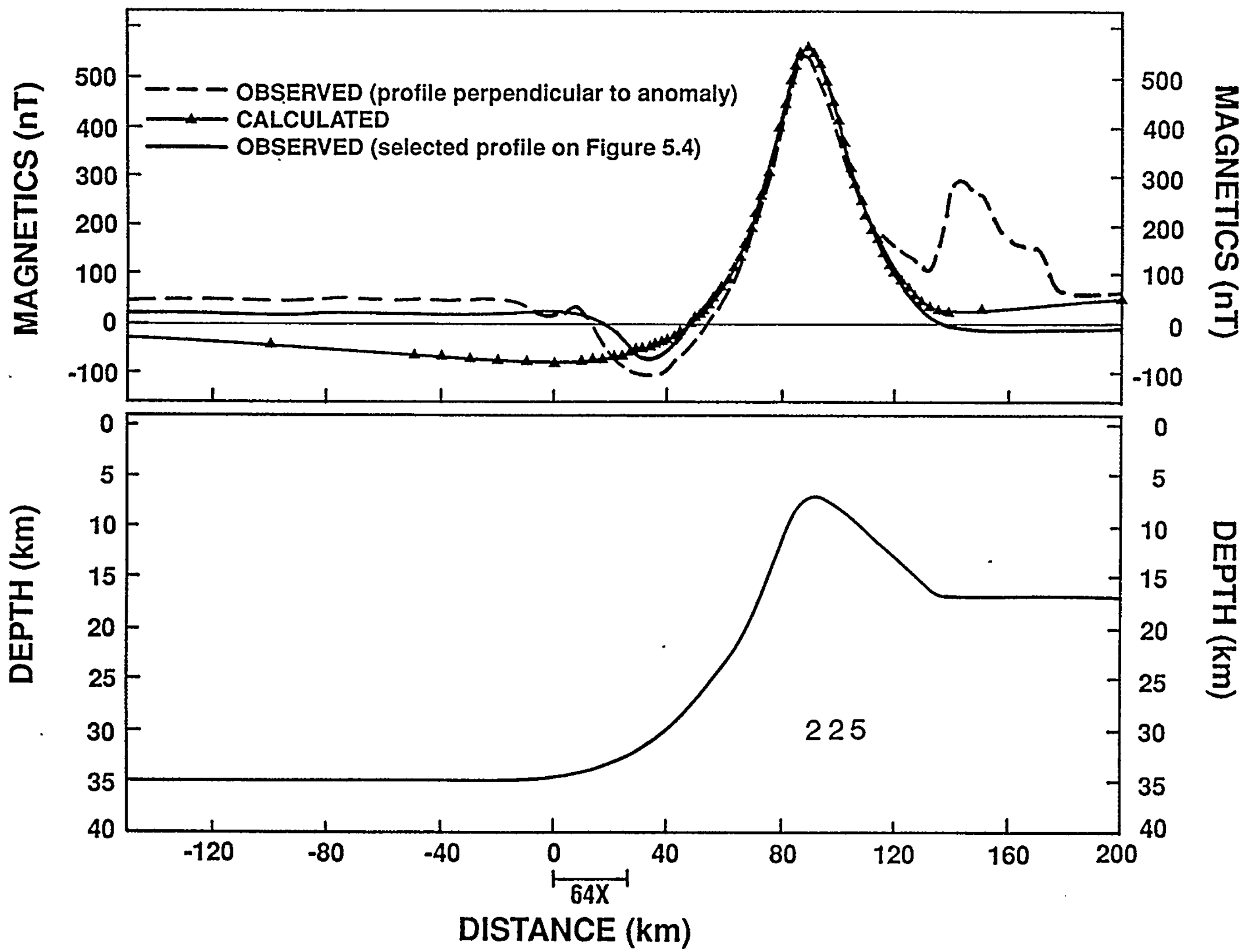

OBSERVED (profile perpendicular to anomaly)
CALCULATED
OBSERVED (selected profile on Figure 5.4)
MAGNETICS (nT)
500
400
300
200
100
0
-100
DEPTH (km)
0
5
10
15
20
25
30
35
40
225
-120
-80
-40
0
40
80
120
160
200
64X
DISTANCE (km)

Figure 4.8

Magnetic profile plotted to the same scale as the seismic constraint used (same as for the gravity).

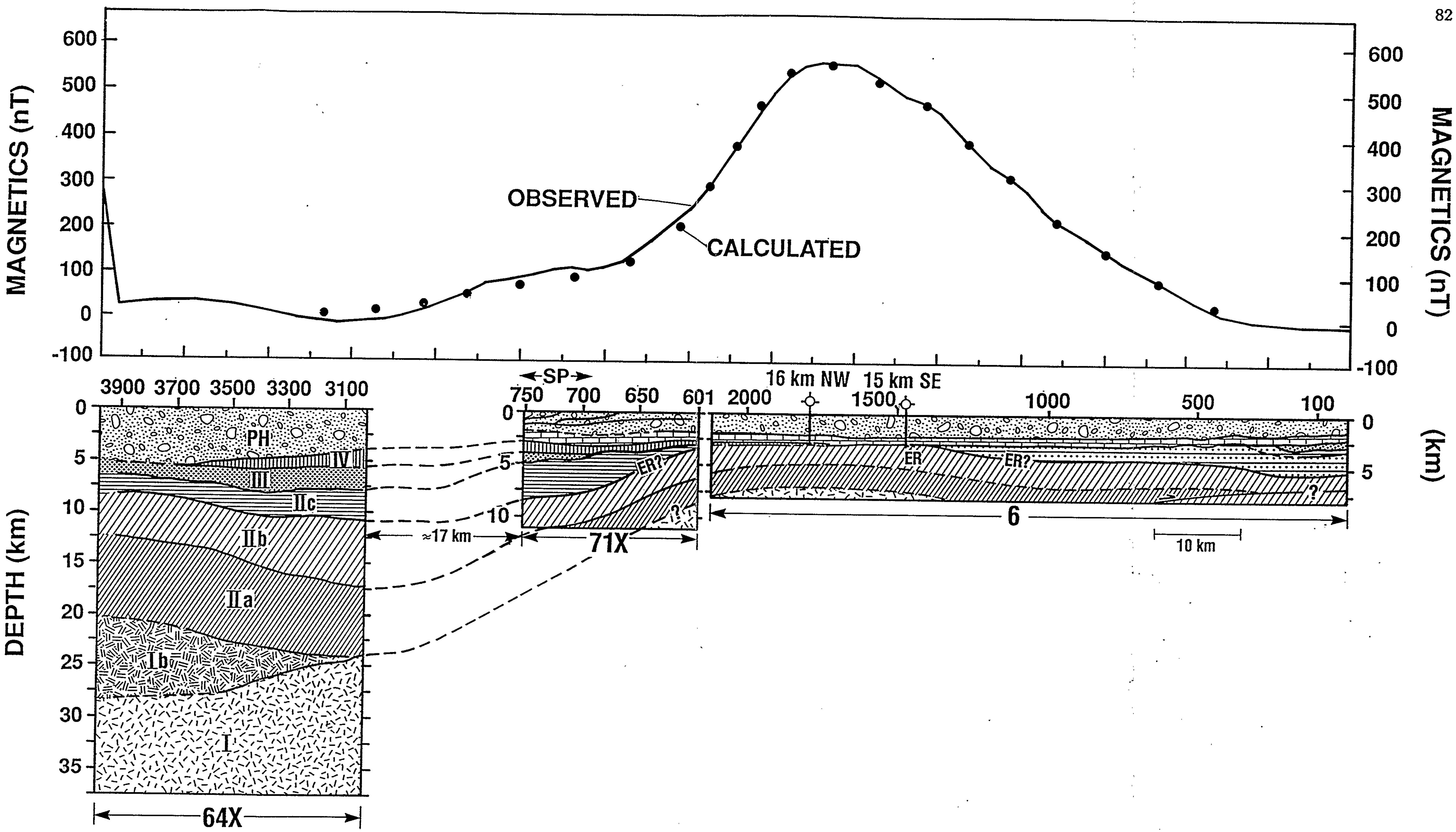
MAGNETICS (nT)
OBSERVED
CALCULATED
DEPTH (km)
3900 3700 3500 3300 3100
SP
750 700 650 601
16 km NW
15 km SE
2000 1500 1000 500 100
PH
IV
III
IIc
IIb
IIa
Ib
I
ER?
ER
?
≈17 km
64X
71X
6
10 km
(km)

CHAPTER 5 : INTERPRETATIONS OF SEISMIC REFLECTION DATA

Introduction

Lines 52X, 64X and 26X are parallel, northeast-southwest trending lines that are located approximately 25 to 30 km due south of the townsite of Fort Norman. Line 29-10 is a north-south line that includes lines CD-29 (4.0 sec) and CD-10 (3.5 sec) and ties lines 52X, 64X and 26X. All of the profiles show regionally consistent reflection patterns that are divisible into zones that can be related from one profile to another (Figures 5.1 through 5.4). Following Cook et al. (1992), these are labelled from deeper to shallower levels as I through IV for the Proterozoic and PH for the Phanerozoic.

Data used in this study are of four different vintages (Table 5.1). Because the lines obtained from NEB are only available in unmigrated stacks, all the profiles are presented as unmigrated stacks. Migrations are available for the more recent data donated by Chevron (discussed in Chapter 3) but the interpretation presented here is not significantly altered by the migration process. The data are described below from north to south.

Data Description

Chevron Seismic Reflection Lines (52X, 64X, and 26X)

The three northeast-southwest Chevron seismic reflection lines are perpendicular to the magnetic trend and parallel to one another. They are tied together by seismic reflection line 29-10. All these lines illustrate the same geological features (with the exception of a fault occurring near the Proterozoic/Phanerozoic boundary on line 52X).

Table 5.1 : A listing of all seismic reflection lines used in the study.

Line	Operator	Source	Date
52X, 64X and 26X	Chevron Canada	dynamite	1992
CD-29 and CD-10	Sigma Explorations	dynamite	1971
71X	Petro-Canada	dynamite	1982
6	B.P.O.G.	dynamite	1974

Seismic Character Common to All Seismic Lines

Seismic reflection lines 52X, 64X, and 26X (Figures 5.1-5.3, respectively) can all be divided into five major Proterozoic zones, I, Ib, II, III, and IV (see also Figures 4.6 and 4.8). Zone I consists of a relatively non-reflective west-dipping pattern which starts between 6.0-10.0 sec on the east side of the lines (at 8.25 sec on 52X, 9.5 sec on 64X and 6.25 sec on 26X; zone Ib is a wedge shaped unit of weak reflectivity which overlies zone I. On the west side of line 52X this zone is 3.5 sec thick between 7.5 sec and 11.0 sec, on line 64X it is 3.0 sec thick from 8.0 to 11.0 sec and on line 26X it is 3.5 to 4.0 sec thick from 9.0 sec to 12.5 or 13.0 sec.

Zone II is a thick package of reflections approximately 6.0 seconds thick that has been subdivided into three packages, IIa, IIb,and IIc. On the west side of seismic lines 52X, 64X, and 26X it occurs between 2.0 to 8.0 sec, 2.0 to 8.0 sec, and 2.5 to 8.5 sec, respectively. The subdivision into these three subzones is based on the seismic reflectivity. Subzone IIa is a 3.0 sec thick sequence of moderate reflectivity. Subzone IIb is a 2.5 sec thick sequence of strong reflectivity. Subzone IIc is a weakly reflective zone which conformably overlies IIb.

Zone III is a wedge of moderately reflective layers which is truncated at the top by the overlying zone IV. It is about 1.0 to 1.5 sec thick positioned at 1.2 to 2.5 sec on the east side of line 52X, at 1.5 to 3.25 on line 64X, and 2.5 to 4.0 sec on line 26X.

The zone named PH represents a fairly thin package of flat, parallel reflections of Phanerozoic cover ranging in thickness from 1.5 to 3 seconds. On the west ends of lines

Figure 5.1

Seismic reflection line 52X is located south of the townsite of Fort Norman oriented in a northwest-southeast direction. L-04 marks the location of the well tie.

a) Coherency filter of seismic line 52X.

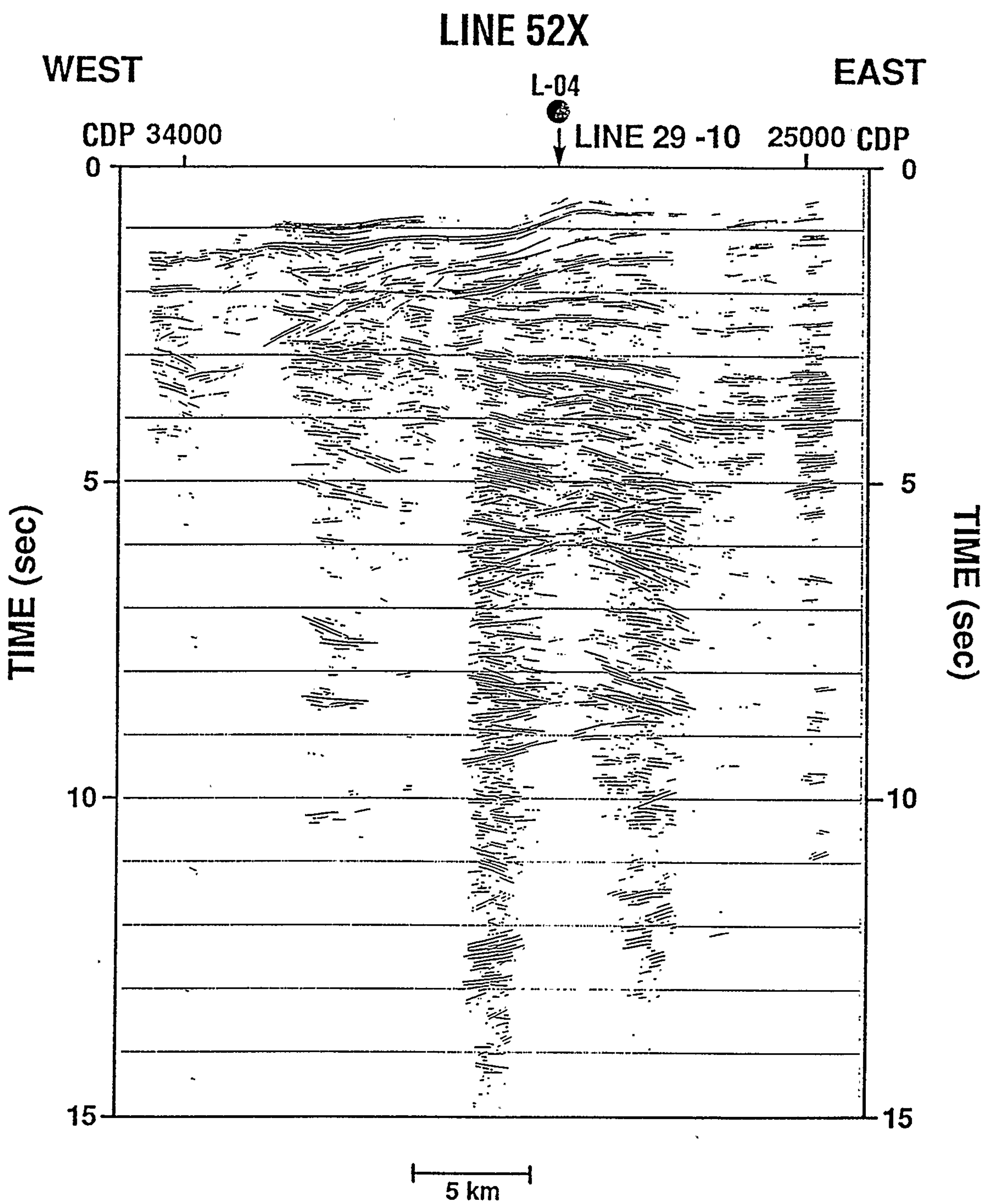
LINE 52X
WEST
EAST
L-04
CDP 34000
LINE 29 -10
25000 CDP
0
5
10
15
TIME (sec)
5 km

Figure 5.1b

Interpretation of seismic line 52X.

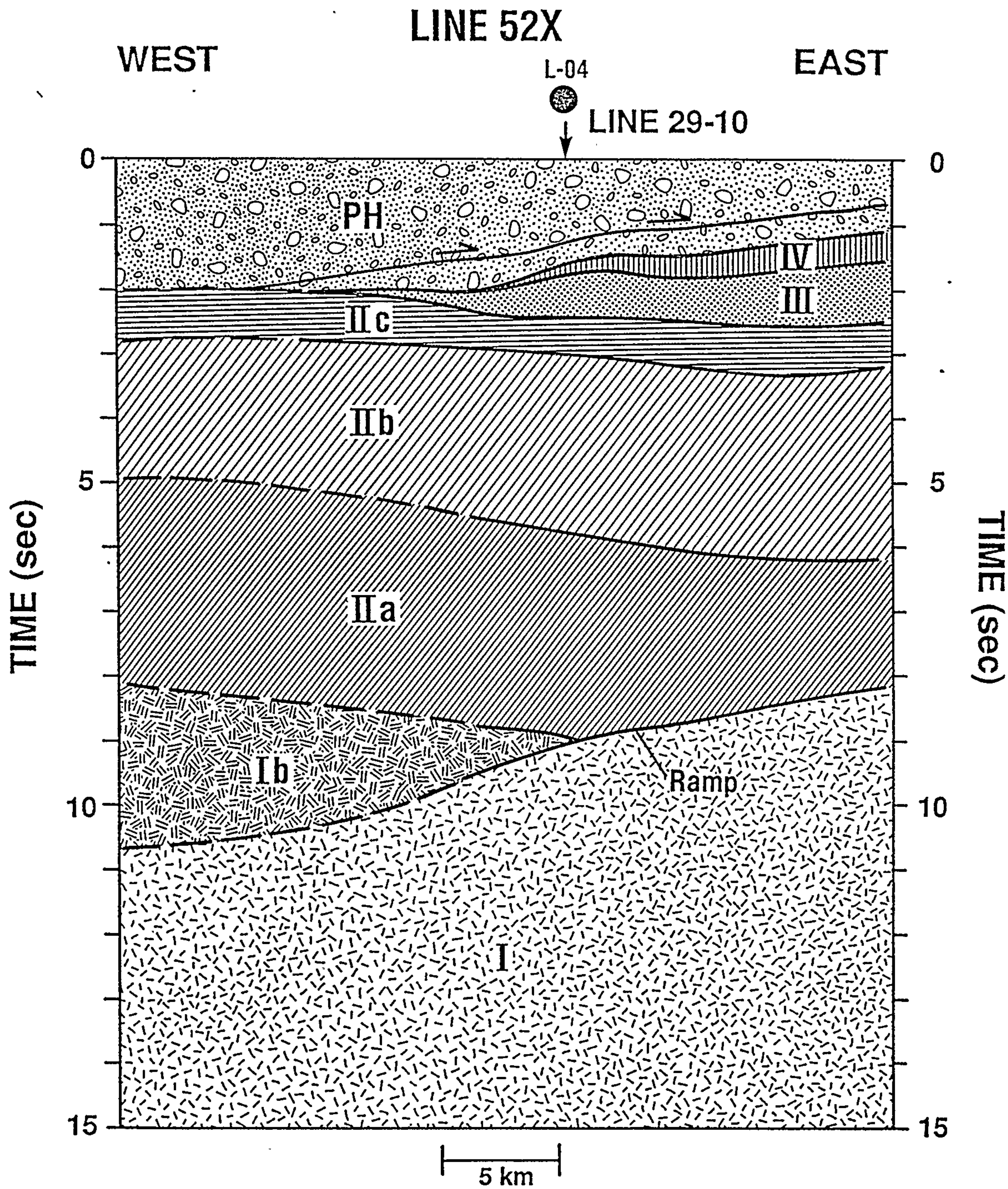
LINE 52X
WEST
EAST
L-04
LINE 29-10
0
5
10
15
TIME (sec)
PH
IV
III
IIc
IIb
IIa
Ib
Ramp
I
5 km

Figure 5.2

Seismic reflection line 64X is parallel to and just north of line 52X.

a) Coherency filter of seismic line 64X.

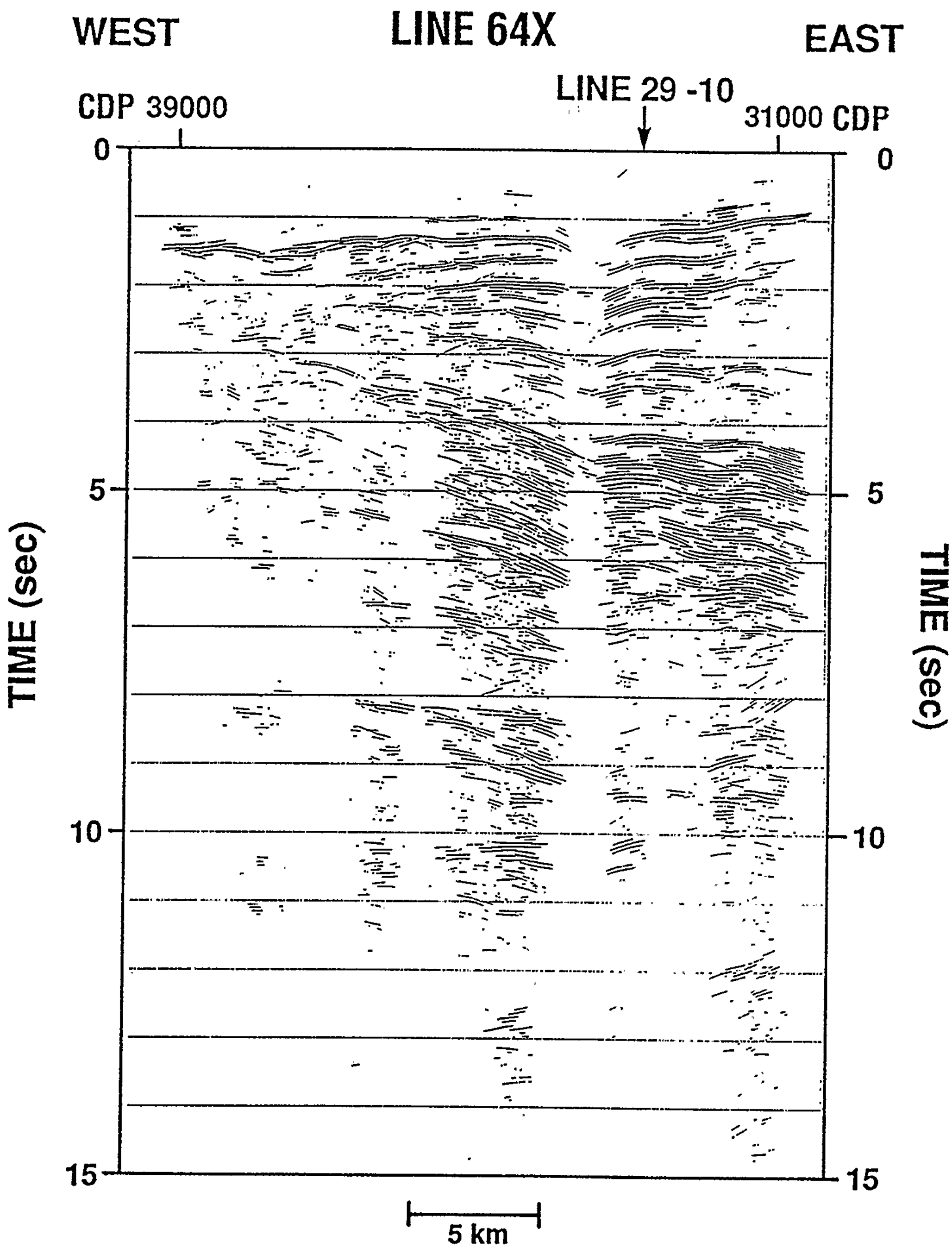
WEST
LINE 64X
EAST
CDP 39000
LINE 29 -10
31000 CDP
0
5
10
15
TIME (sec)
5 km

Figure 5.2b

Interpretation of seismic line 64X.

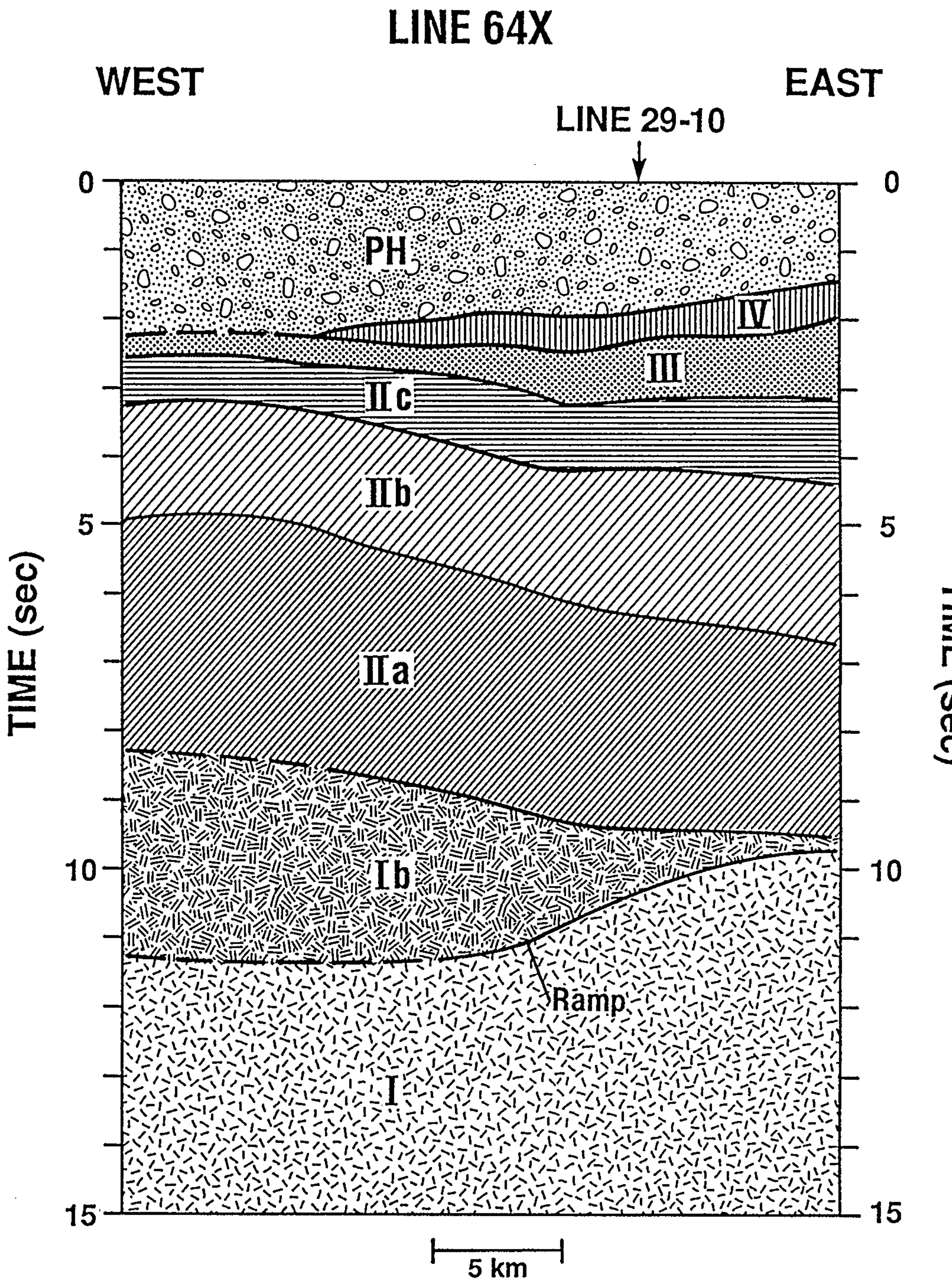

LINE 64X
WEST
EAST
LINE 29-10
0
5
10
15
TIME (sec)
PH
IV
III
IIc
IIb
IIa
Ib
Ramp
I
5 km

Figure 5.3

Seismic reflection line 26X is parallel to lines 52X and 64X and is located just north of line 64X.

a) Coherency filter of seismic line 26X.

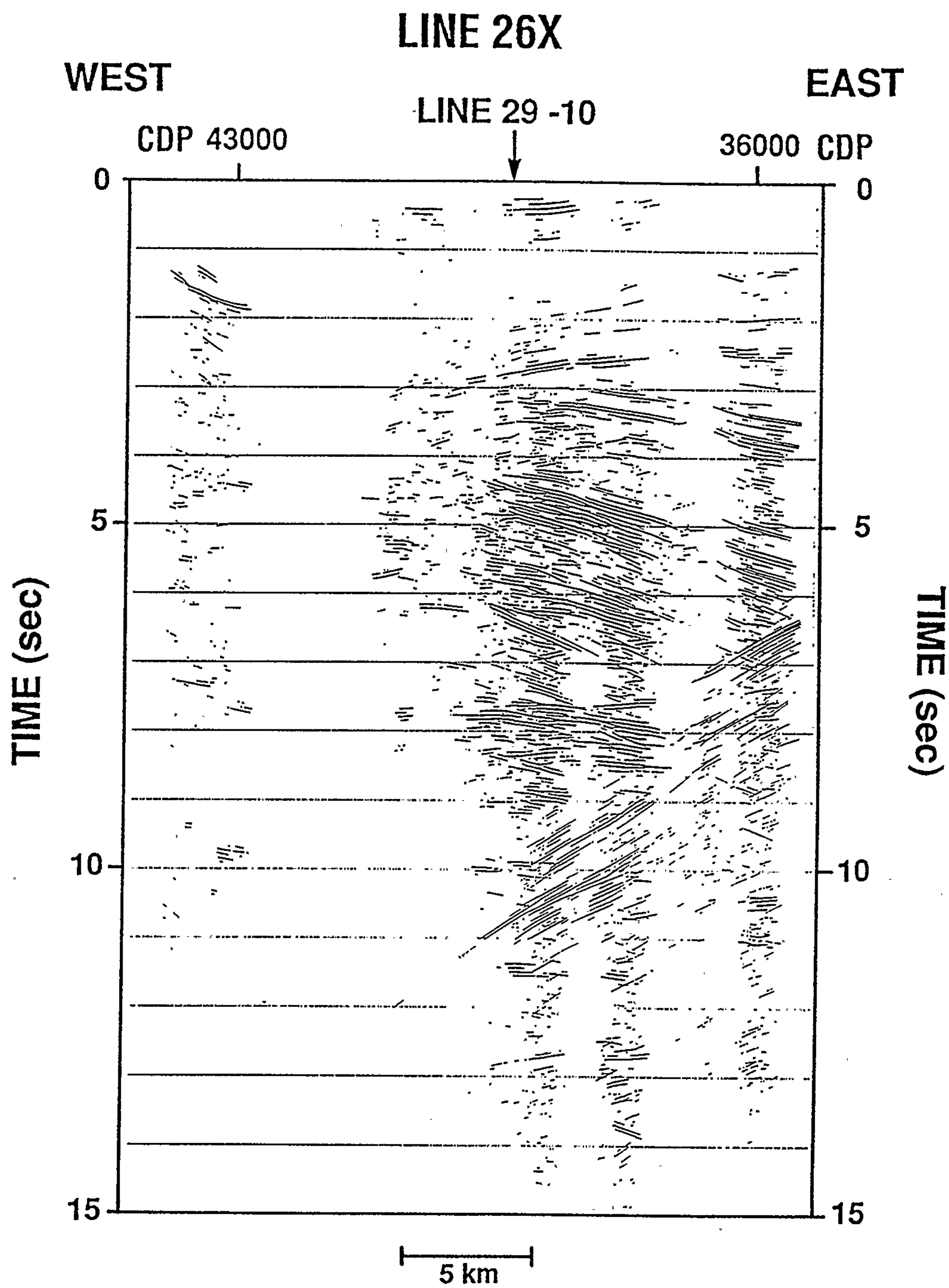
LINE 26X
WEST
EAST
LINE 29 -10
CDP 43000
36000 CDP
0
5
10
15
TIME (sec)
5 km

Figure 5.3b

Interpretation of seismic line 26X.

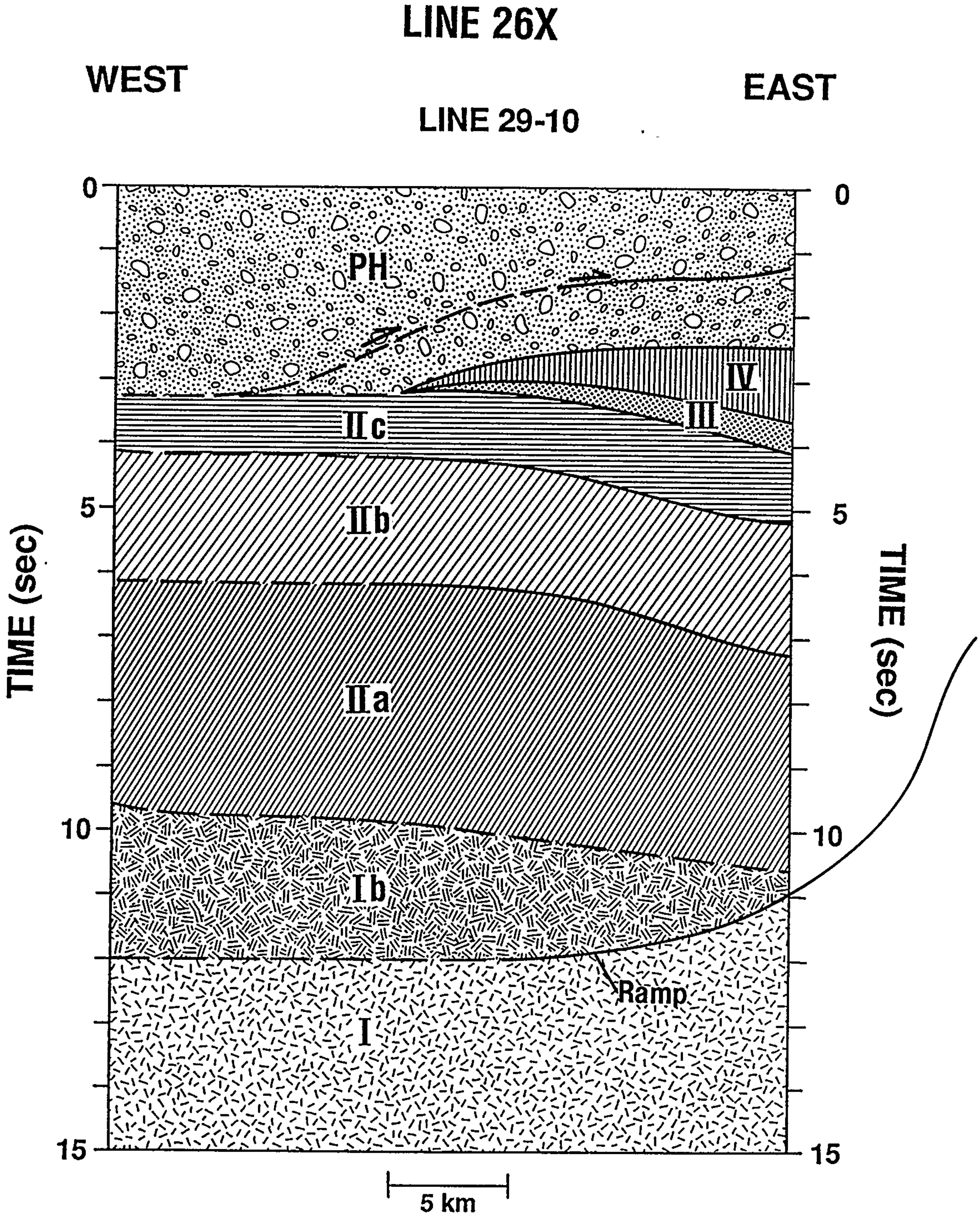
LINE 26X
WEST
EAST
LINE 29-10
PH
IV
III
IIc
IIb
IIa
Ib
I
Ramp
TIME (sec)
TIME (sec)
0
5
10
15
0
5
10
15
5 km

52X, 64X, and 26X this zone extends down to 2.0, 2.2, and 2.6 seconds, respectively.

Seismic Structure

There are two major structural features observed on the seismic reflection data within the Fort Norman study area: the "Tate Lake" antiform and the crustal-scale ramp (homocline). The "Tate Lake" antiform, so named because of its geographic closeness to Tate Lake, is expressed by east-dipping reflections (zone II) having uniform thickness (about 6.0 sec or 18.0 km) and starting at 2.0-3.0 sec on the west side of seismic reflection lines 52X, 64X, and 26X. The ramp is observed deep on the Chevron seismic lines. It is represented by a steep, west-facing reflector below which there is little to no reflectivity.

Seismic Reflection Line 29-10

Seismic reflection line 29-10 (Figure 4.4) is a combination of lines CD-29 and CD-10. It ties with the L-04 well as well as with the three Chevron lines (seismic lines 52X, 64X, and 26X). The lower units (zones I to IIa) discussed above for the Chevron lines are not observed here since this seismic line was only recorded to 3.5 - 4.0 seconds. The lower subzone observed here is zone IIb which begins at 3.0 seconds on the east side of the data. This unit has strong reflectivity and good continuity. It is comformably overlain by subzone IIc which is approximately 1.0 second thick and is characterized by little reflectivity. The 0.5 second thick zone III also displays little reflectivity and is uncomformably overlain by zone IV. Zone IV is observed to deepen to the north and onlap zone III in both the northern and southern portions of the data.

DATA INTERPRETATION

Introduction

Interpretation of these data is difficult because there are no drill holes along them that penetrate to Proterozoic rocks. Nevertheless, comparison of the L-04 well to seismic reflection lines 52X and CD-29 and the B-62 well to line 71X allows a good estimation of the top of the Proterozoic, and correlation of the reflection character on all seismic lines to that observed on data to the east (Cook et al., 1992) and to outcrop allows reasonable interpretations of the deep stratigraphy and structures.

The L-04 Drill Hole

The L-04 well had been used in a correlation by Cook and Yorath (1981) in

Figure 5.4

Seismic reflection line 29-10 is a north-south oriented seismic line combining seismic lines CD-29 and CD-10.

a) Uninterpreted seismic line 29-10.

b) Interpretation of seismic line 29-10.

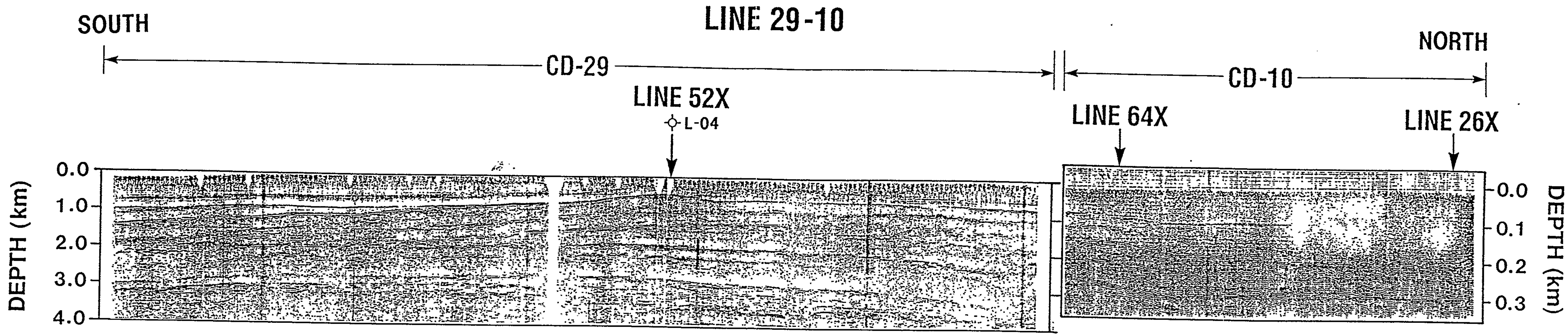
LINE 29-10
SOUTH
NORTH
CD-29
CD-10
LINE 52X
L-04
LINE 64X
LINE 26X
DEPTH (km)
0.0
1.0
2.0
3.0
4.0
DEPTH (km)
0.0
0.1
0.2
0.3

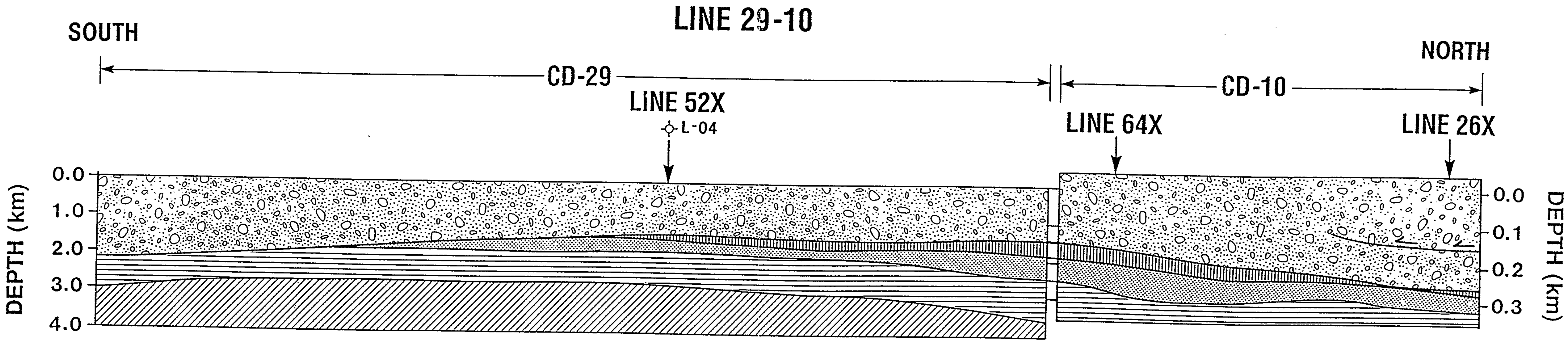
LINE 29-10
SOUTH
NORTH
CD-29
CD-10
LINE 52X
L-04
LINE 64X
LINE 26X
DEPTH (km)
0.0
1.0
2.0
3.0
4.0
DEPTH (km)
0.0
0.1
0.2
0.3

studying the Mesozoic strata. They used only the upper portion of the well (down to the top of the Cambrian at 698 m) but clearly show an unconformity whereby Cretaceous sediments overlie Cambrian sediments (Figure 5.5). Figure 5.6 correlates the L-04 well to the synthetic generated by Veritas. It clearly shows the top of the Cambrian as a large peak at 0.28 sec. In comparing this synthetic with the 52X seismic profile we observe a very thick Cambrian succession and possible thrusting within the Cambrian.

The B-62 Drill Hole

The B-62 well is located about 50-60 km north of Chevron seismic reflection line 26X. Table 5.2 outlines the formations encountered in the well along with the depths at which each was drilled. The uncertainty concerning the formation drilled at 1942 m is what is important to this study. According to a report obtained from the NEB (1986), a white to light grey, medium-grained, well-cemented, quartz-rich sandstone was encountered at a depth of 1942 m. Porosity was tight to poor throughout the sandstone and drilling was very difficult due to the high silica content. The determination of this formation was difficult so comparisons were made to the lithology of the Proterozoic Katherine Formation with a neighbouring well; the P.C.I. Sammons well drilled in 1984 (NEB, 1986). The lithology of the Katherine Formation and the sandstone encountered in the B-62 well were quite similar and had similar drilling properties. Therefore, the formation encountered at 1942 m in the B-62 well has been interpreted as the Proterozoic Katherine Formation of the Mackenzie Mountains Supergroup (NEB, 1986).

If the B-62 drillhole drilled Proterozoic Katherine Formation of the Mackenzie Mountains Supergroup and I-74 drilled Proterozoic unit H1 carbonates (Aitken and Pugh, 1984), then a first order estimate of regional dip of the Mackenzie Mountains Supergroup based on formation thicknesses obtained from Aitken and Pugh (1984) and compared to the seismic data (Figure 5.7a and b) is possible and can be compared to the seismic data. The results of this approach indicate a maximum apparent dip of 2.9° and a minimum dip of 1.4° on layers immediately beneath the Phanerozoic. In either case the dips are quite low and approximate those seen in zone IV. Therefore, zone IV on the seismic data (Figures 5.1-5.3) is at roughly the same structural level as the rocks drilled by the I-74 well, the Mackenzie Mountains Supergroup, and has a similar apparent dip. Seismic reflection lines 71X and 6 (Figure 5.8) illustrate where the I-74 well ties these lines and the depth to which it penetrates.

Correlation of Seismic Reflection Lines 64X and 71X

Line 71X has been interpreted by Cook et al. (1992) with zone IV as the Mackenzie Mountains Supergroup, based on well control. A southward projection of this low along strike with the magnetic trend allows it to be correlated to seismic lines 52X, 64X, and 26X. Hence, a previous interpretation by Cook et al. (1992) is applied here to line 64X (Figure 5.9). According to this comparison, which is based on reflection character, zone I represents the Hudsonian basement, zone Ib is unknown (possibly the lower part of the Wernecke Supergroup), zone II represents the Wernecke Supergroup

Figure 5.5

Stratigraphic correlation of the L-04 well by Cook and Yorath (1981).

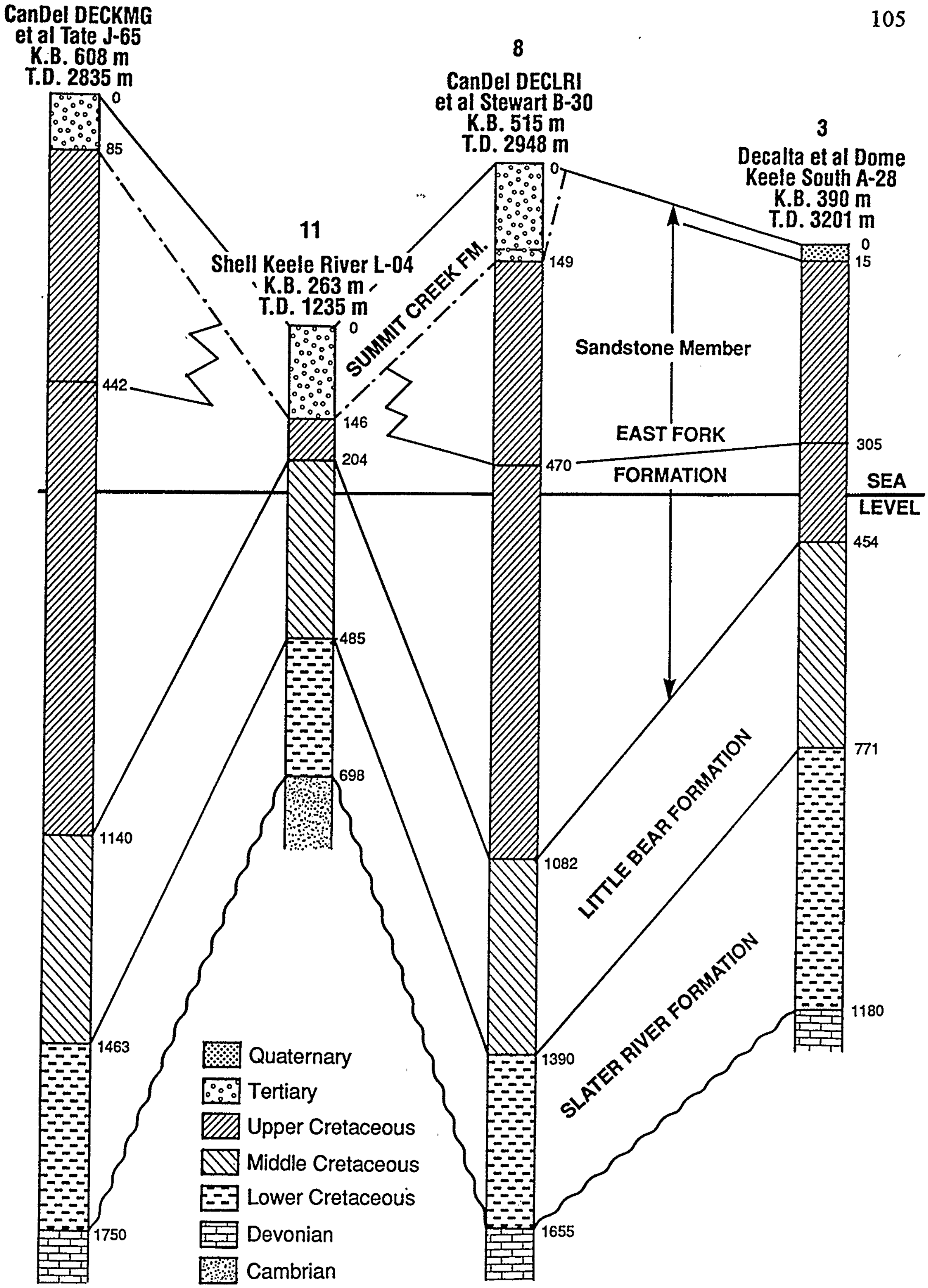

CanDel DECKMG
et al Tate J-65
K.B. 608 m
T.D. 2835 m
11
Shell Keele River L-04
K.B. 263 m
T.D. 1235 m
8
CanDel DECLRI
et al Stewart B-30
K.B. 515 m
T.D. 2948 m
3
Decalta et al Dome
Keele South A-28
K.B. 390 m
T.D. 3201 m
0
85
442
1140
1463
1750
146
204
485
698
149
470
1082
1390
1655
15
305
454
771
1180
SUMMIT CREEK FM.
Sandstone Member
EAST FORK
FORMATION
SEA
LEVEL
LITTLE BEAR FORMATION
SLATER RIVER FORMATION
Quaternary
Tertiary
Upper Cretaceous
Middle Cretaceous
Lower Cretaceous
Devonian
Cambrian

Figure 5.6

Synthetic generated by Veritas Seismic Ltd. from the L-04 well. Here it is correlated to Cook and Yorath's (1981) interpretation of the L-04.

REFLECTION COEFFICIENT SERIES

SHELL KEELE RIVER: 45-9L-4.0-S W M

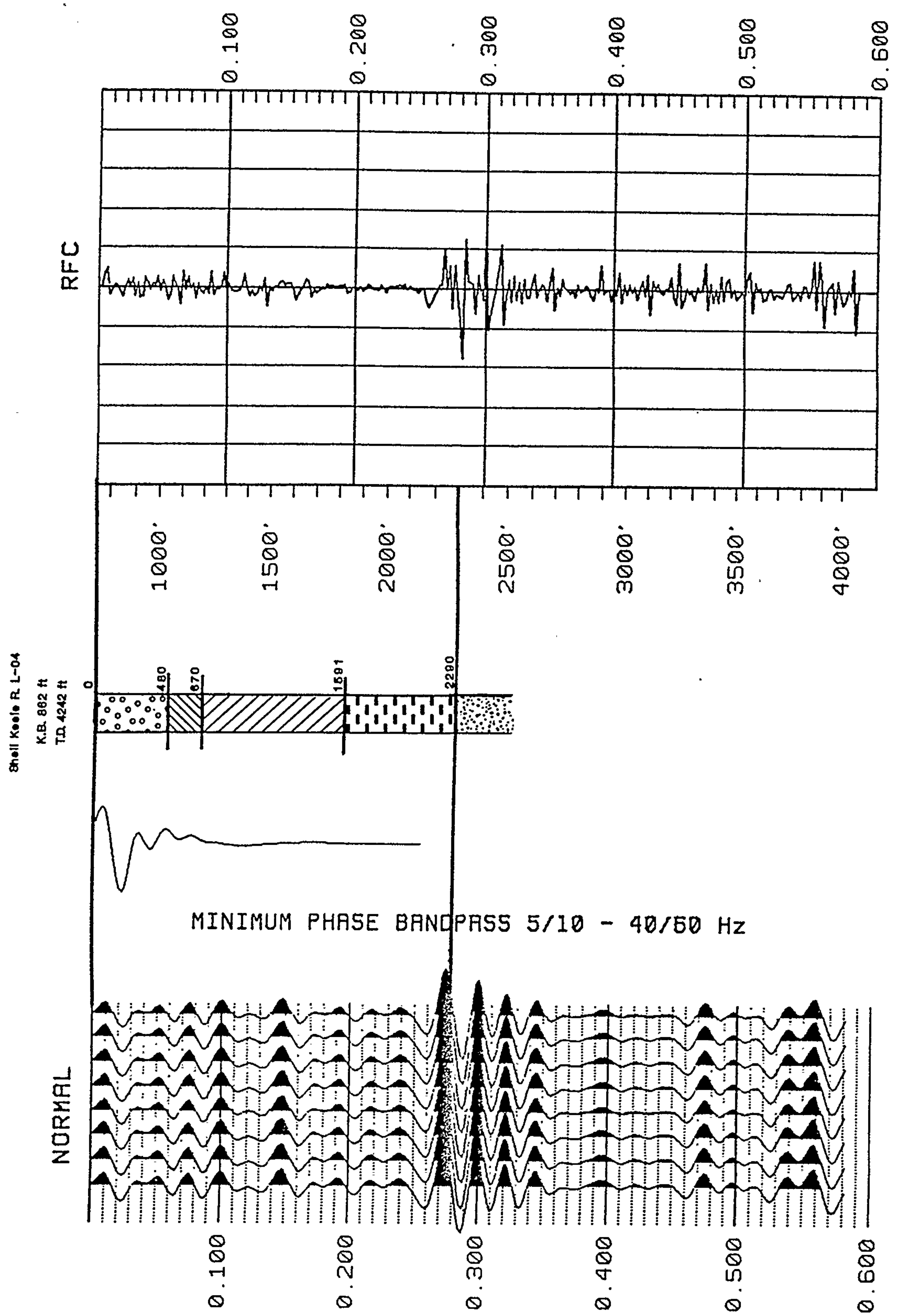

Table 5.2 : Formation tops for the B-62 drill hole.

FORMATION	DEPTH (m)
Detrital Zone	348
Franklin Mt.	366
Saline River	889
Salt Member	939
Mount Cap	1019
Mt. Clarke/Katherine?	1942
F.T.D.	1985

Figure 5.7

a) Schematic geological cross-section between the B-62 and the I-74 drill holes illustrating the dip of the Proterozoic strata from the top of the Katherine Formation to the base of the H1 carbonate map unit.

Figure 5.7

b) Schematic geological cross-section between the B-62 and the I-74 drill holes illustrating the dip of the Proterozoic strata from the base of the Katherine Formation to the top of the H1 carbonate map unit.

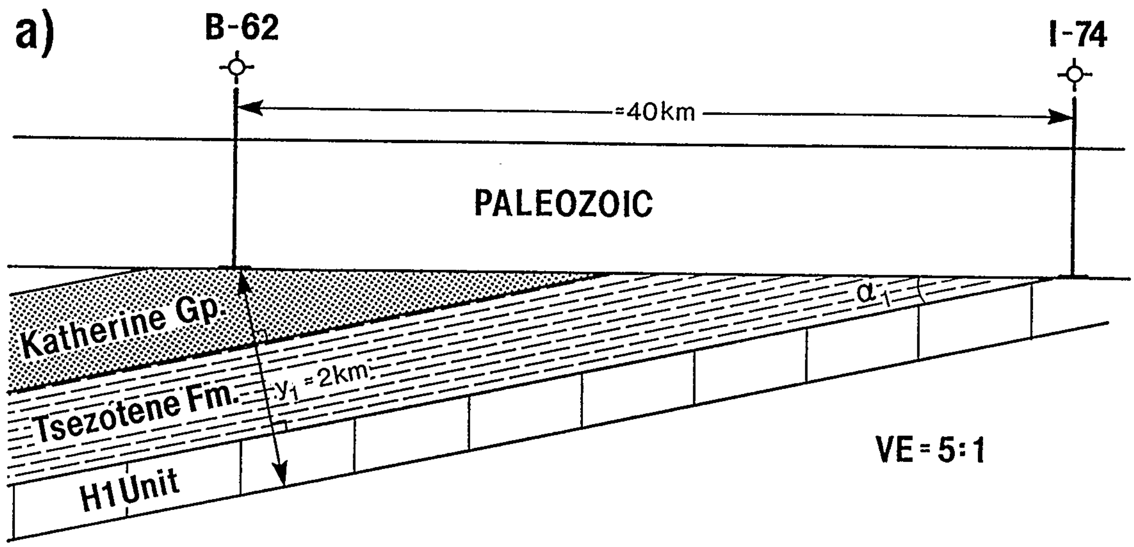

$$\alpha_1 = \tan^{-1} \frac{2}{40} = 2.9$$

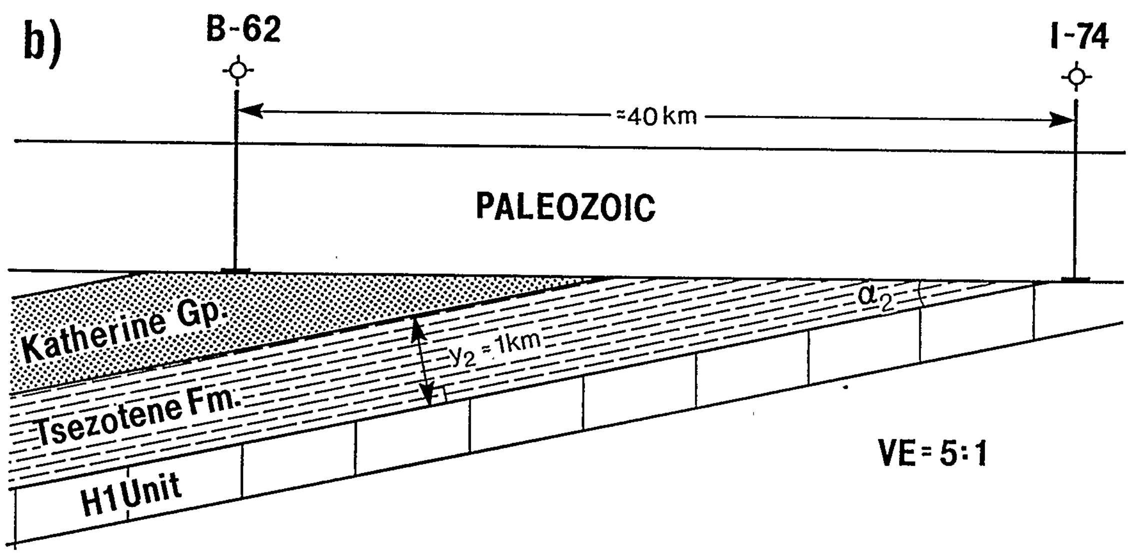

$$\alpha_2 = \tan^{-1} \frac{1}{40} = 1.4$$

Figure 5.8

Interpretation of seismic lines 71X and 6 by Cook et al. (1992).

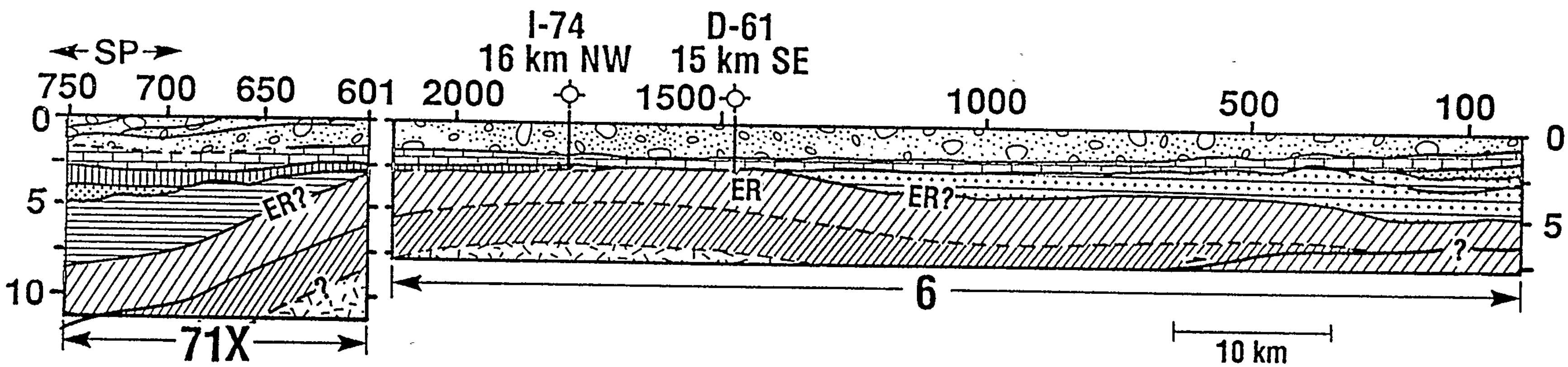
SP
750
700
650
601
2000
I-74
16 km NW
D-61
15 km SE
1500
1000
500
100
0
5
10
ER?
ER
ER?
?
71X
6
10 km

sedimentary package, zone III is unknown, zone IV represents the Mackenzie Mountain Supergroup and, finally, the PH zone represents the Phanerozoic.

Interpretation of Zone IV

According to the correlation discussed above, Zone IV represents rocks of the Mackenzie Mountains Supergroup. This zone is interpreted to thin and onlap underlying structures (Fort Simpson structural high) to the east (Figure 5.8; Cook et al., 1992) and possibly the "Tate Lake" antiform in the west (Figure 5.9). This indicates that these rocks were deposited after uplift of underlying rocks.

Interpretation of Zone III

The exact geological correlation of this zone is unkown. It is observed to onlap underlying structure of zone II to the east (Cook et al., 1992). Therefore, zone III is younger than both zone II and the deformation of zone II, but is older than zone IV.

Interpretation of Zone II

This zone represents sedimentary and metasedimentary rocks of the Dismal Lakes/Hornby Bay Groups (or the equivalent Wernecke Supergroup). Zone II is unconformably overlain by zone III and thickens dramatically to the west. After deposition it was uplifted in the west to form the "Tate Lake" antiform maintaining uniform thickness of strata and acquiring little internal deformation.

Interpretation of Zone Ib

It is not known what zone Ib represents. It is conformably overlain by zone II and unconformably overlies zone I. A possible explanation is that it may represent the lower part of the Fairchild Lake Group as the base of this group of rocks has not yet been seen.

Interpretation of Zone I

Zone I is interpreted to represent the metamorphic and plutonic rocks of the Hudsonian basement. The Bouguer gravity and aeromagnetic data showed very high values in the area east of the crustal-scale ramp (homocline) and may be interpreted as crystalline rocks of the Hudsonian basement (this is discussed in Chapter 4). This interpretation is also strengthened by the correlation made by Cook et al. (1992) of line 71X which has been correlated to seismic reflection line 64X (Figure 5.8).

Relationship of Zonal Interpretations to Regional Stratigraphy

A stratigraphic section for sequence A from the Coppermine area (east) was correlated with one from the Cordillera (west; Figure 5.10). In the Coppermine area the Hornby Bay strata of sequence A conformably overlie the Hudsonian basement. The Dismal Lakes Group strata conformably overlie the Hornby Bay and are in turn unconformably overlain by the Coppermine River Group.

The correlation between the Hornby Bay/Dismal Lakes Groups with the Wernecke Supergroup has been previously discussed in chapter 2 whereby the Hornby Bay Group may be the eastern equivalent of the Fairchild Lake Group because both are carbonate-clastic packages represented by a weakly reflective zone on the seismic reflection data. Lower Dismal Lakes Group has been correlated with the Quartet Group because they both are clastic packages represented by strongly reflective zones on the seismic reflection data. Finally, Upper Dismal Lakes Group of the Coppermine area has been correlated with the Gillespie Lake Group of the Cordillera because both are carbonate packages represented by a non-reflective zone on seismic reflection data.

The Wernecke Supergroup - Hornby Bay/Dismal Lakes Groups can be correlated through the Chevron seismic reflection data (Figure 5.9), such that zone IIa represents the Fairchild Lake Group (Hornby Bay Group), zone IIb represents the Quartet Group (Lower Dismal Lakes Group), and zone IIc represents the Gillespie Lake Group (Upper Dismal Lakes Group). As for the other zones identified on the seismic data, the correlation is outlined in Figure 5.11.

Figure 5.9

Correlation of seismic line 64X to line 71X.

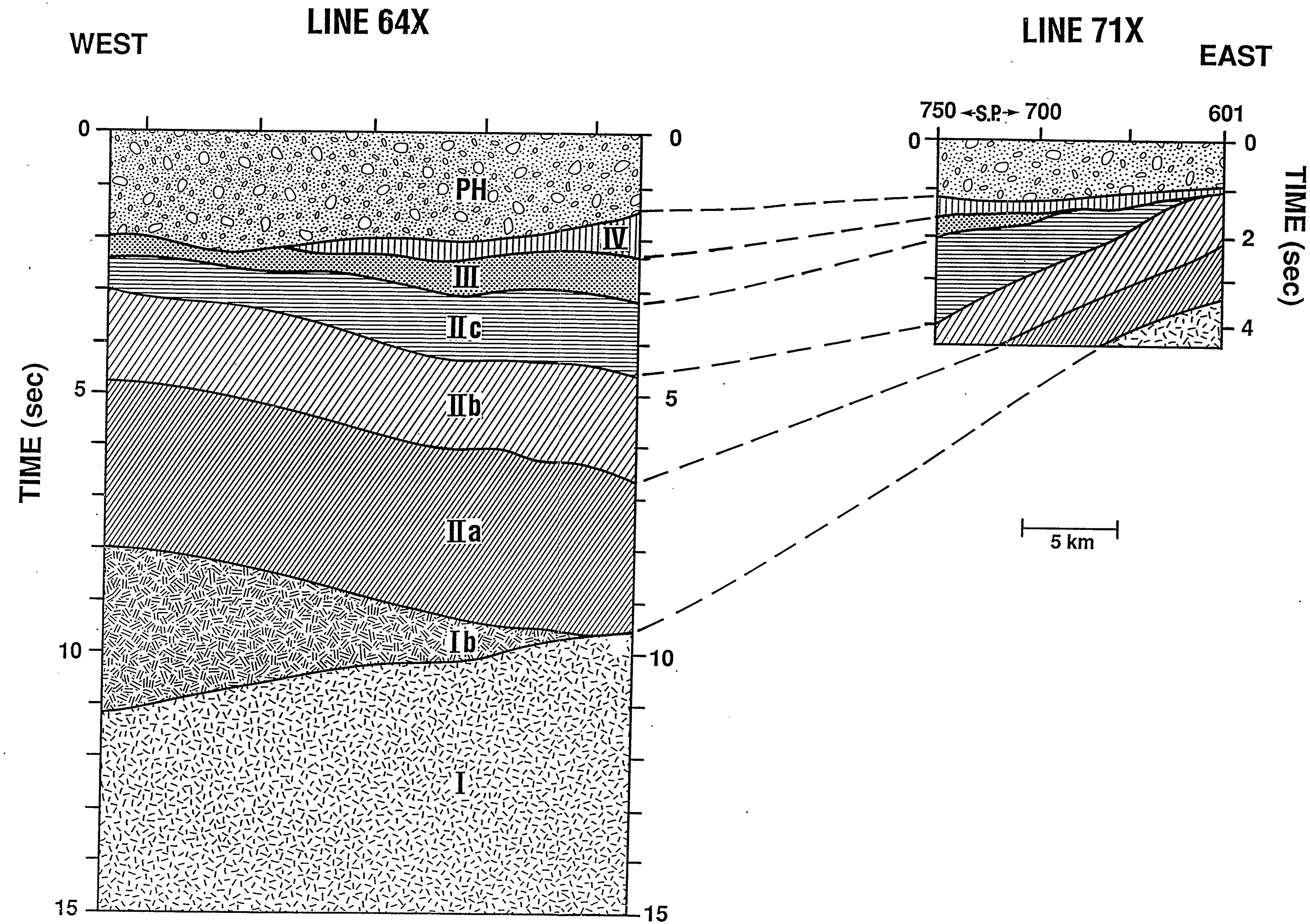
LINE 64X
WEST
LINE 71X
EAST
750 S.P. 700
601
TIME (sec)
TIME (sec)
0
5
10
15
0
2
4
PH
IV
III
IIc
IIb
IIa
Ib
I
5 km

Structure of the Proterozoic

The correlation of the Wernecke Supergroup in the west to the Dismal Lakes/Hornby Bay Groups in the east suggests a major thickening of the rocks occurred from east to west into the Wernecke basin. Accordingly, the underlying ramp is considered to be a transition from thick craton on the east to thin crust on the west. This analysis further implies that these sediments have become uplifted in the west. There are two possible causes for this uplift: 1) extensional faulting and 2) thrust faulting (Figure 5.12). Both can result in the same geometry. In the case of an extensional fault a rock mass must be stretched up section and balanced with the excess rock mass lower in the section whereas a thrust fault would likely push rock up section from the west causing shortening.

The deep west-dipping reflector observed on the Fort Norman data appears to be related to a deep basal detachment, and is possibly the westward projection of the intra-Proterozoic ramp. This interpretation is suggested by correlation to seismic reflection data to the northeast and by the gravity modelling. East of the study area anticlinal culminations have been observed by Cook et al. (1992). Seismic reflection profiles coupled with drilling data, outcrop, and potential field observations show that the culminations are cored by ca. 1.85 Ga crystalline rocks and include overlying sedimentary rocks of the ca. 1.7 to 1.3 Ga Hornby Bay and Dismal Lakes groups (Cook et al., 1992). Mackenzie Mountains Supergroup strata onlap these culminations and are thus younger than the deformation causing the uplifting of crystalline Hudsonian basement.

Figure 5.10

Correlation of generalized stratigraphic columns from the Cordillera through line 64X to the Coppermine area.

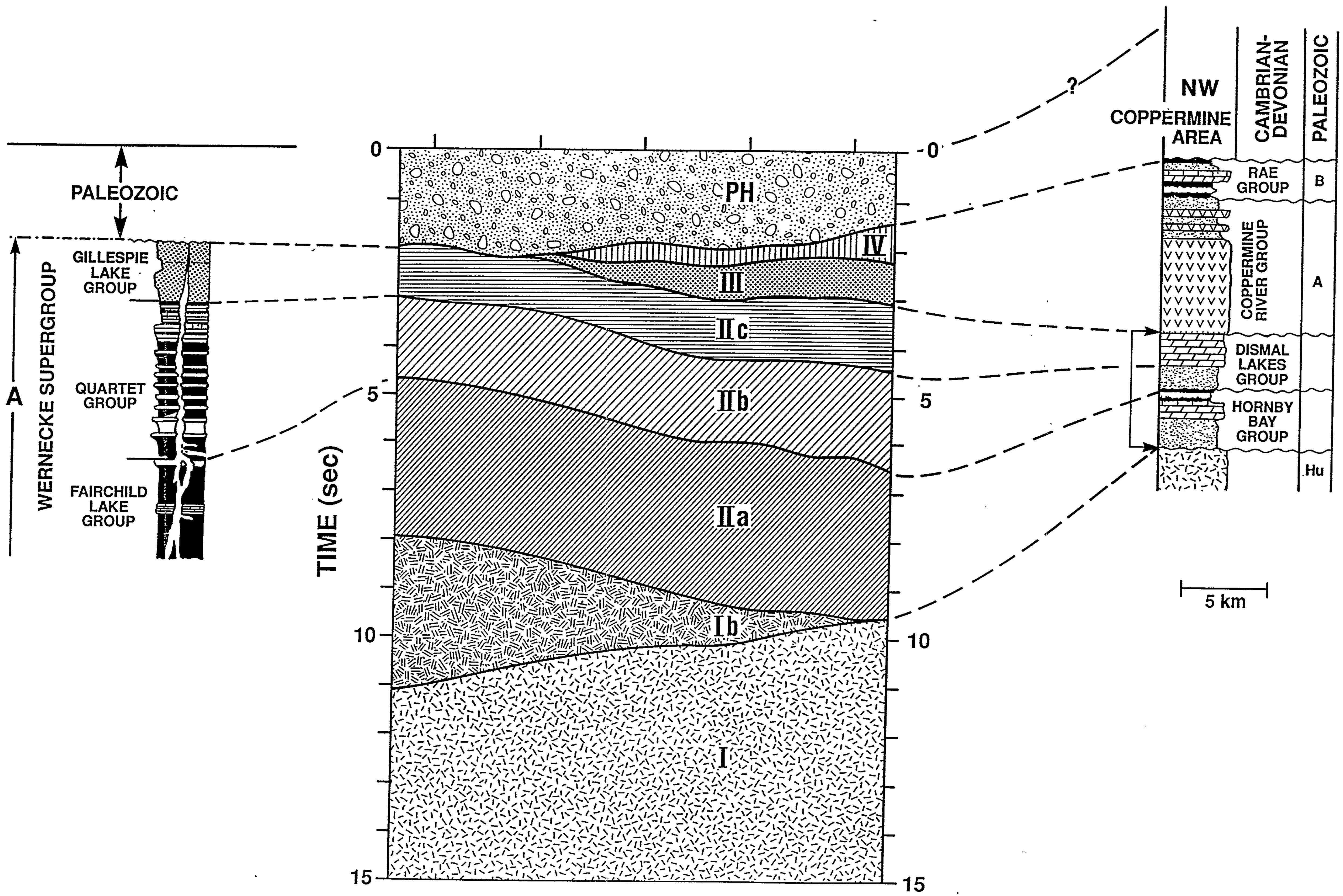

PALEOZOIC
A
WERNECKE SUPERGROUP
GILLESPIE LAKE GROUP
QUARTET GROUP
FAIRCHILD LAKE GROUP
TIME (sec)
0
5
10
15
PH
IV
III
IIc
IIb
IIa
Ib
I
?
NW
COPPERMINE AREA
CAMBRIAN-DEVONIAN
PALEOZOIC
RAE GROUP
B
COPPERMINE RIVER GROUP
A
DISMAL LAKES GROUP
HORNBY BAY GROUP
Hu
5 km

Figure 5.11

Summary of the correlations made between the documented Proterozoic strata and the zones identified on the seismic lines used in this study (modified from Cook et al., 1992)

NAME	AGE (Ga)	STRATIGRAPHIC SEQUENCE	SEISMIC ZONE	SYMBOL	
Phanerozoic	<0.6		Ph		
Windermere	0.6 - 0.8	C	not present	none	
MMSG / Rae	0.8 - 1.1	B	IV		
Uncertain	?	?	III		
Coppermine River Group	1.27	A	not present	none	
Dismal Lakes Group	1.3 - 1.66		IIc		
Upper Hornby Bay Group	>1.66		IIb		ER
Lower Hornby Bay Group			IIa		
Uncertain			Ib		
Hudsonian	>1.8		I (?)		

PROTEROZOIC

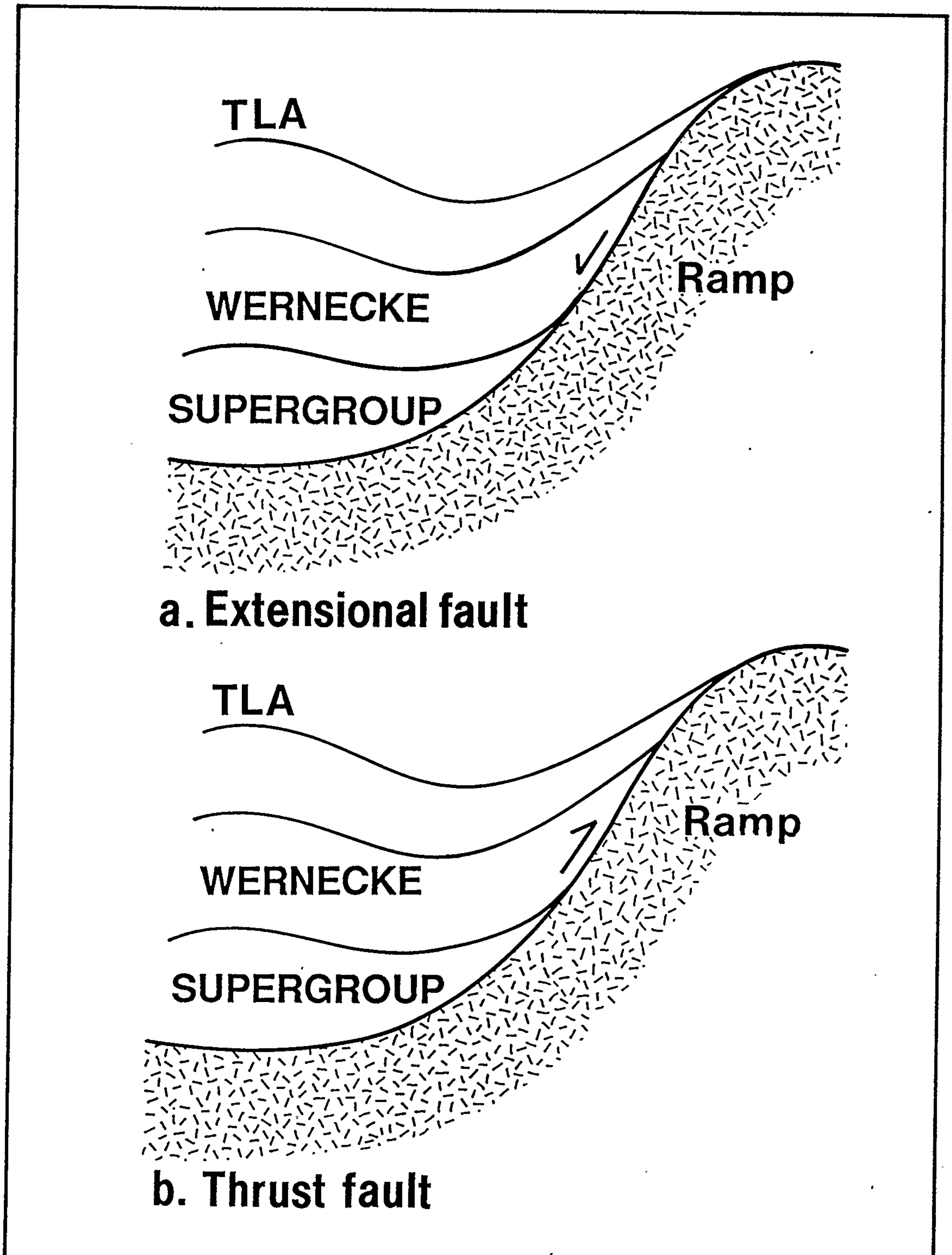
TLA
WERNECKE
SUPERGROUP
Ramp
a. Extensional fault
TLA
WERNECKE
SUPERGROUP
Ramp
b. Thrust fault

In the west, an antiform, referred to as the Tate Lake anticline because of its geographic closeness to Tate Lake, is observed on the reflection seismic data within the Fort Norman study area. It is an uplift of Mid-Proterozoic strata occurring post-Wernecke Supergroup deposition and pre-Mackenzie Mountains Supergroup deposition.

Discussion

The combination of data from seismic reflection lines, drill hole data, outcrop data and potential field data provide a fairly complete picture of the Proterozoic geology in the Fort Norman study area. The most dominant feature within the Proterozoic rocks of this area is the large intra-Proterozoic ramp that has at least 10 km of relief and that may have strongly influenced the depositional events that followed its formation. This large structural relief has been speculated by Cook et al. (1992) to have been a regionally extensive west-facing basement ramp which formed in a passive margin environment. Due to the deepening of the Wernecke basin, which was controlled by the intra-Proterozoic ramp, a greater accumulation of sediment occurred in the west as compared to the east. This sedimentary package (namely the Wernecke Supergroup or Dismal Lakes/Hornby Bay Groups) was deposited directly on top of the basement ramp and later uplifted on the western side probably due to thrust faulting. In the east, anticlinal culminations in the area are probably cored by Hudsonian basement which are flanked by Hornby Bay and Dismal Lakes sedimentary rocks (Cook et al., 1992). The Mackenzie

Mountains Supergroup rocks overlie these structures with angular unconformity and appear to onlap some flanks of the anticlines suggesting the anticlines were topographic highs, at least, during the early stages of deposition of the Mackenzie Mountains Supergroup. Relatively thin, flat layers of Phanerozoic sedimentary rocks unconformably overlie this stratigraphic succession. A suggestion put forward by Cook et al. (1992) to explain the basement uplifts was based on reconstructions of the structures associated with the Fort Simpson structural trend. They stated that the basement uplifts may have been formed as thrust faults rode over a crustal scale basement ramp that originally marked the location of significant stratigraphic thickening of the Hornby Bay and Dismal Lakes strata into the Wernecke basin.

The ramp is observed on the east side of the three Chevron Canada seismic reflection lines (52X, 64X, and 26X). According to the time migrations, the west-dipping crustal-scale ramp migrates up-section such that the Fort Simpson magnetic anomaly marks the top of the ramp in the southern portion of the study area (Figure 5.13). The location of the intra-Proterozoic ramp marks a north-south trending regional gravity gradient from high values in the east to low values in the west. This gravity gradient appears to be a direct result of the thicker accumulation of lower density rocks to the west. The magnetic anomaly indicates the ramp ends in a structural high a few kilometres east of the study area and then flattens out eastward.

Figure 5.13

A schematic diagram illustrating the location of the deep west-dipping ramp reflection event along strike within the Fort Norman area as compared to the locations of deep seismic profiles.

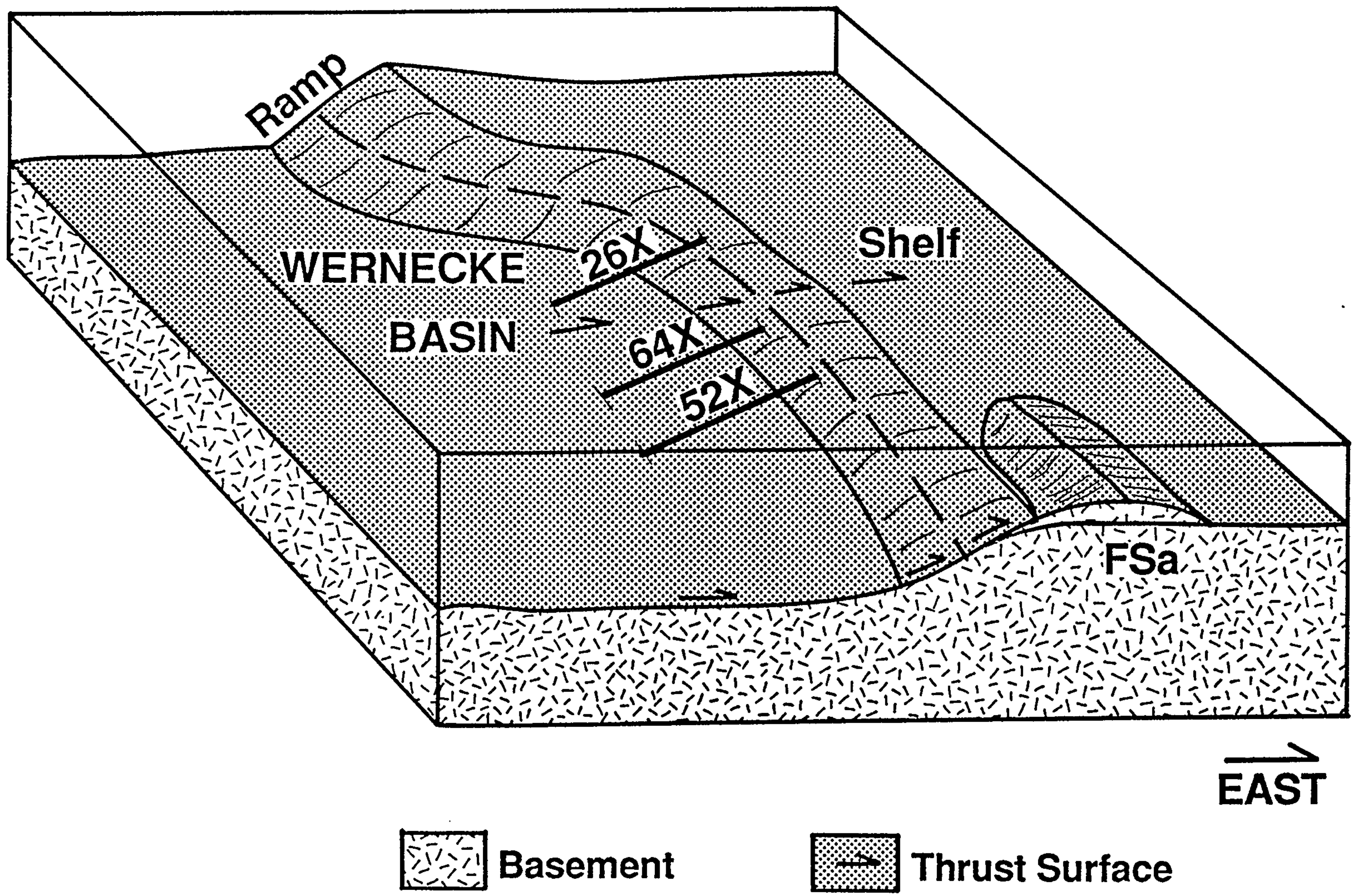
Ramp
WERNECKE
BASIN
26X
64X
52X
Shelf
FSa
EAST
Basement
Thrust Surface

CHAPTER 6 : CONCLUSION

Conclusion

The Fort Norman data illustrates two main geological features, a thick (about 18 km) package of internally undeformed relatively sedimentary/metasedimentary rock which dramatically thickens westward and a steep west-dipping event very deep within the sections (about 20 to 25 km deep). The thick package of rock is observed to lie directly over and west of a basement ramp. The correlation of known stratigraphy to the east (Coppermine area) and the west (Cordillera) allows one to speculate that those layers are part of the Wernecke Supergroup and that the associated steeply dipping event represents the lower part of a crustal-scale intra-Proterozoic ramp.

The potential field data indicate that a rock mass which is structurally higher than the ramp, just east of the study area, has high density and susceptibility. The location of this feature is consistent with the idea that it is indeed part of a regionally extensive west-facing basement ramp that was formed within rocks of the Hudsonian basement. The gradual decrease in gravity values westward has been attributed to the large accumulation of lower density rocks, both Proterozoic and Phanerozoic, above the basement ramp.

As a result of this deep crustal study of the Fort Norman area, prominent variations in potential field data (gravity and magnetic) anomalies coupled with seismic reflection data and drill hole information, have provided new insight relating to the stratigraphic and structural evolution of the Proterozoic rocks of northwestern Canada. At the base of the Proterozoic sequence is the Hudsonian basement ramp upon which we interpret sediments of the Wernecke Supergroup to have accumulated. Due to the large relief on the west-dipping, crustal-scale ramp, the sediment accumulation was thicker in the west. East-west contraction followed causing the Wernecke Supergroup sedimentary rocks to be thrust up resulting in an antiform in the west but to remain relatively undeformed internally. This was followed by deposition of the Mackenzie Mountain Supergroup which unconformably overlies the Wernecke Supergroup. Finally, the flat-lying sediments of the Phanerozoic were unconformably deposited over the Proterozoic package, and then deformed at shallow levels during the Cordilleran (Mesozoic) orogenic events. Although other interpretations can be made from this data, the interpretation presented in this text is consistent with the available information and is geologically possible.

Future Recommendations

Much more work is necessary for the complete understanding of the Proterozoic of northwestern Canada. There are still large areas of unexplored Proterozoic which would serve to link all the studied areas. I have attempted to link the Fort Norman area stratigraphy and structure with that of the Cordillera and the Coppermine areas, but there are still linkages needed to the Richardson Mountains and the Colville Hills, just to name a couple. Companies actively engaged in the exploration of petroleum can help in this quest to further understand the Proterozoic by simply donating deep crustal data to the LSPF.

REFERENCES

Aitken, J.D., and Pugh D.C., 1984. The Fort Norman and Leith Ridge structures: major, buried, Precambrian features underlying Franklin Mountains and the Great Bear and MackenziePlains. Bulletin of Canadian Society of Petroleum Geology, V. 32, No. 2, p. 139-146.

Balkwill, H.R., 1971. Reconnaissance Geology, Southern Great Bear Plain, District of Mackenzie; Geological Survey of Canada, Paper 71-11.

Clark, E., and Cook, F., 1989. Proterozoic structures in the subsurface of the Fort Good Hope area, N.W.T. (abs.), Exploration update '89, Canadian Society of Exploration Geophysists National Convention Program and Abstracts, p. 89.

Cook, D., and Yorath, C.J., 1981. Cretaceous and Tertiary stratigraphy and paleogeography, Northern Interior Plains, District of Mackenzie, Geological Survey of Canada, Memoir 398.

Cook, F., 1988. Middle Proterozoic compressional orogen in Northwestern Canada, Journal of Geophysical Research V. 93, No. B8, p. 8985-9005.

Cook, F., Dredge, M., and Clark, E., 1992. The Proterozoic Fort Simpson structural trend in Northwestern Canada, Geological Society of America Bulletin, V. 104, p. 1121-1137.

Cook, F., and Taylor, G., 1991. Seismic reflection trace synthesized from Proterozoic outcrop and its correlation to seismic profiles in northwestern Canada, Tectonophysics, V. 191, p. 111-126.

Cook, F., Varsek, J., and Clark, E., 1991. Proterozoic craton to basin crustal transition in western Canada and its influence on the evolution of the Cordillera, Canadian Journal of Earth Sciences, p. 1148-1158.

Delaney, G., 1981. The Mid-Proterozoic Wernecke Supergroup, Wernecke Mountains, Yukon Territory: In F.H.A. Campbell, (ed.), Proterozoic Basins of Canada, Geological Survey of Canada Paper 81-10, p. 1-24.

Geological Society of America, 1987a. Gravity anomaly map of North America. Continential scale map 002, scale 1:5 000 000.

Geological Society of America, 1987b. Magnetic anomaly map of North America. Continential scale map 003, scale 1:5 000 000.

Kerans, C., Ross, G., Donaldson, J., and Geldsetzer, H., 1981. The Helikian Hornby Bay and Dismal Lakes groups, District of Mackenzie. in, F. Campbell (editor), Proterozoic Basins of Canada, Geological Survey of Canada Paper 81-10, p. 157-182.

Kong, S.M., Phinney, R.A., and Chowdhury, K.R., 1985. Nonlinear signal detector for enhancement of noisy seismic record sections, Geophysics, V. 50, No. 4, p. 539-550.

Le Cheminant, and Heaman, L., 1989. Mackenzie igneous events, Canada: Middle Proterozoic hotspot magmatism associated wilth ocean opening, Earth and Planet. Sci. Letters, V. 96, p. 38-48.

National Energy Board, 1986. Geological summary for B-62 drill hole, file PCI K'ALO B-62, Stratigraphic interpretation made by Pro Geo Consultants.

Sevigny, J., Cook, F., and Clark, E., 1991. Geochemical signature and seismic stratigraphic setting of Coppermine Basalts drilled beneath the Anderson Plains in northwestern Canada, Canadian Journal of Earth Sciences, V. 28, p. 184-194.

Villeneuve, M.E., Theriault, R.J., and Ross, G.M., 1991. U-Pb ages and Sm-Nd signature of two subsurface granites from the Fort Simpson magnetic high, northwest Canada, Canadian Jourmal of Earth Sciences, p. 1003-1008.

Young, G., 1984. Proterozoic plate tectonics in Canada with emphasis on evidence for a late Proterozoic rifting event, Elsevier Science Publishers B.V.

Young, G., Jefferson, C., Delaney, G., and Yeo, G., 1979. Middle and upper Proterozoic correlation of the northern Canadian Cordillera and Shield, Geology, V. 7, p. 125-129.